BOW VARIETIES—GEOMETRY, COMBINATORICS, CHARACTERISTIC CLASSES

Yiyan Shou

A dissertation submitted to the faculty at the University of North Carolina at Chapel Hill in partial fulfillment of the requirements for the degree of Doctor of Philosophy in the Department of Mathematics in the College of Arts and Sciences.

Chapel Hill
2021

Approved by:

Richárd Rimányi

Prakash Belkale

Lev Rozansky

Andrey Smirnov

Alexander Varchenko

ABSTRACT

Yiyan Shou: Bow Varieties—Geometry, Combinatorics, Characteristic Classes
(Under the direction of Richárd Rimányi)

Motivated by the study of 3d mirror symmetry from the perspective of characteristic classes, we develop a combinatorial framework for the study of Cherkis Bow Varieties. Bow varieties are believed to be a natural setting where 3d mirror symmetry for characteristic classes can be observed. We take the first steps toward a general theory of mirror symmetry by describing the geometry of bow varieties in terms of brane diagrams, binary contingency tables, and various combinatorial operations on these objects. We then give a conjectural formula for the cohomological stable envelope of a bow variety. An overview of 3d mirror symmetry for characteristic classes in Schubert calculus is also provided.

To Maya

ACKNOWLEDGEMENTS

I would like to acknowledge, first and foremost, my advisor, Richárd Rimányi. It was truly an honor studying mathematics under his supervision. Without his guidance, this work would have never come to fruition. Second, I would like to thank the wonderful faculty and staff of the UNC mathematics department. I learned a great deal of mathematics from them over the years, my committee especially, and have relied on Laurie Straube to keep me on top of paperwork, administrative requirements, and deadlines. Sara Kross was always prepared to brighten my day with a smile and free office supplies. Third, I would like to thank my fellow graduate students. Our mathematical discussions have been an invaluable source of knowledge and fresh ideas and perspectives. Our non-mathematical discussions have been an invaluable source of levity amidst the stress of a doctoral program. My interactions with Bradley Hicks, Wesley Hamilton, Marc Besson, Samuel Jeralds, Joshua Kiers, Hunter Dinkins, Paul Kruse, and Joseph Graves in particular have been of great personal and professional value. Finally, I am grateful to my family for their love and support. I am especially indebted to my parents for the opportunities they have provided me, to which I owe my academic accomplishments.

TABLE OF CONTENTS

LIST OF FIGURES

LIST OF TABLES

CHAPTER 1

Introduction

This thesis is an expansion of the work done in [RS]. The motivation of this work is the study of enumerative geometry through characteristic classes in cohomology associated to subvarieties of interest within a smooth ambient variety. An example of this approach is the assignment of characteristic classes to Schubert varieties. This makes up an important part of Schubert calculus. Classically, one might consider fundamental classes of closed subvarieties, which encode information about intersection multiplicites. The fundamental classes of Schubert varieties in (equivariant) cohomology or K-theory are well-studied objects called "Schubert classes". These classes can be used to solve certain enumerative Schubert problems, but are also intersting in their own right, connecting with various areas of combinatorics, geometry, and representation theory. The fundamental class can be generalized in many ways. In the case of smooth closed subvarieties, one could consider the pushforward of the total Chern class of the tangent bundle of the subvariety. This is generalized to constructible subsets by the Chern-Schwartz-MacPherson class in (equivariant) cohomology and the Motivic Chern class in (equivariant) K-theory. These classes can be applied to either Schubert varieties or Schubert cells giving rise to $\hbar$-deformed Schubert calculus [Ri].

Recently, motivated by relations with quantum integrable systems, Okounkov and his coauthors introduced torus equivariant characteristic classes assigned to the torus fixed points of a torus equivariant symplectic resolution. These classes are called the "stable envelope" [AO, O, MO]. They depend on other parameters, and varying those parameters gives a geometric quantum group action on cohomology, K-theory, and elliptic cohomology. In certain settings where both the aformentioned Chern classes and stable envelopes are defined, they can be shown to agree. This coincidence not only made the study of the classical characteristic classes even more interesting than before, but also brought fresh ideas and new ways of calculating them [RV, FRW1, FRW2, AMSS1, AMSS2, RW1, KRW]. Rather than generalizing the class, one could also generalize the cohomology theory. Passing to elliptic cohomology reveals a hidden structure.

Elliptic stable envelopes depend on two sets of parameters. There are the usual equivariant parameters coming from the torus action. There is also a new set of "Kähler" or "dynamical" parameters. For certain pairs of equivariant symplectic resolutions, the elliptic stable envelopes of the two spaces "match". This "matching" is explained in detail in Section 4.1.6, but its key feature is interchanging the two sets of parameters. Motivated by ideas from physics [BFN, BDGH, GW, GMMS, IS], we call this phenomenon "3d mirror symmetry for characteristic classes". Some instances of 3d mirror symmetry for characteristic classes are proven in [RSVZ1, RSVZ2, RW2, SZ] using ad hoc methods, but a general theory is not yet known.

There are indications that the right collection of spaces for the study of 3d mirror symmetry for characteristic classes is the collection of Cherkis bow varieties. For bow varieties, the equivariant and Kähler parameters appear on equal footing, corresponding to two "dual" combinatorial objects called "5-branes". There is a duality operation that interchanges the 5-branes, paralleling the interchange of equivariant and Kähler parameters in 3d mirror symmetry for characterstic classes. Moreover, the collection of bow varieties is closed under this operation. The goal of the work in this thesis and [RS] is to introduce Cherkis bow varieties to enumerative geometry and work out the necessary combinatorial structures for their enumerative analysis and the study of 3d mirror symmetry for characteristic classes.

This thesis is organized into three main chapters on combinatorics, geometry, and characteristic classes. In Chapter 2, we define the basic combinatorial objects of our framework, "brane diagrams", and explore their properties. Important combinatorial operations—brane duality and Hanany-Witten transition—on brane diagrams are also studied. These objects can be connected to binary contingency tables from statistics and combinatorics, giving us an alternative combinatorial perspective, which has certain advantages. Brane diagrams and related constructions, while interesting in their own right, encode the geometry of bow varieties, our principle objects of study.

In Chapter 3, we review the "quiver" construction of bow varieties [NT]—as well as the construction of quiver varieties [N1], which arise as a special case of bow varieties. We then connect the combinatorial objects of Chapter 2 to the geometry of bow varieties. To each brane diagram we will associate a bow variety: a holomorophic symplectic torus equivariant manifold, which possesses a distinguished family of "tautological" vector bundles. Certain properties of this manifold can be read from the combinatorics of the brane diagram. The main result of this chapter establishes a

bijection between certain configurations of "ties" on a brane diagram—or binary contingency tables with certain margin vectors—and the torus fixed points of the corresponding bow variety. We also give a combinatorial formula for the weights of fixed point restrictions of tautological bundles and the K-theory class of the tangent bundle. Finally, we construct certain torus invariant curves using combinatorial "surgery" operations. Fixed points, fixed point restrictions of tautological bundles, and invariant curves are key to the study of characteristic classes.

Chapter 4 is devoted to initiating the study of characteristic classes on bow varieties. Here, we give an overview of characteristictic classes in Schubert calculus, and especially 3d mirror symmetry. This notion of 3d mirror symmetry is an important motivator for the study of characteristic classes on bow varieties, as it connects very naturally with the combinatorics of bow varieties. We then discuss the equivariant cohomology and K-theory of bow varieties, and introduce a notion of cohomological stable envelope class adapted to bow varieties. Several examples of these classes are shown, and we give a conjectural formula for calculating their fixed point restrictions.

The bow varieties considered in this work are special cases of the more general construction of [NT]. Appendix A shows how to translate between our bow varieties and those of [NT]. Finally, we have included the appendix in [RS] on Maya diagrams [N3] as Appendix B, for the sake of completeness.

CHAPTER 2

Combinatorics

This chapter establishes a combinatorial framework for the study of Cherkis bow varieties. This framework includes brane diagrams, binary contingency tables, and the related combinatorial operations of brane duality and Hanany-Witten transition.

2.1 Brane Configurations and Diagrams

In this section we will construct the primary combinatorial objects of our framework, *brane diagrams*, and explore their basic combinatorial properties. We begin with a 3-dimensional view. Consider a configuration of distinct lines in $\mathbb{R}^3$ parallel to the y- and z-axis. Call those lines parallel to the y-axis *NS5 branes* and those parallel to the z-axis *D5 branes*. Collectively, D5 and NS5 branes are referred to as *5-branes*. Insert distinct line segments parallel to the x-axis with endpoints on the 5-branes. Call these line segments *D3 branes*. NS5, D5, and D3 branes are collectively referred to as *branes*. Thinking of the 5-branes as being fixed in place and the D3 branes as rigid but able to slide along their endpoints, a configuration of branes is completely fixed in place if and only if the endpoints of each D3 brane are on 5-branes of opposite type. Note that only one D3 brane may connect a pair of 5-branes of opposite type.

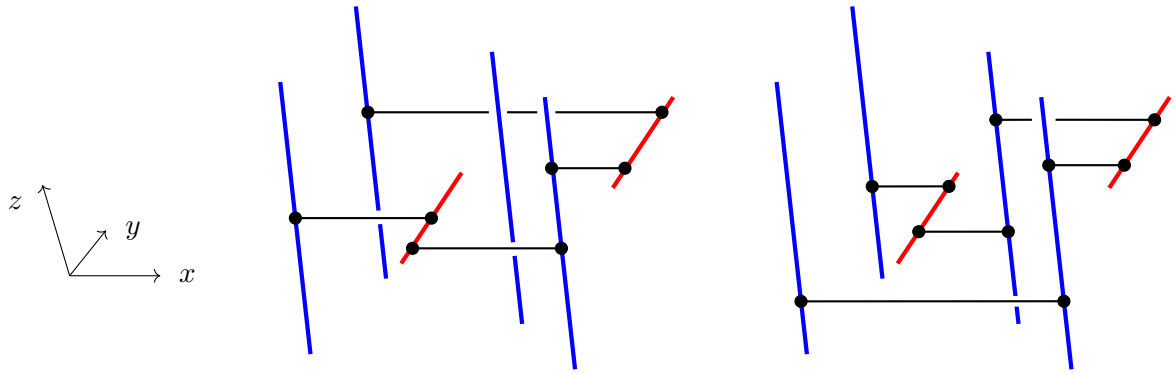

Figure 2.1: A fixed (left) and nonfixed (right) brane configuration. NS5 branes are red, D5 branes are blue, and D3 branes are black.

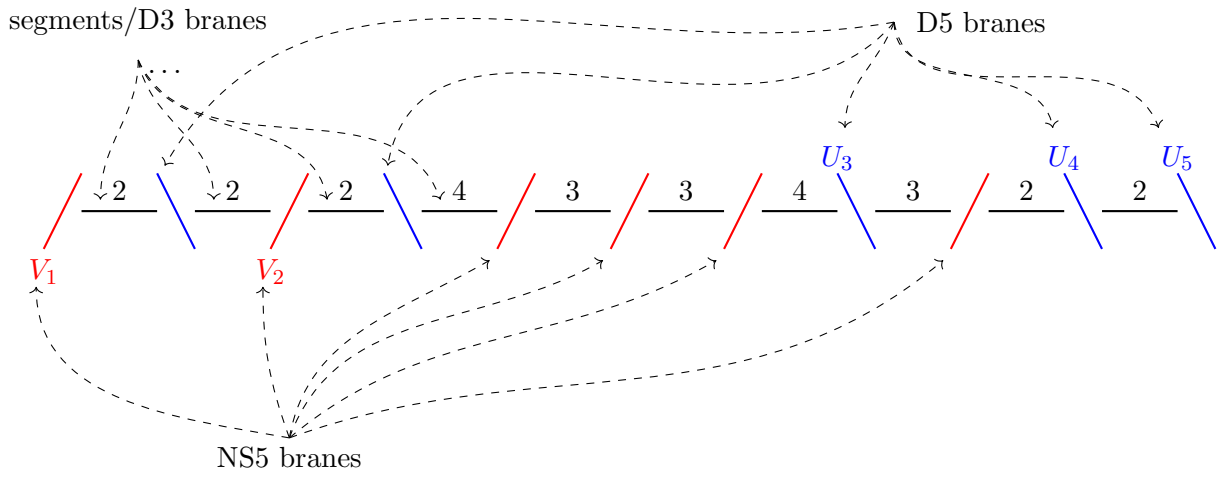

Figure 2.2: A typical brane diagram.

Given a configuration of branes, we may project onto the x-axis, retaining the x-coordinates of the 5-branes and the number of D3 branes spanning the space between the 5-branes. We lose the endpoints of the D3 branes. This projection is called a *brane diagram*. Graphically, we draw the x-axis horizontally, and represent the projected NS5 branes by lines with positive slope and D5 branes by lines with negative slope. These lines subdivide the x-axis into segments, which we label with the number of D3 branes spanning the space between the bounding 5-branes. Note that there are two infinite segments on the far left and right of the diagram with label 0. We will not draw these segments, but they are necessary in what follows. Drawing the brane diagrams can be cumbersome, so we will often condense them. For example, we can represent the brane diagram in Figure 2.2 more compactly by /2\2/2\4/3/3/4\3/2\2\.

If we wish to retain the endpoints of the D3 branes, we may represent the D3 branes with dashed lines, which we call *ties*. Such a diagram is called a *tie diagram*. The numerical labels of the segments record the number of ties that "cover" that segment. Once the ties are drawn, these labels become redundant, and we will often ommit them.

From now on, we will be concerned only with fixed brane configurations. For instance, tie diagrams like the one on the right of Figure 2.3 will no longer be considered.

Assumption 2.1.1. All tie diagrams correspond to fixed configurations of branes. In other words,

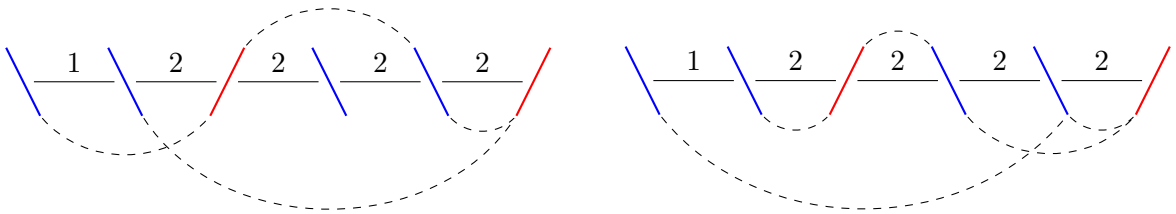

Figure 2.3: The tie diagrams corresponding to the brane configurations in Figure 2.1.

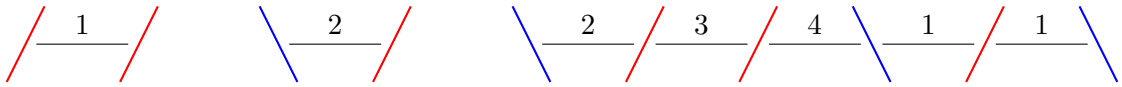

Figure 2.4: Brane diagrams that cannot be extended to a tie diagram.

each tie joins 5-branes of opposite type, and no two ties join the same pair of 5-branes.

Under this assumption, it may not be possible to add ties to a brane diagram to obtain a valid tie diagram (see Figure 2.4 for simple examples). When we draw ties between a pair of 5-branes of opposite type, we place them above the diagram if the NS5 brane is left of the D5 brane and below the diagram if the D5 brane is left of the NS5 brane (see the left tie diagram of Figure 2.3). This convention has both aesthetic and combinatorial advantages.

We will also adopt the convention that NS5 branes are denoted V, D5 branes are denoted U, and segments in the brane diagram are denoted X. Given a 5-brane/segment $\mathcal{B}$, let $\mathcal{B}^-$ and $\mathcal{B}^+$ denote the segment/5-brane immediately to the left and right, respectively, of $\mathcal{B}$. Let $\mathcal{B}^=$ and $\mathcal{B}^\ddagger$ denote the 5-brane/segment two positions to the left and right, respectively, of $\mathcal{B}$. Given a segment X, call its integer label the *multiplicity* of X and denote it by d_X. The two hidden segments at the far ends of the diagram have multiplicity 0. When speaking of brane diagrams, the terms "segment" and "D3 brane" will be used interchangeably. By convention, branes will always be listed from left to right. Brane and tie diagrams can be augmented with additional combinatorial structures and possess alternative combinatorial descriptions, which will be explored in the remainder of this chapter. This section concludes with an example.

Example 2.1.2. Consider the underlying brane diagram of Figure 2.3

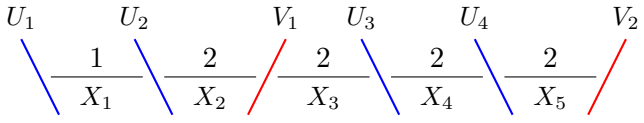

.

Let us enumerate all of the tie diagrams that can be obtained from this brane diagram. Since U_1 is the leftmost 5-brane and $d_{U_1^+} = d_{X_1} = 1$, there must be a tie between U_1 and V_1 or V_2. Either way, this tie covers X_2. Since $d_{X_2} = 2$, there must be one additional tie covering X_2. This additional tie cannot cover X_1, so it must join U_2 with V_1 or V_2.

First, consider the case where there is a tie between U_1 and V_1. If the additional tie joins U_2 with V_1, there must be two ties starting at V_1 going to the right. This is because $d_{V_1^+} = d_{X_3} = 2$, and no more ties can cover X_1 and X_2. There are only two D5 branes to the right of V_1, so these two ties must end at U_3 and U_4. The mutliplicities of X_4 and X_5 force us to place ties between U_3, U_4, and V_2. We obtain the tie diagram

(1) 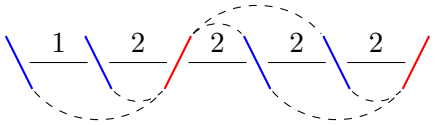

.

If on the other hand the additional tie joins U_2 with V_2, then X_3, X_4, X_5 must each be covered by one more tie. There must be one tie starting at V_1 and going to the right. This tie can end either at U_3 or U_4. Regardless of the endpoint, we are forced to place a tie between it and V_2. The two tie diagrams obtained this way are

(2) 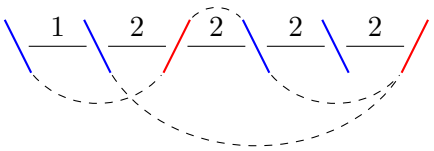

(3) 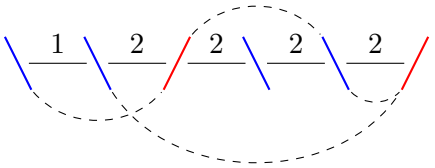

.

Second, consider the case where there is a tie between U_1 and V_2. If the additional tie is placed between U_2 and V_1, then X_3, X_4, X_5 must each be covered by one more tie. The reasoning above gives us two possible tie diagrams

(4) 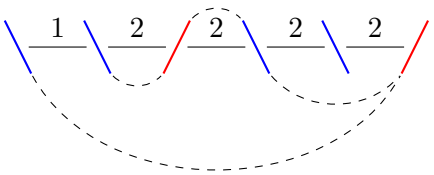

(5) 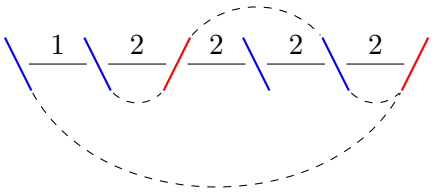

.

Finally, if the additional tie is placed between U_2 and V_2, then all segments are covered by the requisite number of ties. We immediately obtain

(6) 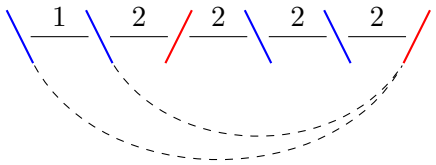

We have now listed all six tie diagrams with the given underlying brane diagram.

Enumerating tie diagrams with a given underlying brane diagram is an important problem. While the argument given here is ad hoc, the general line of reasoning can be applied to arbitrary brane diagrams. More sophisticated techniques will be discussed in Section 2.2.

2.2 Brane Charge and Binary Contingency Tables

Motivated by ideas from physics, we introduce a notion of "charge" for each 5-brane in a brane diagram. This gives rise to an alternate description of tie diagrams in terms of binary contingency tables (BCTs).

2.2.1 The Charge of a 5-Brane and Margin Vectors

To every 5-brane will be associated an integer called the *brane charge*.

Definition 2.2.1. 1. For an NS5 brane V, let

$$\text{charge}(V) = d_{V^+} - d_{V^-} + \#\{\text{D5 branes left of } V\}.$$

2. For a D5 brane U, let

$$\text{charge}(U) = d_{U^-} - d_{U^+} + \#\{\text{NS5 branes right of } U\}.$$

Remark 2.2.2. In string theory, the brane charge is defined as an integral, and is calculated to be $(d_{\mathcal{B}^+} - d_{\mathcal{B}^-}) + \#\{\text{opposite type 5-branes left of } \mathcal{B}\}$ for both types of 5-branes. Hence, for D5 branes our definition is not identical with the physics definition, rather it is a simple linear function of it. In physics this can be interpreted as integrating on a different cycle.

In general, the charge may be negative. However, brane configurations with 5-branes of negative charge cannot be fixed. In other words, they do not admit tie diagrams.

Proposition 2.2.3. *If a brane configuration is fixed, all brane charges are nonnegative.*

Proof. Suppose we have a tie diagram for a fixed brane configuration. Let V be an NS5 brane. Denote the number of ties with an endpoint on V extending to the right (respectively left) by t_+ (respectively t_-). We have

$$\text{charge}(V) = d_{V^+} - d_{V^-} + \#\{\text{D5 branes left of } V\} = t_+ - t_- + \#\{\text{D5 branes left of } V\}.$$

Since each tie has endpoints on 5-branes of opposite type, there are at least t_- D5 branes to the left of V. It follows that $\text{charge}(V) \geq t_+ \geq 0$. A similar argument applies to D5 branes. □

Let m be the number of NS5 branes and n be the number of D5 branes in a brane diagram. Denote the NS5 branes by $V_1, ..., V_m$ and the D5 branes by $U_1, ..., U_n$ (indexed from left to right). Let $r \in \mathbb{Z}^m$ and $c \in \mathbb{Z}^n$ be the vectors of charges of NS5 branes and D5 branes respectively. These vectors are the *margin vectors* of the brane diagram.

Example 2.2.4. Consider the brane diagram in Figure 2.2. The charges of V_1, V_3, U_3 are calculated as

$$\text{charge}(V_1) = 2 - 0 + 0 = 2 \quad , \quad \text{charge}(V_3) = 3 - 4 + 2 = 1 \quad , \quad \text{charge}(U_3) = 4 - 3 + 1 = 2.$$

The margin vectors are

$$r = (2, 1, 1, 2, 3, 2) \quad , \quad c = (5, 2, 2, 0, 2).$$

Lemma 2.2.5. *For any brane diagram,* $\sum r_i = \sum c_i$.

Proof. Consider the expression $\sum r_i - \sum c_i$. Collecting the d_X terms yields a telescoping sum that simplifies to the difference of the multiplicities of the infinite leftmost and rightmost segments. These multiplicites are 0. The remaining terms are $\sum_i \#\{\text{D5 branes left of } V_i\} - \sum_j \#\{\text{NS5 branes right of } U_j\}$. Fix i. Then, each D5 brane to the left of V_i contributes 1 to the sum. However, V_i will be right of each of these $D5$ branes, so V_i contributes -1 to the sum for each D5 brane to the left of V_i. All terms cancel, and we get $\sum r_i - \sum c_i = 0$. □

2.2.2 Tables-with-Margins

The *separating line* of the brane diagram is a lattice path in $\{0, ..., n\} \times \{0, ..., m\}$ that encodes the order of the 5-branes. So that our conventions match the conventions for matrices, draw the

y-axis pointing downwards. The separating line is uniquely defined by the following properties:

1. starts at $(0,0)$ and ends at (n,m),
2. only moves down or right (monotonicity),
3. passes through the segment from $(x-1,y)$ to (x,y) if and only if $V_1,...,V_y$ are to the left of U_x and $V_{y+1},...,V_m$ are to the right.

The separating line is well defined, since as j increases, the highest index i for which V_i is to the left of U_j increases. Hence, the horizontal segments of the path are moving downward as we move to the right.

Alternatively, we may define the separating line in a step-by-step fashion. Start at $(0,0)$, and read the 5-branes from left to right. Each time you encounter an NS5 brane, move one step down. Each time you encounter a D5 brane, move one step to the right. The number of downward steps is m, the number of NS5 branes, and the number of rightward steps is n, the number of D5 branes. Therefore, this path ends at (n,m). It is easy to see that these two definitions of the separating line agree.

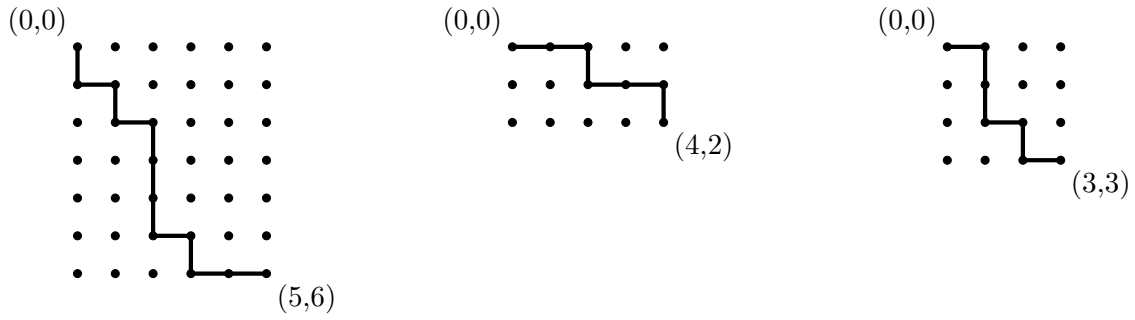

Figure 2.5: The separating line of the brane diagram in Figure 2.2, Example 2.1.2, and the right of Figure 2.4.

The margin vectors along with the separating line uniquely determine the brane diagram. Define $MV_{m,n}$ to be the set of pairs of integer vectors $r \in \mathbb{Z}^m, c \in \mathbb{Z}^n$ satisfying $\sum r_i = \sum c_i$. Let $Sep_{m,n}$ be the set of lattice paths satisfying properties 1 and 2 above.

Lemma 2.2.6. *There is a bijective correspondence*

$$\{\textit{brane diagrams with } m \textit{ NS5 branes and } n \textit{ D5 branes}\} \longleftrightarrow MV_{m,n} \times Sep_{m,n}.$$

Proof. We will construct the inverse. To a pair of vectors $(r, c) \in MV_{m,n}$ and a path in $Sep_{m,n}$, we must associate a brane diagram. The number of NS5 and D5 branes can be recovered from m and n respectively. The path determines the order of the 5-branes, as described by the step-by-step description above: each downward step gives an NS5 brane and each rightward step gives a D5 brane. We must now use the charges r, c to recover the multiplicites d_X.

Assign a multiplicity of 0 to the leftmost segment. Assume that the leftmost 5-brane is the NS5 brane V_1. Then,

$$\text{charge}(V_1) = d_{V_1^+} - d_{V_1^-} + \#\{\text{D5 branes to the left of } V_1\} = d_{V_1^+}.$$

If the leftmost 5-brane is the D5 brane U_1, then

$$\text{charge}(U_1) = d_{U_1^-} - d_{U_1^+} + \#\{\text{NS5 branes to the right of } U_1\} = m - d_{U_1^+}.$$

Now we induct. Let V be an NS5 brane and assume d_{V^-} is known. We can read charge(V) from the vector r, and we know the ordering of the 5-branes. Therefore, the multiplicity d_{V^+} can be deduced from the formula charge$(V) = d_{V^+} - d_{V^-} + \#\{\text{D5 branes to the left of } V\}$. The same procedure applies to D5 branes U.

It remains to show that the rightmost segment is assigned a multiplicty of 0. By assumption, we have $0 = \sum_i \text{charge}(V_i) - \sum_j \text{charge}(U_j)$. The proof of Lemma 2.2.5 shows that our inductive procedure assigns the same multiplicity to the leftmost and rightmost segment. The leftmost segment is assigned a multiplicty of 0, so the rightmost is also assigned a multiplicty of 0. □

Create an m by n table. Label the rows by the entries of r from top to bottom. Label the columns by the entries of c from left to right. Superimpose the separating line with the table, so that it runs in between the entries, separating the table into upper and lower parts. This collection of combinatorial data is the *table-with-margins* code of the brane diagram. Lemma 2.2.6 says that brane diagrams are in bijective correspondence with table-with-margins.

2.2.3 Binary Contingency Tables

As one might expect, ties can be encoded by filling in the entries of the table-with-margins.

Definition 2.2.7. For given $r \in \mathbb{Z}^m, c \in \mathbb{Z}^n$, an $m \times n$ matrix M is called a *binary contingency*

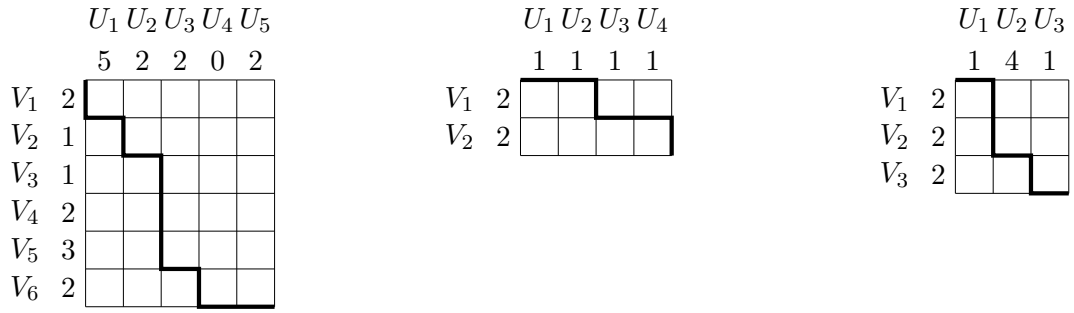

Figure 2.6: The table-with-margins of the brane diagram in Figure 2.2, Example 2.1.2, and the right of Figure 2.4.

table (BCT) with margins r, c if

$$M_{ij} \in \{0,1\}, \quad \sum_j M_{ij} = r_i, \quad \text{and } \sum_i M_{ij} = c_j.$$

Given a tie diagram, define a binary matrix M_{ij} as follows. If V_i is left of U_j (i.e. if a tie connecting V_i to U_j would be drawn above the diagram), let

$$M_{ij} = \begin{cases} 1 & \text{if } V_i, U_j \text{ are connected by a tie,} \\ 0 & \text{if } V_i, U_j \text{ are not connected by a tie.} \end{cases}$$

If V_i is to the right of U_j (i.e. if a tie connecting V_i to U_j would be drawn below the diagram), let

$$M_{ij} = \begin{cases} 0 & \text{if } V_i, U_j \text{ are connected by a tie,} \\ 1 & \text{if } V_i, U_j \text{ are not connected by a tie.} \end{cases}$$

The matrix M will be a BCT for all tie diagrams. Thus, we have

Proposition 2.2.8. *There is a bijective correspondence between BCTs of tables-with-margins and tie diagrams.*

Proof. We begin by proving that the matrix M is a BCT by inducting on the number of ties. The base case is when there are no ties. All multiplicities are 0, so

$$r_i = \text{charge}(V_i) = \#\{\text{D5 branes left of } V_i\} \quad , \quad c_j = \text{charge}(U_j) = \#\{\text{NS5 branes right of } U_j\}.$$

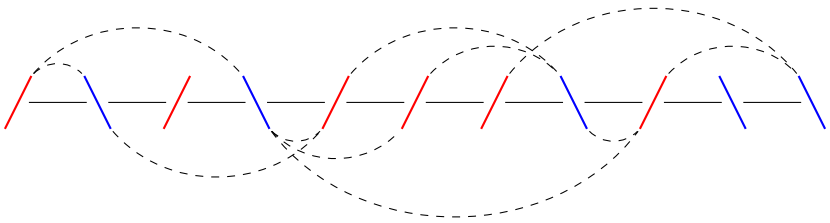

		U_1	U_2	U_3	U_4	U_5
		5	2	2	0	2
V_1	2	1	1	0	0	0
V_2	1	1	0	0	0	0
V_3	1	0	0	1	0	0
V_4	2	1	0	1	0	0
V_5	3	1	1	0	0	1
V_6	2	1	0	0	0	1

Figure 2.7: A tie diagram with the underlying brane diagram of Figure 2.2 and its BCT.

All entries of M above the separating line are 0 and all entries below the separating line are 1. It follows immediately from the description of the separating line that $\sum_j M_{ij} = r_i$ and $\sum_i M_{ij} = c_j$.

If V_i is left of U_j, then adding a tie between V_i and U_j increases $r_i = \text{charge}(V_i)$ by 1 and also switches a 0 in row i of M to a 1. On the other hand, if V_i is right of U_j, then adding a tie decreases r_i by 1 and switches a 1 in row i of M to a 0. By induction, it follows that $\sum_j M_{ij} = r_i$. A similar argument shows that $\sum_i M_{ij} = c_j$.

There is an obvious way to invert the construction of M. We must show that the ties obtained from a BCT cover each D3 brane the requisite number of times. Similarly to the above, induct on the number of 1's above the separating line and 0's below the separating line. The base case, where all entries above the separating line are 0 and all entries below the separating line are 1, is addressed above. For the inductive step, suppose we take an entry $M_{ij} = 0$ above the separating line and change it to 1. Then $r_i = \text{charge}(V_i)$ and $c_j = \text{charge}(U_j)$ increase by 1, but no other charges change. Since the entry is above the separating line, V_i is to the left of U_j. It follows from the definition of charge and the fact that the leftmost and rightmost segments have multiplicity 0 that the multiplicities of all segments between V_i and U_j increase by 1, while all other multiplicities remain the same. We have, however, added a tie between V_i and U_j, so each segment is still covered by the correct number of ties by induction. A similar argument applies below the separating line.

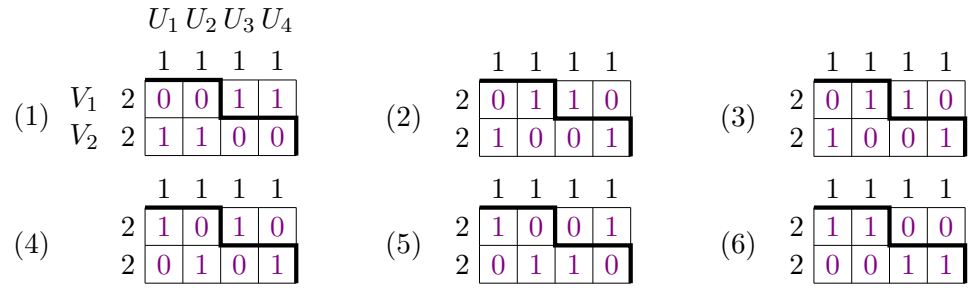

Figure 2.8: BCTs for the six tie diagrams of Example 2.1.2.

Applying Lemma 2.2.6 completes the proof. □

Remark 2.2.9. The set $\mathrm{BCT}(r, c)$ of BCTs with margins r, c is studied in combinatorics and statistics. Here is a list of some relations between BCTs and other algebraic combinatorial notions. Clearly

$$\prod_{i=1}^{m}\prod_{j=1}^{n}(1+x_i y_j) = \sum_{r,c} \#\mathrm{BCT}(r,c)\cdot x_1^{r_1}x_2^{r_2}\dots x_m^{r_m}y_1^{c_1}y_2^{c_2}\dots y_n^{c_n}.$$

The number $\#\mathrm{BCT}(r, c)$ can be evaluated in terms of the Kostka numbers associated with Young tableaux. The Gale-Ryser theorem is a simple numerical criterion on r, c determining whether $\mathrm{BCT}(r, c)$ is empty. The Robinson-Schensted-Knuth correspondence establishes a bijection between $\mathrm{BCT}(r, c)$ and pairs of certain Young tableaux. For exact statements and more on the relevance of BCTs see e.g. [Br, B] and references therein. Enumerating BCTs will be important in later sections.

Proposition 2.2.8 gives another proof of Proposition 2.2.3. If a BCT exists, then it also gives an alternative proof of Lemma 2.2.5. Given a table-with-margins with nonnegative margin vectors whose sums of entries are equal, there may not be a BCT associated with it. For instance, it is easy to see that the table-with-margins on the right in Figure 2.6 does not admit a BCT, consistent with the fact that the brane diagrams in Figure 2.4 do not admit tie diagrams. From now on, we restrict our attention to those that do possess BCTs.

Assumption 2.2.10. All tables-with-margins admit a BCT. Equivalently, all brane diagrams can be extended to a tie diagram.

With this assumption in place, there is an easy way to read off the D3 multiplicities from a BCT, forgoing the inductive procedure of Lemma 2.2.6. The step-by-step definition of the separating line

gives us a natural correspondence between integer points $P = (x, y)$ on the separating line and segments X_P of the brane diagram:

1. if the next integer point on the separating line is $(x, y+1)$, then X_P is the segment bounded on the right by V_{y+1},
2. if the next integer point on the separating line is $(x+1, y)$, then X_P is the segment bounded on the right by U_{x+1},
3. if P is the last integer point on the separating line, X_P is the infinite segment on the right of the brane diagram.

We claim that the number of ties covering X_P is given by $\#\{1\text{'s NE of } P\} + \#\{0\text{'s SW of } P\}$. Indeed, for each 1 NE of P, we have a tie between a 5-brane to the left of X_P and a 5-brane to the right of X_P. The same is true for each 0 SW of P.

Proposition 2.2.11. *Fix a BCT. Let P be an integer point on the separating line, and let X_P be the corresponding D3 brane. Then, we have*

$$d_{X_P} = \#\{\textit{1's NE of } P\} + \#\{\textit{0's SW of } P\}.$$

2.3 Brane Duality

A natural combinatorial operation on brane/tie diagrams is to change the NS5 branes to D5 branes and vice versa. This operation is referred to as *duality*. Let $\mathcal{D}$ be a brane diagram with margin vectors $r \in \mathbb{Z}^m, c \in \mathbb{Z}^n$. Denote the dual brane diagram by $\mathcal{D}'$ and its margin vectors by $r' \in \mathbb{Z}^n, c' \in \mathbb{Z}^m$. From the definition of charge (Definition 2.2.1), we have

$$r'_i = m - c_i \quad , \quad c'_j = n - r_j. \tag{2.1}$$

Indeed, switching the type of a 5-brane negates the contribution of the D3 multiplicities to the charge, and instead of adding the number of branes of opposite type on the left/right, we add the number of branes of opposite type on the right/left. It is also easy to see that the separating line is transposed from the step-by-step description: every downward step becomes a rightward step and vice versa. Finally, entries of a BCT above/below the separating line of $\mathcal{D}$ move below/above the

separating line of $\mathcal{D}'$ upon transposition. This is reflected in the fact that ties that are drawn above $\mathcal{D}$ are drawn below $\mathcal{D}'$. Hence, duality transposes BCTs and interchanges 0's and 1's. In summary, we have

Proposition 2.3.1. *Given a dual pair of brane/tie diagrams $\mathcal{D}, \mathcal{D}'$, their table-with-margins are related by transposition and a renormalization* (2.1) *of the margin vectors. Their BCTs are related by transposition and interchanging 0's and 1's.*

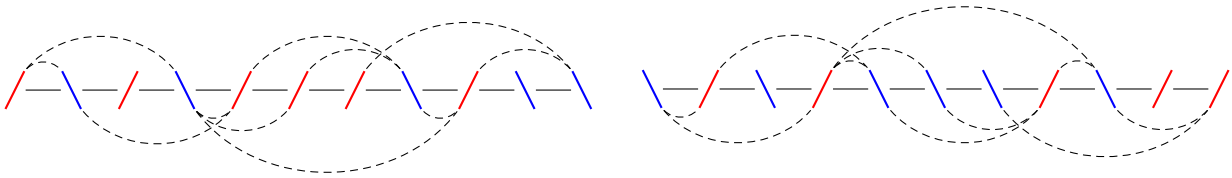

		U_1	U_2	U_3	U_4	U_5
		5	2	2	0	2
V_1	2	1	1	0	0	0
V_2	1	1	0	0	0	0
V_3	1	0	0	1	0	0
V_4	2	1	0	1	0	0
V_5	3	1	1	0	0	1
V_6	2	1	0	0	0	1

		U'_1	U'_2	U'_3	U'_4	U'_5	U'_6
		3	4	4	3	2	3
V'_1	1	0	0	1	0	0	0
V'_2	4	0	1	1	1	0	1
V'_3	4	1	1	0	0	1	1
V'_4	6	1	1	1	1	1	1
V'_5	4	1	1	1	1	0	0

Figure 2.9: The tie diagram and BCT of Figure 2.7 (left) and their duals (right).

2.4 Hanany-Witten Transitions

We will now define a combinatorial operation on brane diagrams that changes the order of the 5-branes. These operations will be defined in such a way that the margin vectors are preserved. Let $\mathcal{B}_1$ be a 5-brane and suppose $\mathcal{B}_2 = \mathcal{B}_1^{\ddagger}$ is a 5-brane of opposite type. Define $d_1 = d_{\mathcal{B}_1^-}$, $d_2 = d_{\mathcal{B}_1^+}$, $d_3 = d_{\mathcal{B}_2^+}$. The operation of switching the positions of $\mathcal{B}_1$ and $\mathcal{B}_2$ and replacing d_2 with $\tilde{d_2} = d_1 + d_3 - d_2 + 1$ is called a *Hanany-Witten transition*. We will use the abbreviation "HW" for "Hanany-Witten". The new multiplicty $\tilde{d_2}$ is chosen precisely so that the charges of the 5-branes are preserved. Moreover, applying a Hanany-Witten transition twice to the same pair of 5-branes recovers the original brane diagram. Two brane diagrams related by a sequence of HW transitions will be called *Hanany-Witten equivalent*.

Since the charges are preserved, the only change in the table-with-margins is the separating line. If $\mathcal{B}_1 = V_i$ and $\mathcal{B}_2 = U_j$, then the separating line contains the segments $(i-1, j)$ to (i, j) followed

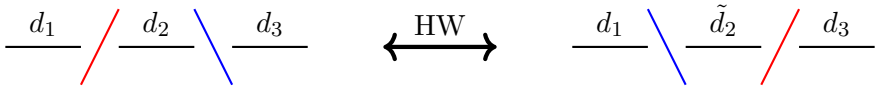

Figure 2.10: A local illustration of the Hanany-Witten transition.

by (i, j) to $(i, j+1)$. Upon performing the HW transition, these segments are replaced by $(i-1, j)$ to $(i-1, j+1)$ followed by $(i-1, j+1)$ to $(i, j+1)$. In fact, all $\binom{m+n}{m}$ possible separating lines are related by HW transition. This immediately extends the HW transition to BCTs, and hence tie diagrams. Since one of the entries of the BCT moves to the other side of the separating line, all ties are preserved except those joining B_1 and B_2. If there was such a tie to begin with, then it is removed. Otherwise, a new tie is created.

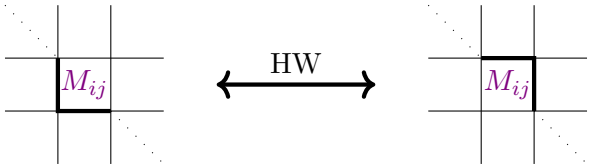

Figure 2.11: A local illustration of the action of a Hanany-Witten transition on the separating line.

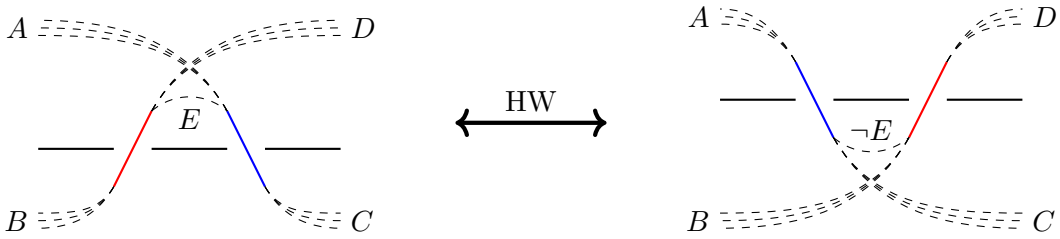

Figure 2.12: A local illustration of the action of a Hanany-Witten transition on a tie diagram. The symbols $E, \neg E$ mean that if tie E is part of the diagram, then tie $\neg E$ is not and vice versa.

Remark 2.4.1. It is tempting to consider the analogous transitions interchanging two 5-branes of the same type in such a way that their brane charges do not change, that is,

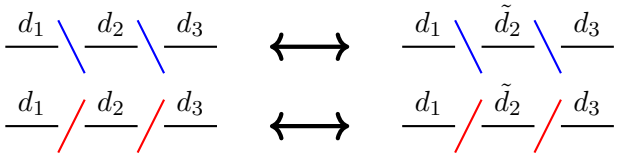

for $d_2 + \tilde{d}_2 = d_1 + d_3$.

In fact, these transitions make sense and are important in physics, but not for our purposes, until Section 4.5.

Example 2.4.2. We will illustrate the HW transition by using them to transform the tie diagram of Figure 2.1.2 (1) into two forms (the cobalanced and separated forms), which will be discussed in Section 2.5, 2.6. We will begin by moving V_1 to the far left. This is accomplished by a sequence of two HW transitions

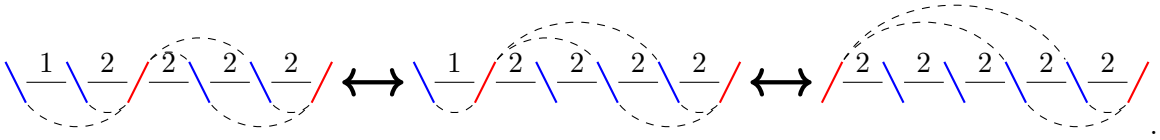

The resulting brane diagram has the property that for each D5 brane U, we have $d_{U^+} = d_{U^-}$. Such a brane diagram is called "cobalanced" (see Section 2.5).

Next, we will move V_2 into the second position, so that both NS5 branes are on the far left. Rather than performing the HW transitions on tie diagrams, we will manipulate BCTs and recover the tie diagrams using Proposition 2.2.8, 2.2.11. Moving all NS5 branes to the left results in a separating line that runs along the left and bottom side of the BCT. Hence, from the BCT in Figure 2.8 (1), we obtain the HW equivalent BCT and tie diagram

		U_1	U_2	U_3	U_4
		1	1	1	1
V_1	2	0	0	1	1
V_2	2	1	1	0	0

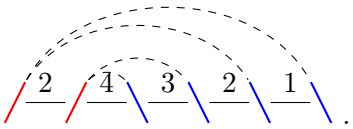

Brane diagrams with all NS5 branes on the left side are called "separated" (see Section 2.6).

2.5 (Co)balanced Brane Diagrams

A brane diagram is called *balanced* if for all NS5 branes V, we have $d_{V^+} = d_{V^-}$. A brane diagram is called *cobalanced* if for all D5 branes U we have $d_{U^+} = d_{U^-}$. In other words, cobalanced brane diagrams are those whose duals are balanced and vice versa. Cobalanced brane diagrams will be of special importance (see Section 3.3). It is possible that a brane diagram that is not cobalanced is HW equivalent to one that is. For instance, see Example 2.4.2. We will establish a numerical criterion for a brane diagram being HW equivalent to a cobalanced one.

Theorem 2.5.1. *A brane diagram is Hanany-Witten equivalent to a cobalanced brane diagram if and only if the margin vector c is weakly decreasing.*

Proof. In a cobalanced brane diagram, for all D5 branes U, we have

$$\text{charge}(U) = d_{U^+} - d_{U^-} + \#\{\text{NS5 branes right of } U\} = \#\{\text{NS5 branes right of } U\}.$$

It follows that c is weakly decreasing. Since c is preserved by HW transitions, all HW equivalent brane diagrams have weakly decreasing c as well.

Conversely, if a brane diagram with weakly decreasing margin vector c is given, then we may apply HW transitions to obtain the separating line illustrated by the picture

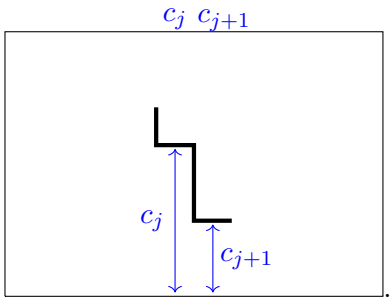

This separating line is well-defined by Lemma 2.2.5. Fix a BCT. By Proposition 2.2.11, it suffices to show that for $j = 1, ..., n$,

$$\#\{\text{1's NE of } P_j^-\} + \#\{\text{0's SW of } P_j^-\} = \#\{\text{1's NE of } P_j^+\} + \#\{\text{0's SW of } P_j^+\}$$

where P_j^- is the left endpoint of the horizontal step of the separating line across column j and P^+ is the right endpoint. From the shape of the separating line, we see that

$$\begin{aligned}
\#\{\text{1's NE of } P_j^-\} - \#\{\text{1's NE of } P_j^+\} &= \#\{\text{1's in the first } m - c_j \text{ entries of column } j\}, \\
\#\{\text{0's SW of } P_j^-\} - \#\{\text{0's SW of } P_j^+\} &= -\#\{\text{0's in the last } c_j \text{ entries of column } j\} \\
&= \#\{\text{1's in the last } c_j \text{ entries of column } j\} - c_j.
\end{aligned}$$

Adding these two expressions together yields $\#\{\text{1's in column } j\} - c_j = 0$, as required. □

By dualizing, we immediately obtain a numerical criterion for a brane diagram being HW equivalent to a balanced brane diagram from Theorem 2.5.1 and Proposition 2.3.1.

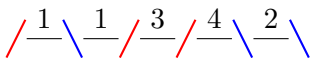

$r = (1, 3, 2)$
$c = (2, 2, 2)$

(a)

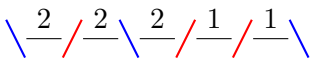

$r = (1, 1, 2)$
$c = (1, 2, 1)$

(b)

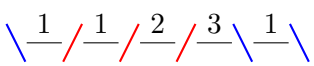

$r = (1, 2, 2)$
$c = (2, 2, 1)$

(c)

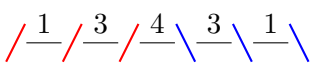

$r = (1, 2, 1)$
$c = (1, 2, 1)$

(d)

Figure 2.13: A brane diagram that is Hanany-Witten equivalent to (a) a cobalanced brane diagram but not a balanced brane diagram, (b) a balanced brane diagram but not a cobalanced brane diagram, (c) both a balanced brane diagram and a cobalanced brane diagram, and (d) neither a balanced nor a cobalanced brane diagram.

Corollary 2.5.2. *A brane diagram is balanced if and only if the margin vector r is weakly increasing.*

It is possible for brane diagrams to be HW equivalent to cobalanced brane diagrams but not balanced, balanced but not cobalanced, both balanced and cobalanced, or neither. Some simple examples are given in Figure 2.13. Of course, the only brane diagrams which are simultaneously balanced and cobalanced are those with all D3 multiplicities equal to 0.

2.6 Separated Brane Diagrams

A brane diagram is called *separated* if all NS5 branes are on the left and all D5 branes are on the right. In terms of table-with-margins, the separating line runs along the left and bottom sides. Separated brane diagrams offer some advantages when studying invariant curves and characteristic classes, which will be discussed in Section 3.4, 4.4.3.

First, we note that all HW equivalence classes of brane diagrams have a unique separated representative. Moreover, the D3 multiplicites can be related to the entries of the margin vectors r, c as an immediate consequence of Proposition 2.2.11.

Proposition 2.6.1. *The unique separated representative of the HW equivalence class of a brane*

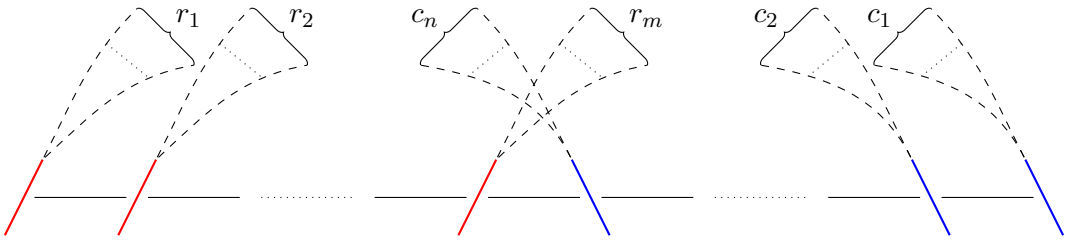

Figure 2.14: The general form of a separated tie diagram.

diagram $\mathcal{D}$ *with margin vectors* $r \in \mathbb{Z}^m, c \in \mathbb{Z}^n$ *is*

$$/r_1/r_1 + r_2/\cdots/r_1 + \cdots + r_m = c_1 + \cdots + c_n\backslash c_1 + \cdots + c_{n-1}\backslash\cdots\backslash c_1\backslash.$$

Consider a tie diagram $\mathcal{D}$ with m NS5 branes and n D5 branes. Fix a D5 brane U. Since there are no NS5 branes to the right of U, all ties attached to U must go to the left. It follows that the d_{U^+} ties covering U^+ must also cover U^-. Therefore, $d_{U^-} \geq d_{U^+}$ and there are $d_{U^-} - d_{U^+}$ ties attached to U going to the left. A symmetric argument shows that $d_{V^+} \geq d_{V^-}$ and there are $d_{V^+} - d_{V^-}$ ties attached to V going to the right for all NS5 branes V.

Create a partite set of m vertices corresponding to the NS5 branes and a partite set of size n vertices corresponding to the D5 branes. Then, each tie diagram can be realized as a bipartite graph where r and c are the sequences of degrees for the partite sets. Studying bipartite graphs with specified degree sequences is a useful approach to BCTs in general [G]. Given a bipartite graph with partite sets of size m and n, the adjacency matrix has the block structure

$$\begin{pmatrix} 0_m & M \\ M^T & 0_n \end{pmatrix},$$

where M is a BCT with margins equal to the degree sequences of the partite sets. When the bipartite graph comes from a separated brane diagram, this matrix M is precisely the matrix described in Section 2.2.

CHAPTER 3

Geometry

Cherkis bow varieties are torus equivariant holomorphic symplectic manifolds associated to brane diagrams. This chapter connects the geometry of bow varieties with the combinatorics of Chapter 2. In particular, we will see that tie diagrams correspond to torus fixed points and Hanany-Witten transitions correspond to certain natural isomorphisms of bow varieties.

3.1 The Nakajima-Takayama Quiver Description of Bow Varieties

In this section, we recount the so called "quiver description" of bow varieties of [NT, Section 2.2]. For our purposes, we will only need a special case of the [NT] construction. The exposition in this section is adapted to this special case. For comparisons between our special case and the more general construction, see Appendix A.

Remark 3.1.1. Readers familiar with [NT] can use this picture

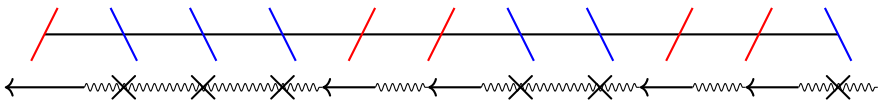

for comparison between diagrams of this paper (top) and diagrams of [NT] (bottom).

3.1.1 Bow Varieties

Fix a brane diagram $\mathcal{D}$. The first step is to associate a vector space to each brane of $\mathcal{D}$.

- For each segment X, let $W_X = \mathbb{C}^{d_X}$, and define

$$\mathbb{N}_X = \mathrm{End}(W_X), \qquad \text{illustrated by } \circlearrowright W_X \ .$$

- For each D5 brane U, let $\mathbb{C}_U = \mathbb{C}$, and define the "triangle part"

$$\begin{aligned}\mathbb{M}_U =& \mathrm{Hom}(W_{U+}, W_{U-}) \oplus \mathrm{Hom}(W_{U+}, \mathbb{C}_U) \oplus \mathrm{Hom}(\mathbb{C}_U, W_{U-}) \\ &\oplus \mathrm{End}(W_{U-}) \oplus \mathrm{End}(W_{U+}),\end{aligned}$$

  whose elements will be denoted by $(A_U, B_U, B'_U, a_U, b_U)$, as shown in the diagram

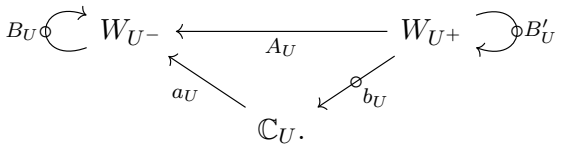

  Moreover, define a space

$$\mathbb{N}_U = \mathrm{Hom}(W_{U+}, W_{U-}), \qquad \text{illustrated by} \quad W_{U-} \longleftarrow\!\circ\!\!- W_{U+}.$$

- For each NS5 brane, define the "two-way part"

$$\mathbb{M}_V = \mathrm{Hom}(W_{V+}, W_{V-}) \oplus \mathrm{Hom}(W_{V-}, W_{V+}),$$

  whose elements will be denoted by (C_V, D_V), as shown in the diagram

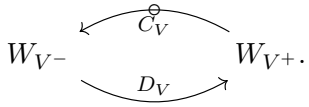

The significance of the circles in the diagrams will be explained in Section 3.1.2. Ignore them for now. Finally, define

$$\mathbb{M} = \bigoplus_{U \text{ D5}} \mathbb{M}_U \oplus \bigoplus_{V \text{ NS5}} \mathbb{M}_V \quad , \quad \mathbb{N} = \bigoplus_{U \text{ D5}} \mathbb{N}_U \oplus \bigoplus_{X \text{ D3}} \mathbb{N}_X.$$

Next, we define the "moment map" $\mu : \mathbb{M} \to \mathbb{N}$. The moment map will split as a sum of maps $\mu = \mu_1 + \mu_2$ where

$$\mu_1 : \mathbb{M} \to \bigoplus_{U \text{ D5}} \mathbb{N}_U \quad , \quad \mu_2 : \mathbb{M} \to \bigoplus_{X \text{ D3}} \mathbb{N}_X.$$

The definition of μ_1, μ_2 is component-wise:

1. For each D5 brane U, the $\mathbb{N}_U$ component of μ_1 is $B_U A_U - A_U B'_U + a_U b_U$.

2. For each segment X, the $\mathbb{N}_X$ component of μ_2 is

   - $B'_{X^-} - B_{X^+}$ if X is in between two D5 branes ($\backslash - X - \backslash$),
   - $C_{X^+} D_{X^+} - D_{X^-} C_{X^-}$ if X is in between two NS5 branes ($/ - X - /$),
   - $-D_{X^-} C_{X^-} - B_{X^+}$ if X^- is an NS5 brane and X^+ is a D5 brane ($/ - X - \backslash$),
   - $C_{X^+} D_{X^+} + B'_{X^-}$ if X^- is a D5 brane and X^+ is an NS5 brane ($\backslash - X - /$).

Consider the 0-momentum set $\mu^{-1}(0)$. Note that we do not need the full data of $\mathbb{M}$ to specify an element of $\mu^{-1}(0)$. Namely, the $\mu_2 = 0$ condition implies that if a D3 brane X is between two D5 branes, then $B'_{X^-} = B_{X^+}$. By convention, we will associate the B maps to D3 branes X with a neighboring D5 brane, so that $B_X \in \mathrm{End}(W_X)$, and only distinguish between B_U and B'_U when necessary. If X has a neighboring NS5 brane, then the $\mu_2 = 0$ condition also allows us to rewrite B_X in terms of C and D maps.

Next, two "stability conditions", (S1) and (S2), on $\mu^{-1}(0)$ will be introduced.

(S1) For all D5 branes U, the only B_{U^+}-invariant subspace $S \subset W_{U^+}$ with $A_U(S) = 0, b_U(S) = 0$ is $S = 0$.

(S2) For all D5 branes U, the only B_{U^-}-invariant subspace $T \subset W_{U^-}$ with $\mathrm{im}(A_U) + \mathrm{im}(a_U) \subset T$ is $T = W_{U^-}$.

Let $\widetilde{\mathcal{M}}$ be the open subset of $\mu^{-1}(0)$ consisting of elements satisfying (S1) and (S2).

There is a natural action of $\mathcal{G} = \prod_{X\ \mathrm{D3}} \mathrm{GL}(W_X)$ on $\mathbb{M}$ and $\mathbb{N}$ by conjugation. Indeed, $\mathcal{G}$ acts on $\mathrm{Hom}(W_X, W_{X'})$ by $(g_X)_X.\phi = g_{X'} \phi g_X^{-1}$, and $\mathbb{M}$ and $\mathbb{N}$ are direct sums of such spaces. It is clear that the moment map μ is equivariant with respect to this action, and the (S1) and (S2) stability conditions are invariant under this action, so there is an induced action of $\mathcal{G}$ on $\mu^{-1}(0)$ and $\widetilde{\mathcal{M}}$. Define a character

$$\chi : \mathcal{G} \to \mathbb{C}^\times \quad , \quad (g_X)_X \mapsto \prod_{X'} \det(g_{X'}),$$

where the product runs over all segments X' where X'^- is an NS5 brane. The *bow variety* corresponding to $\mathcal{D}$ is the GIT quotient $\mathcal{M}_{\text{quiver}} = \widetilde{\mathcal{M}}^{ss}//_\chi \mathcal{G}$. We will be interested in only the smooth locus, which is identified with $\widetilde{\mathcal{M}}^s/\mathcal{G}$.

Definition 3.1.2. Given a brane diagram $\mathcal{D}$, let

$$\mathcal{C}(\mathcal{D}) = \widetilde{\mathcal{M}}^s/\mathcal{G}.$$

Remark 3.1.3. From general GIT considerations, we know only that $\widetilde{\mathcal{M}}^s$ has finite stabilizers. Hence, $\widetilde{\mathcal{M}}^s/\mathcal{G}$ may have orbifold singularities. In the case of bow varieties, however, all stabilizers are trivial, and $\widetilde{\mathcal{M}}^s/\mathcal{G}$ is smooth [NT, Lemma 2.10].

As stated, the definition of $\mathcal{C}(\mathcal{D})$ is rather technical, due to the technical nature of GIT stability. We will instead appeal to a much more natural notion of stability. Let $\mathbb{W} = \bigoplus_X W_X$ and define the (ν) stability condition:

(ν) The only subset $T = \bigoplus_X T_X \subset \mathbb{W}$ invariant under all A, B, C, D maps such that $\text{im}(a_U) \subset T$ and A_U induces an isomorphism $W_{U^+}/T_{U^+} \to W_{U^-}/T_{U^-}$ for all D5 branes U is $T = \mathbb{W}$.

Lemma 3.1.4. *The stable locus $\widetilde{\mathcal{M}}^s$ is the open subset of $\widetilde{\mathcal{M}}$ consisting of elements satisfying (ν).*

Proof. This is a special case of [NT, Proposition 2.8]. □

Example 3.1.5 (an empty bow variety and a bow variety with a single point). Consider the brane diagram \2/ from Figure 2.4. Note that Assumption 2.2.10 is not satisfied. The space $\mu^{-1}(0)$ is illustrated by the diagram

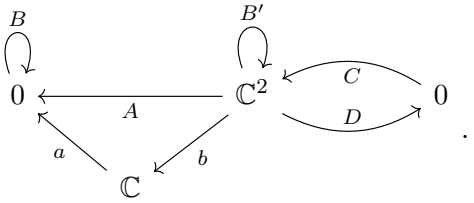

Since $B' = CD$, we have $B' = 0$. It follows that all subspaces of $\mathbb{C}^2$ are B'-invariant. In particular, $\ker(b)$ is B'-invariant, and $A(\ker(b)) = 0, b(\ker(b)) = 0$. In order for (S1) to hold, $\ker(b)$ must vanish. This is impossible, so $\mathcal{C}(\backslash 2/) = \emptyset$.

Next, consider the brane diagram \1/. By the argument above, b must be an isomorphism in order for (S1) to be satisfied. In this case, the (S2) and (ν) conditions are trivially satisfied. It follows $\widetilde{\mathcal{M}}^s$ is obtained by taking b to be all possible isomorphisms and all other maps to be 0. All such isomorphisms are related by the $\mathcal{G}$-action, so $\mathcal{C}(\backslash 1/) = \{\text{pt}\}$.

Example 3.1.6 (another degenerate example). In Example 3.1.5, we saw that a brane diagram not satisfying Assumption 2.2.10 gave rise to an empty bow variety. This need not be the case. Consider $\mathcal{C}(\backslash 1\backslash)$. This bow variety is illustrated by the diagram

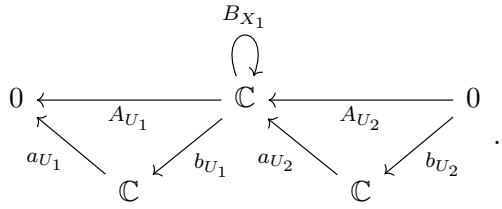

The (S1) and (S2) conditions force a_{U_2} and b_{U_1} to be isomorphisms. In this case, the (ν) condition is automatically satisfied. There are no additional constraints on $B_{X_1}, b_{U_1}, a_{U_2}$. Hence, $\widetilde{\mathcal{M}}^s = \mathbb{C} \times \mathbb{C}^\times \times \mathbb{C}^\times$, with $\mathcal{G} = \mathbb{C}^\times$ acting by

$$g.(z_1, z_2, z_3) = (z_1, g^{-1}z_2, gz_3).$$

The quotient space is isomorphic to $\mathbb{C} \times \mathbb{C}^\times$ via $(z_1, z_2, z_3) \mapsto (z_1, z_2 z_3^{-1})$. Therefore, we have $\mathcal{C}(\backslash 1\backslash) = \mathbb{C} \times \mathbb{C}^\times$. The action of $\mathbb{T} = \mathbb{C}^\times \times \mathbb{C}^\times$ is given by

$$(u_1, u_2).(\zeta_1, \zeta_2) = (\zeta_1, u_1 u_2 \zeta_2).$$

Example 3.1.7 ($T^*\mathbb{P}^1$). Consider the brane diagram $\mathcal{D} = /1\backslash 1\backslash 1/$. The space $\mu^{-1}(0)$ is illustrated by the diagram

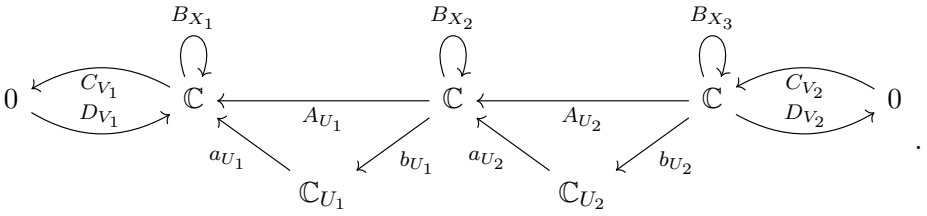

Note that $B_{X_1} = 0, B_{X_3} = 0$. We would like to describe $\widetilde{\mathcal{M}}$. Suppose $A_{U_2} = 0$. Then, the 0-momentum condition implies $a_{U_2} b_{U_2} = 0$. It follows that $a_{U_2} = 0$ or $b_{U_2} = 0$. The former would violate (S2), and the latter (S1). Therefore, A_{U_2} is an isomorphism. The same argument can be used to show that A_{U_1} must be an isomorphism as well. We now know that a_{U_1} and a_{U_2} cannot both vanish, for if they did, the 0 subspace would violate the (ν) condition. Finally, the 0-momentum condition gives us the relation

$$A_{U_1}^{-1} a_{U_1} b_{U_1} = B_{X_2} = -a_{U_2} b_{U_2} A_{U_2}^{-1}. \tag{3.1}$$

By identifying W_{X_1} and W_{X_3} with W_{X_2} via isomorphisms A_{U_1} and A_{U_2}, we may realize $\widetilde{\mathcal{M}}$ as the space illustrated by the diagram

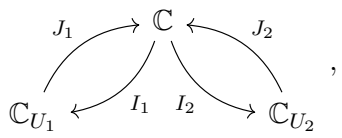

,

where $I_1 = b_{U_1}, I_2 = b_{U_2} A_{U_2}^{-1}, J_1 = A_{U_1}^{-1} a_{U_1}, J_2 = a_{U_2}$. The relation (3.1) can be rephrased as $J_1 I_1 + J_2 I_2 = 0$. The (ν) condition is equivalent to $\mathrm{im}(J_1) + \mathrm{im}(J_2) = \mathbb{C}$. The group $\mathcal{G}$ acts by change of basis at $\mathbb{C}$. Readers familiar with Nakajima quiver varieties [N1] will recognize the quotient of this space by the action of $\mathcal{G}$ as the quiver variety description of $T^*\mathbb{P}^1$. For completeness, we will now show the explicit identification $\mathcal{C}(\mathcal{D}) \cong T^*\mathbb{P}^1$.

Let $I : \mathbb{C} \to \mathbb{C}_{U_1} \oplus \mathbb{C}_{U_2} = \mathbb{C}^2, J : \mathbb{C}^2 = \mathbb{C}_{U_1} \oplus \mathbb{C}_{U_2} \to \mathbb{C}$ be defined by $I = I_1 + I_2, J = J_1 + J_2$. The space $\widetilde{\mathcal{M}}$ consists of pairs of maps $I : \mathbb{C} \to \mathbb{C}^2, J : \mathbb{C}^2 \to \mathbb{C}$ such that J is surjective and $JI = 0$. Taking duals, this space is isomorphic to the space of pairs of maps $I^\vee : \mathbb{C}^2 \to \mathbb{C}, J^\vee : \mathbb{C} \to \mathbb{C}^2$ such that $J^\vee$ is injective and $I^\vee J^\vee = 0$. It follows that $I^\vee$ induces a map $\mathbb{C}^2/\mathrm{im}(J^\vee) \to \mathbb{C}$. After quotienting by the action of $\mathcal{G}$, we obtain $\mathcal{C}(\mathcal{D}) = \mathrm{Hom}(Q, S)$, where $S \to \mathbb{P}^1$ is the tautological bundle and $Q = (\mathbb{P}^1 \times \mathbb{C}^2)/S$ is the quotient of the trivial rank 2 bundle by the tautological bundle. This is precisely the classical description of $T^*\mathbb{P}^1$.

All Nakajima quiver varieties appear as special cases of bow varieties. See Section 3.3 for details. In Example 3.1.7, we showed that the A maps were isomorphisms. In general, we have

Lemma 3.1.8 ([T, Lemma 2.18])**.** *For any element* $(A, B, B', a, b, C, D) \in \mu_1^{-1}(0)$ *satisfying (S1)*

and (S2), A_U has full rank for all D5 branes U.

3.1.2 Additional Structures

In this section, we will endow the bow variety $\mathcal{C}(\mathcal{D})$ with the following additional structures:

- a holomorphic symplectic form,
- tautological vector bundles $\xi_X \to \mathcal{C}(\mathcal{D})$,
- a symplectic action of an n-dimensional torus $\mathbb{A}$,
- an additional (non-symplectic) action of $\mathbb{C}^\times$.

Let $\widetilde{\mathcal{M}}_{\text{sym}}$ denote the open subset of $\mu_1^{-1}(0)$ satisfying (S1) and (S2). This space can be thought of as being similar to $\widetilde{\mathcal{M}}$ except we treat each triangle part and two-way part as being disjoint. Namely, there is no identification of B maps coming from adjacent triangle parts, and the C, D maps of two-way parts are uncoupled from the B maps of any adjacent triangle parts. The space $\widetilde{\mathcal{M}}_{\text{sym}}$ is a holomorphic symplectic manifold, and μ_2 is a moment map for the action of $\mathcal{G}$ [NT, Section 3]. It follows that $\mathcal{C}(\mathcal{D})$ is a symplectic reduction, and hence carries a symplectic structure. While it is important for theoretical reasons that $\mathcal{C}(\mathcal{D})$ carries a symplectic structure, the specifics of this structure are not important for our purposes. We refer the reader to [NT, Section 3, 5] for details.

The quotient map $\widetilde{\mathcal{M}}^s \to \widetilde{\mathcal{M}}^s/\mathcal{G} = \mathcal{C}(\mathcal{D})$ is a principle $\mathcal{G}$-bundle. Hence, for each D3 brane X, there is a vector bundle

$$\xi_X = \widetilde{\mathcal{M}}^s \times_{\mathcal{G}} W_X \to \mathcal{C}(\mathcal{D}),$$

associated with the standard action of $\mathcal{G}$ on W_X, given by $(g_{X'})_{X'}.w = g_X w$. These bundles are called the *tautological bundles* of $\mathcal{C}(\mathcal{D})$.

Define an n-dimensional torus $\mathbb{A} = \prod_{U \text{ D5}} \mathbb{C}_U^\times$. Denote the coordinate of $\mathbb{C}_U^\times$ by $\mathbf{u}$. An element $(\mathbf{u}') \in \mathbb{A}$ acts on $\mathbb{M}$ by sending

$$a_U \mapsto {\mathbf{u}'}^{-1} a_U \quad , \quad b_U \mapsto \mathbf{u}' b_U \quad \text{for all D5 branes } U$$

and leaving all other maps fixed. In other words, the action of $\mathbb{T}$ is the natural extension of the $\mathcal{G}$-action that involves the spaces $\mathbb{C}_U$ as well. Let the 1-dimensional torus $\mathbb{C}_\hbar^\times$ with coordinate $\mathbf{h}$ act

on $\mathbb{M}$ by sending

$$b_U \mapsto \mathbf{h} b_U \quad , \quad B_U \mapsto \mathbf{h} B_U \quad , \quad B'_U \mapsto \mathbf{h} B'_U \quad , \quad C_V \mapsto \mathbf{h} C_V \quad \text{for all D5 branes } U, \text{ NS5 branes } V$$

and leaving all other maps fixed. The circles in the diagrams of Section 3.1.1 denote the action of $\mathbb{C}^\times_\hbar$. There is also an action of $\mathbb{C}^\times_\hbar$ on $\mathbb{N}$ by scaling. Let $\mathbb{T} = \mathbb{A} \times \mathbb{C}^\times_\hbar$.

Lemma 3.1.9. *The map $\mu : \mathbb{M} \to \mathbb{N}$ is $\mathbb{T}$-equivariant. The stability conditions (S1), (S2), (ν) are preserved by the action of $\mathbb{T}$ on $\mu^{-1}(0)$.*

Proof. The only contribution of a_U, b_U to μ is the $\mathbb{N}_U$ component $B_U A_U - A_U B'_U + a_U b_U$. The action of $\mathbb{A}$ on a_U cancels the action of $\mathbb{A}$ on b_U, proving $\mathbb{A}$-equivariance. For $\mathbb{C}^\times_\hbar$-equivariance, it is easy to verify that the $\mathbb{C}^\times_\hbar$ action scales each component of μ. For instance, acting on the $\mathbb{N}_U$ component yields

$$(\mathbf{h} B_U) A_U - A_U (\mathbf{h} B'_U) + a_U (\mathbf{h} b_U) = \mathbf{h}(B_U A_U - A_U B'_U + a_U b_U).$$

It follows that μ is T-equivariant. The three stability conditions are clearly insensitive to scaling of the maps. □

The action of the torus $\mathbb{T}$ descends to the quotient $\mathcal{C}(\mathcal{D})$. The action of $\mathbb{A}$ preserves the symplectic form, while the action of $\mathbb{C}^\times_\hbar$ does not. There is also an induced action on the tautological bundles ξ_X. We will denote the characters (multiplicative) of $\mathbb{T}$ by $\mathbf{u}, \mathbf{h}$, as above. The weights (additive) will be denoted by $u, \hbar$ (i.e. $\mathbf{u} = \exp(u), \mathbf{h} = \exp(\hbar)$).

Remark 3.1.10. This action of $\mathbb{C}^\times_\hbar$ differs from that of [NT]. Our $\mathbb{T}$-action, however, agrees with that of [NT] up to a reparametrization of $\mathbb{T}$. See Appendix A for details.

3.1.3 The Tangent Bundle

In this section, we will give a formula for the $\mathbb{T}$-equivariant K-theory class of the tangent bundle of a bow variety in terms of tautological bundles. Let $\mathbf{h} \in K^0_\mathbb{T}(\mathcal{C}(\mathcal{D}))$ also denote the class of the trivial line bundle on $\mathcal{C}(\mathcal{D})$ whose fibres are acted upon by $\mathbb{T}$ with character $\mathbf{h}$. For a D5 brane U, let $\mathbf{u} \in K^0_\mathbb{T}(\mathcal{C}(\mathcal{D}))$ also denote the class of the trivial line bundle with fibre acted upon by $\mathbf{u}$. We will first find the tangent space $T_p \widetilde{\mathcal{M}}^s$ at a point $p \in \widetilde{\mathcal{M}}^s$ by analyzing the differential of μ.

Throughout this section, we will be identifying the tangent spaces of vector spaces with the vector spaces themselves. For notational clarity, elements of the base vector space will be underlined.

Lemma 3.1.11 ([NT, Section 2.5]). *Let $p = (\underline{A}, \underline{B}, \underline{B}', \underline{a}, \underline{b}, \underline{C}, \underline{D}) \in \mathbb{M}$, and consider the differentials $\mu_{1*,p} : \mathbb{M} \to \bigoplus_{U\ D5} \mathbb{N}_U$, $\mu_{2*,p} : \mathbb{M} \to \bigoplus_{X\ D3} \mathbb{N}_X$. Then, we have*

$$\begin{aligned}\mu_{1*,p}(A, B, B', a, b, C, D) &= \underline{B}A + B\underline{A} - \underline{A}B' - A\underline{B'} + \underline{a}b + a\underline{b},\\ \mu_{2*,p}(A, B, B', a, b, C, D) &= \sum_{X\ D3} \mu_{*,p,X}(A, B, B', a, b, C, D),\end{aligned}$$

where

$$\mu_{*,p,X}(A, B, B', a, b, C, D) = \begin{cases} B'_{X^-} - B_{X^+} & \text{if } \mathcal{D} = \cdots \backslash - X - \backslash \cdots, \\ \underline{C}_{X^+} D_{X^+} + C_{X^+} \underline{D}_{X^+} & \\ \qquad - \underline{D}_{X^-} C_{X^+} - D_{X^-} \underline{C}_{X^+} & \text{if } \mathcal{D} = \cdots / - X - / \cdots, \\ -\underline{D}_{X^-} C_{X^+} - D_{X^-} \underline{C}_{X^+} - B_{X^+} & \text{if } \mathcal{D} = \cdots / - X - \backslash \cdots, \\ \underline{C}_{X^+} D_{X^+} + C_{X^+} \underline{D}_{X^+} + B'_{X^-} & \text{if } \mathcal{D} = \cdots \backslash - X - / \cdots. \end{cases}$$

Proof. The formulas are straightforward calculations of derivatives. For example,

$$\begin{aligned}\mu_{1*,p}(A, B, B', a, b, C, D) &= \frac{d}{dt} \mu_1(p + t(A, B, B', a, b, C, D))|_{t=0}\\ &= \frac{d}{dt} \left((\underline{B} + tB)(\underline{A} + tA) - (\underline{A} + tA)(\underline{B} + tB) + (\underline{a} + ta)(\underline{b} + tb)\right)|_{t=0}\\ &= \underline{B}A + B\underline{A} - \underline{A}B' - A\underline{B'} + \underline{a}b + a\underline{b},\end{aligned}$$

where the last equality is obtained by expanding in powers of t and extracting the linear term. □

The kernel of $\mu_{*,p}$ is precisely the tangent space $T_p\mu^{-1}(0)$ whenever $p \in \mu^{-1}(0)$. Since the stability conditions are open conditions, if additionally $p \in \widetilde{\mathcal{M}}^s$, then $T_p\widetilde{\mathcal{M}}^s = \ker(\mu_{*,p})$ as well.

Next, we obtain $T_p\mathcal{C}(\mathcal{D})$ by quotienting out those vectors in $T_p\widetilde{\mathcal{M}}^s$ that are tangent to the $\mathcal{G}$-orbit through p. This can be accomplished by analyzing the infinitesimal vector field induced by the action of $\mathcal{G}$. Namely, given $\gamma = (\gamma_X)_X \in \mathrm{Lie}(\mathcal{G}) = \bigoplus_{X\ \mathrm{D3}} \mathrm{End}(W_X)$, the induced infinitesimal

vector field $\gamma^\sharp$ on $\widetilde{\mathcal{M}}^s$ is given by

$$\gamma_p^\sharp = \frac{d}{dt}\exp(t\gamma).p|_{t=0}.$$

Lemma 3.1.12 ([NT, Section 2.5]). *Let $\mu_p^* : \bigoplus_{X\ D3}\mathrm{End}(W_X) \to T_p\widetilde{\mathcal{M}}^s \subset \mathbb{M}$ be the "comoment" map $\gamma \mapsto \gamma_p^\sharp$. Then, we have*

$$\mu_p^*(\gamma) = ([\gamma,\underline{A}],[\gamma,\underline{B}],[\gamma,\underline{B'}],[\gamma,\underline{a}],[\gamma,\underline{b}],[\gamma,\underline{C}],[\gamma,\underline{D}]),$$

where the commutator brackets $[\gamma,*]$ are interpreted as $\gamma_X * - * \gamma_{X'}$ for suitable D3 branes X, X' depending on the map $*$ (e.g. $[\gamma,\underline{D}_V] = \gamma_{V^+}\underline{D}_V - \underline{D}_V\gamma_{V^-}$ and $[\gamma,A_U] = \gamma_{U^-}\underline{A}_U - \underline{A}_U\gamma_{U^+}$).

Proof. This is a straightforward calculation of derivatives. For instance, to find the A_U component of $\mu_p^*(\gamma)$, we calculate

$$\begin{aligned}\frac{d}{dt}\exp(t\gamma).\underline{A}_U|t=0 &= \frac{d}{dt}\exp(t\gamma_{U^-})\underline{A}_U\exp(-t\gamma_{U^+})|_{t=0}\\ &= \frac{d}{dt}(1+t\gamma_{U^-}+O(t^2))\underline{A}_U(1-t\gamma_{U^+}+O(t^2))|_{t=0}\\ &= \gamma_{U^-}\underline{A}_U - \underline{A}_U\gamma_{U^+},\end{aligned}$$

where the last equality is obtained by expanding in powers of t and extracting the linear term. □

Hence, the tangent space is given by $T_p\mathcal{C}(\mathcal{D}) = \ker(\mu_{*,p})/\mathrm{im}(\mu_p^*)$. The key properties of μ_* and μ^* are summarized by

Proposition 3.1.13 ([NT, Proposition 2.12]). *Let $p \in \widetilde{\mathcal{M}}^s$. Then,*

1. *μ_p^* is injective, and*
2. *$\mu_{*,p}$ is surjective.*

Consider the short exact sequences

(1) $0 \longrightarrow \bigoplus_{X\ \mathrm{D3}}\mathrm{End}(W_X) \xrightarrow{\mu_p^*} \ker(\mu_{*,p}) \longrightarrow T_p\mathcal{C}(\mathcal{D}) \longrightarrow 0$,

(2) $0 \longrightarrow \ker(\mu_{*,p}) \longrightarrow \mathbb{M} \xrightarrow{\mu_{*,p}} \mathbb{N} \longrightarrow 0$.

By varying $p \in \widetilde{\mathcal{M}}^s$, we may interpret (1) and (2) as sequences of trivial bundles over $\widetilde{\mathcal{M}}^s$

(1) $0 \longrightarrow \widetilde{\mathcal{M}}^s \times \bigoplus_{X \text{ D3}} \mathrm{End}(W_X) \xrightarrow{\mu^*} \ker(\mu_*) \longrightarrow \widetilde{T\mathcal{C}(\mathcal{D})} \longrightarrow 0$,

(2) $0 \longrightarrow \ker(\mu_*) \longrightarrow \widetilde{\mathcal{M}}^s \times \mathbb{M} \xrightarrow{\mu_*} \widetilde{\mathcal{M}}^s \times \mathbb{N} \longrightarrow 0$.

Moreover, these sequences are $\mathcal{G} \times \mathbb{T}$-equivariant. It follows that they descend to sequences of $\mathbb{T}$-equivariant bundles over $\mathcal{C}(\mathcal{D})$.

Definition 3.1.14. For each D5 brane U, define the bundle

$$T_U = \mathrm{Hom}(\xi_{U^+}, \xi_{U^-}) \oplus \mathbf{h}\mathrm{Hom}(\xi_{U^+}, \mathbb{C}_U) \oplus \mathrm{Hom}(\mathbb{C}_U, \xi_{U^-}) \oplus \mathbf{h}\mathrm{End}(\xi_{U^+}) \oplus \mathbf{h}\mathrm{End}(\xi_{U^-}),$$

and for each NS5 brane V, define the bundle

$$T_V = \mathbf{h}\mathrm{Hom}(\xi_{V^+}, \xi_{V^-}) \oplus \mathrm{Hom}(\xi_{V^-}, \xi_{V^+}).$$

We have the short exact sequences

(1) $0 \longrightarrow \bigoplus_{X \text{ D3}} \mathrm{End}(\xi_X) \xrightarrow{\mu^*} \ker(\mu_*) \longrightarrow T\mathcal{C}(\mathcal{D}) \longrightarrow 0$,

(2) $0 \longrightarrow \ker(\mu_*) \longrightarrow \bigoplus_{U \text{ D5}} T_U \oplus \bigoplus_{V \text{ NS5}} T_V$
$\xrightarrow{\mu_*} \bigoplus_{U \text{ D5}} \mathbf{h}\mathrm{Hom}(\xi_{U^+}, \xi_{U^-}) \oplus \bigoplus_{X \text{ D3}} \mathbf{h}\mathrm{End}(\xi_X) \longrightarrow 0$,

of $\mathbb{T}$-equivariant bundles over $\mathcal{C}(\mathcal{D})$. From (1) and (2), we obtain

Theorem 3.1.15. *The bow variety $\mathcal{C}(\mathcal{D})$ is a smooth holomorphic symplectic manifold of dimension*

$$\dim(\mathcal{C}(\mathcal{D})) = \sum_{U \ D5} ((d_{U^-} + 1)d_{U^-} + (d_{U^+} + 1)d_{U^+}) + 2 \sum_{V \ NS5} d_{V^+} d_{V^-} - 2 \sum_{X \ D3} d_X^2.$$

The tangent bundle of $\mathcal{C}(\mathcal{D})$ can be expressed as an element of $K^0_{\mathbb{T}}(\mathcal{C}(\mathcal{D}))$ in terms of the tautological bundles as

$$T\mathcal{C}(\mathcal{D}) = \bigoplus_{U \ D5} T_U \oplus \bigoplus_{V \ NS5} T_V \ominus \bigoplus_{U \ D5} \mathbf{h}\mathrm{Hom}(\xi_{U^+}, \xi_{U^-}) \ominus \bigoplus_{X \ D3} (1 + \mathbf{h})\mathrm{End}(\xi_X).$$

Remark 3.1.16. The phenomenon of negative signs in the formula for the tangent bundle also occurs in the formula $T\mathrm{Gr}(k, n) = \mathrm{Hom}(S, Q)$ for the Grassmannian. Here S is the rank k tautological

bundle, and $Q = (\mathrm{Gr}(k,n) \times \mathbb{C}^n)/S$ is the quotient of the trivial rank n bundle by the tautological bundle. If we wish to express the tangent bundle strictly in terms of the tautological and trivial bundles, we must use negative signs: $T\mathrm{Gr}(k,n) = \mathrm{Hom}(S, (\mathrm{Gr}(k,n) \times \mathbb{C}^n) \ominus S)$.

Example 3.1.17. In Example 3.1.5, we showed that $\mathcal{C}(\backslash 2/) = \emptyset$. Theorem 3.1.15 does not apply in this case, because the proof relies on the existence of a point $f \in \widetilde{\mathcal{M}}^s$. If we naively apply the dimension formula of Theorem 3.1.15 to this empty bow variety, we obtain

$$\dim(\mathcal{C}(\backslash 2/)) = (2+1)\cdot 2 - 2(2^2) = -2.$$

In fact, if this dimension formula returns a negative number, we know the bow variety must be empty.

We also showed that $\mathcal{C}(\backslash 1/) = \{\mathrm{pt}\}$. Indeed, according to Theorem 3.1.15,

$$\dim(\mathcal{C}(\backslash 1/)) = (1+1)\cdot 1 - 2(1^2) = 0.$$

Example 3.1.18. In Example 3.1.6, we showed that $\mathcal{C}(\backslash 1\backslash) = \mathbb{C} \times \mathbb{C}^\times$. Theorem 3.1.15 gives

$$\dim(\mathcal{C}(\backslash 1\backslash)) = (1+1)\cdot 1 + (1+1)\cdot 1 - 2(1^2+0^2+0^2) = 2,$$

as expected.

Example 3.1.19. Let $\mathcal{D} = /1\backslash 1\backslash 1/$. In Example 3.1.7, we showed that $\mathcal{C}(\mathcal{D}) = T^*\mathbb{P}^1$. From Theorem 3.1.15, we have

$$T\mathcal{C}(\mathcal{D}) = (1-\mathbf{h})\left(\frac{\xi_{X_1}}{\xi_{X_2}} + \frac{\xi_{X_2}}{\xi_{X_3}}\right) + \frac{\xi_{X_1}}{\mathbf{u}_1} + \frac{\mathbf{h}\mathbf{u}_1}{\xi_{X_2}} + \frac{\xi_{X_2}}{\mathbf{u}_2} + \frac{\mathbf{h}\mathbf{u}_2}{\xi_{X_3}} + \mathbf{h} - 3.$$

Moreover, we have

$$\dim(\mathcal{C}(\mathcal{D})) = (1+1)\cdot 1 + (1+1)\cdot 1 + (1+1)\cdot 1 + (1+1)\cdot 1 + 2(1\cdot 0 + 0\cdot 1) - 2(1^2+1^2+1^2) = 2,$$

as expected.

Example 3.1.20. Let $\mathcal{D}$ be the brane diagram $/2\backslash 2/2\backslash 4/3/3/4\backslash 3/2\backslash 2\backslash$ in Figure 2.2. Then, we

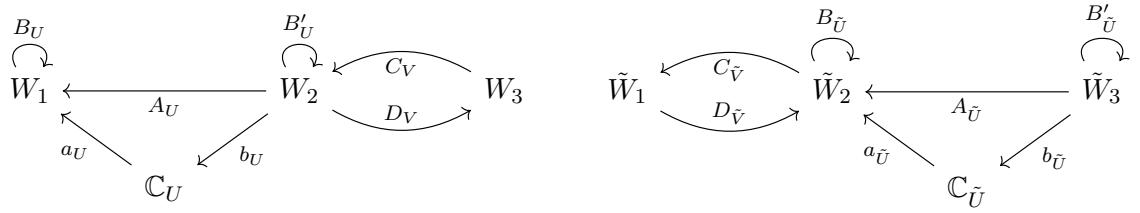

Figure 3.1: A local illustration of $\widetilde{\mathcal{M}}^s(\mathcal{D})$ (left) and $\widetilde{\mathcal{M}}^s(\tilde{\mathcal{D}})$ (right).

have $\dim(\mathcal{C}(\mathcal{D})) = 16$.

3.1.4 Hanany-Witten Transitions

In [NT, Section 7], a $\mathbb{T}$-equivariant isomorphism is constructed between the bow varieties associated to Hanany-Witten equivalent brane diagrams. We will give the construction of this isomorphism for completeness. Consider two brane diagrams $\mathcal{D}, \tilde{\mathcal{D}}$ that differ locally as shown in the diagram

where $\tilde{d}_2 = d_1 + d_3 + 1 - d_2$. Denote the tautological bundles over $\mathcal{C}(\mathcal{D})$ and $\mathcal{C}(\tilde{\mathcal{D}})$ corresponding to the displayed segments by ξ_1, ξ_2, ξ_3 and $\tilde{\xi}_1, \tilde{\xi}_2, \tilde{\xi}_3$. Recall that the tori

$$\mathbb{T} = \prod_{U \text{ D5 in } \mathcal{D}} \mathbb{C}_U^\times \quad \text{and} \quad \tilde{\mathbb{T}} = \prod_{\tilde{U} \text{ D5 in } \tilde{\mathcal{D}}} \mathbb{C}_{\tilde{U}}^\times$$

act on $\mathcal{C}(\mathcal{D})$ and $\mathcal{C}(\tilde{\mathcal{D}})$ respectively. Define a homomorphism $\rho : \mathbb{T} \to \tilde{\mathbb{T}}$ by mapping

$$\mathbb{C}_U^\times \times \mathbb{C}_\hbar^\times \to \mathbb{C}_{\tilde{U}}^\times \times \mathbb{C}_\hbar^\times \quad \text{by} \quad (\mathbf{u}, \mathbf{h}) \mapsto (\mathbf{uh}, \mathbf{h}),$$

and leaving all other components fixed. We will now construct a ρ-equivariant homomorphism $\mathcal{C}(\mathcal{D}) \to \mathcal{C}(\tilde{\mathcal{D}})$.

Fix $p = (A, B, B', a, b, C, D) \in \widetilde{\mathcal{M}}^s(\tilde{\mathcal{D}})$. Our goal is to specify an element $\tilde{p} \in \widetilde{\mathcal{M}}^s(\tilde{\mathcal{D}})$ Let $W_1 = W_{X^=}, W_2 = W_X, W_3 = W_{X^\ddagger}$, and define $\tilde{W}_1, \tilde{W}_2, \tilde{W}_3$ analogously for $\tilde{\mathcal{D}}$. Define a map

$\alpha : W_2 \to W_1 \oplus W_3 \oplus \mathbb{C}_U$ by

$$\alpha = \begin{pmatrix} A_U \\ D_V \\ b_U \end{pmatrix}.$$

Define a map $\beta : W_1 \oplus W_3 \oplus \mathbb{C}_U \to W_1$ by

$$\beta = (B_U, A_U C_V, a_U).$$

One can check that α is injective and $\beta\alpha = 0$. Make identifications $\tilde{W}_1 = W_1, \tilde{W}_2 = \mathrm{coker}(\alpha), \tilde{W}_3 = W_3, \mathbb{C}_U = \mathbb{C}_{\tilde{U}}$, and define the maps

- $A_{\tilde{U}}$ and $a_{\tilde{U}}$ to be the composition of of the inclusion of W_3 and $\mathbb{C}_U$, respectively, into $W_1 \oplus W_3 \oplus \mathbb{C}_U$ followed by the quotient,
- $D_{\tilde{V}}$ to be the composition of the inclusion $W_1 \to W_1 \oplus W_3 \oplus \mathbb{C}_U$ followed by the quotient multiplied by -1,
- $C_{\tilde{V}}$ to be the map induced by β,
- $b_{\tilde{U}} = b_U C_V$.

The 0-momentum condition forces $B_{\tilde{U}} = -D_{\tilde{V}} C_{\tilde{V}}$ and also fixes the value of $B'_{\tilde{U}}$ depending on $\tilde{U}^{\ddagger}$.

Theorem 3.1.21 ([NT, Proposition 7.1])**.** *With ρ and $\tilde{p}$ as above, we have the following.*

1. *The map $p \mapsto \tilde{p}$ is a ρ-equivariant isomorphism $\mathcal{C}(D) \to \mathcal{C}(\tilde{D})$.*
2. *There is a short exact sequence of bundles*

$$0 \to \xi_2 \to \xi_3 \oplus \xi_1 \oplus \mathbb{C}_U \to \tilde{\xi}_2 \to 0.$$

Remark 3.1.22. In Remark 2.4.1, we discussed combinatorial operations that interchange 5-branes of the same type while preserving charges. It is easy to see from the dimension formula of Theorem 3.1.15 that switching D5 branes can change the dimension. Therefore, there is no isomorphism between bow varieties related by switching D5 branes in general. On the other hand, switching NS5 branes

preserves the dimension. While we do not expect there to be an algebraic isomorphism between bow varieties related by switching NS5 branes in general, in certain cases there are C^∞ isomorphisms (see Section 4.5).

3.2 Torus Fixed Points

In Section 3.1.1, we assigned a symplectic holomorphic $\mathbb{T}$-manifold $\mathcal{C}(\mathcal{D})$ to each brane diagram $\mathcal{D}$. These manifolds have finitely many $\mathbb{T}$-fixed points, which as one might expect, are in bijection with tie diagrams. In this section, we will discuss three combinarial codes for the torus fixed points of a bow variety: tie diagrams, BCTs, and butterfly diagrams.

3.2.1 Butterflies

The identification of tie diagrams and BCTs to torus fixed points will pass through intermediate combinatorial objects called "butterflies". Fix a brane diagram $\mathcal{D}$. Let $X_0, ..., X_{s+1}$ be the segments of $\mathcal{D}$ including the infinite left and right segments.

Definition 3.2.1. Choose a D5 brane U. A vector $d^U = (d^U_{X_1}, ..., d^U_{X_s}) \in \mathbb{N}^s$ is called a *butterfly dimension vector with center* U if

1. $d^U_{X_1} \leq \cdots \leq d^U_{U^-}$ and $d^U_{U^+} \geq \cdots \geq d^U_{X_s}$,
2. for all NS5 branes V, we have $|d^U_{V^+} - d^U_{V^-}| \leq 1$, where $d^U_{X_0} = d^U_{X_{s+1}} = 0$,
3. for all D5 branes $U' \neq U$, we have $d^U_{U'^+} = d^U_{U'^-}$.

Fix a butterfly dimension vector d^U with center U. The *butterfly* associated with d^U is a connected directed graph constructed through the following steps. First, we place the vertices of the graph relative to the brane diagram $\mathcal{D}$:

1. Place a vertex below U. This vertex will be called the *framing vertex* of the butterfly.
2. Create a column of d^U_X uniformly spaced vertices below segment X.
3. Align the columns below U^- and U^+ at the bottom, so that their lowest vertices are at the same height.
4. Align columns to the right of U at the top, so that the highest vertices in each column are at the same height.

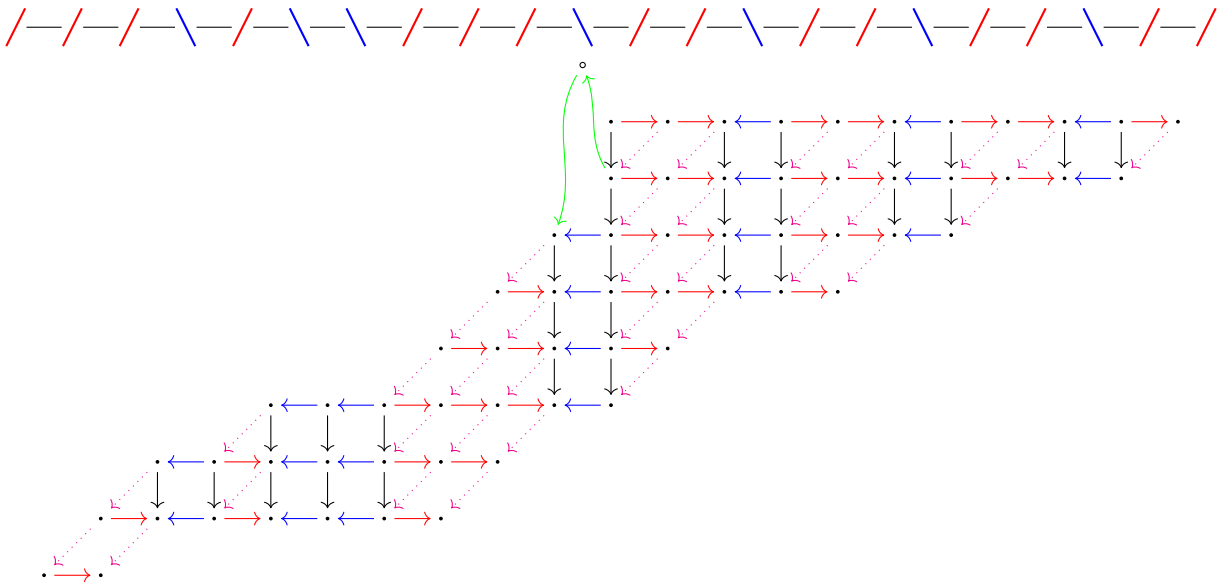

Figure 3.2: The butterfly with dimension vector $(1, 2, 2, 2, 3, 3, 3, 4, 4, 4, 6, 5, 4, 4, 4, 3, 3, 2, 2, 2, 1)$ and center U_4 with respect to the displayed brane diagram. Note that the D3 multiplicites do not play a role in the construction of a butterfly.

5. Align the columns to the left of U, so that

   - if U' is a D5 brane left of U, then the columns below U'^- and U'^+ are aligned at the top, and
   - if V is an NS5 brane left of U, the highest vertex below V^- is at the same height as the second highest vertex below V^+.

Second, we create the directed edges:

1. Create an edge (green) from the framing vertex to the highest vertex below U^-, if such a vertex exists.

2. Create an edge (green) from the vertex below U^+ one position up and right of the highest vertex below U^-, if such a vertex exists, to the framing vertex. If $d^U_{U^-} = 0$, then create an edge from the lowest vertex below U^+ to the framing vertex.

3. For all D5 branes U', create downward edges (black) between all consecutive pairs of vertices under U'^- and U'^+. Also add all possible leftward edges (blue) between vertices of U'^- and U'^+ with the same height.

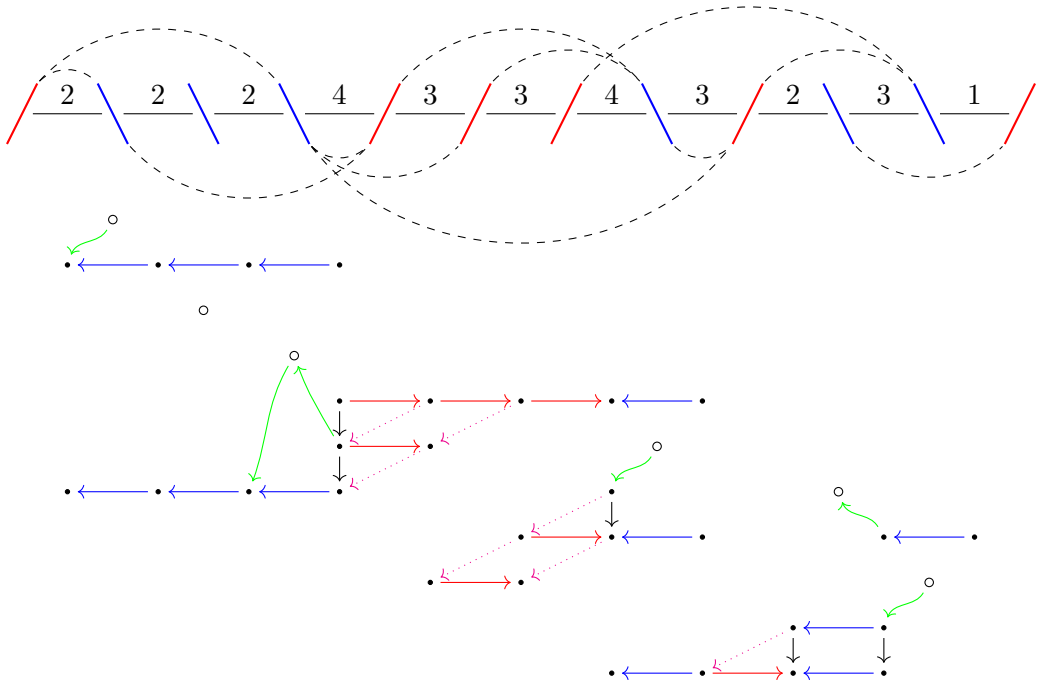

Figure 3.3: A tie diagram and corresponding butterfly diagram.

4. For all NS5 branes V, add all possible rightward edges (red) between vertices under V^- and V^+ with the same height. Also add all possible edges (magenta, dotted) starting at a vertex under V^+ and ending at the vertex one position left and down.

A *butterfly diagram* for $\mathcal{D}$ is a collection of butterflies, one centered on each D5 brane U, such that the corresponding dimension vectors d^U sum to $d = (d_{X_1}, ..., d_{X_s})$. By convention, we think of the butterflies as being stacked vertically, so that the centers of the butterflies go from left to right as we go from the top of the butterfly diagram to the bottom. The condition on the sum of dimension vectors may be rephrased as saying the total number of vertices under each segment X is d_X. Note that butterflies and butterfly diagrams are merely visual representations of butterfly dimension vectors and collections of butterfly dimension vectors compatible with $\mathcal{D}$, respectively. They contain equivalent combinatorial information.

Lemma 3.2.2. *Butterfly diagrams for $\mathcal{D}$ are in bijection with tie diagrams on $\mathcal{D}$.*

Proof. Let $\mathcal{D}$ be a tie diagram, and fix a D5 brane U. Let d^U_X be the number of ties attached to U that cover X. Then, $d^U = (d^U_{X_1}, ..., d^U_{X_s})$ is a butterfly dimension vector centered on U. Indeed, condition 1 of Definition 3.2.1 follows from the fact that the entries of d^U count ties that all emanate

from U, condition 2 follows from the fact that no pair of 5-branes may be joined by multiple ties, and condition 3 follows from the fact that U is the only D5 brane to which the ties under consideration attach, and the endpoints of the ties determine where the entries of d^U change. Repeating this construction for each D5 brane of $\mathcal{D}$ yields a collection of butterfly dimension vectors summing to d: every tie is attached to a unique D5 brane, and the entries of d count the total number of ties covering each segment. This construction has an obvious inverse. □

3.2.2 Combinatorial Codes for Fixed Points

We will now construct a bijection between butterfly diagrams for $\mathcal{D}$ and the fixed point locus $\mathcal{C}(\mathcal{D})^{\mathbb{T}}$. Fix a butterfly diagram for $\mathcal{D}$. For each D5 brane U, choose a basis vector for $\mathbb{C}_U$, and identify the framing vertex of the butterfly centered on U with this basis vector. For each segment X, choose a basis for W_X, and identify the basis vectors with the vertices of the butterfly diagram below X. Interpret the edges as mappings to obtain an element of $\widetilde{\mathcal{M}}^s$. Namely,

- the green edges represent a and $-b$,
- the blue edges represent A,
- the black edges represent $-B$,
- the red edges represent C,
- the dotted magenta edges represent D.

The 0-momentum condition is satisfied by construction, but we must check (S1), (S2), and (ν).

It is sufficient to check the conditions at each D5 brane U restricted to the butterfly centered on U. This is because A_U is an isomorphism outside of the butterfly centered on U. Consider the two cases $d^U_{U-} < d^U_{U+}$ and $d^U_{U-} \geq d^U_{U+}$. The columns of the butterfly adjacent to the center are depicted for both cases by

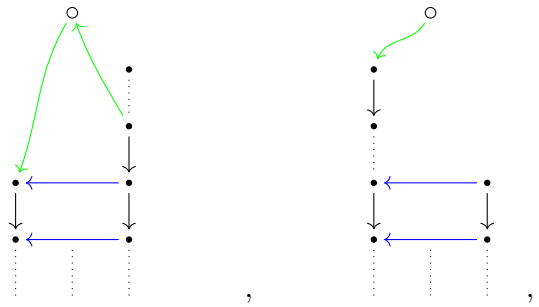

,

,

respectively. In the first case, it is clear from the picture that $\mathrm{im}(a_U)$ generates W_{U^-} as a $\mathbb{C}[B_{U^-}]$-module, so (S2) is satisfied. Any nonzero subspace contained in $\ker(A_U) \cap \ker(b_U)$ must spanned by some of the basis vectors corresponding to the dots above the source of the green b_U edge. However, no such subspace is B_{U^+}-invariant, so (S1) is satisfied. In the second case, (S1) is trivially satisfied, and (S2) is satisfied for the same reason as in case 1. To check the (ν) condition in both cases, note that any A, B, C, D-invariant subspace $\mathrm{im}(a_U) \subset T \subset \mathbb{W}$ contains the span of the portion of the butterfly left of the center. If we also insist that A_U induces an isomorphism on $\mathbb{W}/T$, then the picture shows that T contains the span of the column to the right of the center. Since T is A, B, C, D-invariant, T must contain the span of the portion of the butterfly to the right of the center. It follows that $T = \mathbb{W}$.

Our goal now is to show that the fixed points constructed from butterfly diagrams account for all $\mathbb{T}$-fixed points of $\mathcal{C}(\mathcal{D})$. Given a fixed point $f \in \mathcal{C}(\mathcal{D})^{\mathbb{T}}$, we may identify each vector space W_X with the fibre $\xi_X|_f$ of the corresponding tautological bundle. This endows $\mathbb{W}$ with the structure of a $\mathbb{T}$-representation. The following lemma shows that the weight spaces of $\mathbb{W}$ are modeled by butterflies.

Lemma 3.2.3. *Let $f \in \mathcal{C}(\mathcal{D})^{\mathbb{T}}$ and consider the $\mathbb{T}$-representation $\mathbb{W}$. For each D5 brane U and segment X, denote the u-weight space of the $\mathbb{A}$-action on W_X by W_X^U. Let $d_X^U = \dim(W_X^U)$, and $\mathbb{W}^U = \bigoplus_{X \ D3} W_X^U$. Then, we have the following.*

1. *All A, B, C, D maps send weight spaces to weight spaces. The C and B maps lower the $\hbar$ weight, while A and D maps are homomorphisms of $\mathbb{T}$-representations.*

2. *All $\mathbb{A}$-weights of $\mathbb{W}$ are of the form u, the weight corresponding to a D5 brane U. All $\mathbb{T}$-weights of $\mathbb{W}$ are of the form $u + k\hbar$, where $k \in \mathbb{Z}$.*

3. *The image of a_U is contained in the u-weight space of the $\mathbb{T}$-action, and b_U vanishes on all weight spaces except the $(u + \hbar)$-weight space.*

4. *Let $U' \neq U$ be two distinct D5 branes. Then, $A_{U'}$ is an isomorphism outside of $\mathbb{W}^U$.*

5. *We have $W_{U^-}^U \neq 0$ if and only if $a_U \neq 0$, and $d_{U^-}^U < d_{U^+}^U$ if and only if $b_U \neq 0$.*

6. *The vector $a_U(1)$ is a vector of highest $\hbar$-weight and generates $W_{U^-}^U$ as a $\mathbb{C}[B_{U^-}]$-module. The*

highest $\hbar$-weight of W^U_{U+} is $d^U_{U+} - d^U_{U-}$, and any highest $\hbar$-weight vector generates W^U_{U+} as a $\mathbb{C}[B_{U+}]$-module. All $\mathbb{T}$-weight spaces of $\mathbb{W}$ are 1-dimensional.

Proof. Parts 1, 2, and 3 of the lemma follow immediately from the structure of $\widetilde{\mathcal{M}}$ and the $\mathbb{T}$-action. Fix a D5 brane U, and let $U' \neq U$ be another D5 brane. From 3, we know that $a_{U'}, b_{U'} = 0$ on $\mathbb{W}^U$. Hence, the 0-momentum condition reduces to $B_{U'-}A_{U'} - A_{U'}B_{U'+} = 0$ on this weight space. It follows that the u-weight spaces of the $\mathbb{A}$-action on both $\mathrm{im}(A_{U'})$ and $\ker(A_{U'})$ are B-invariant. The (S1) and (S2) conditions imply part 4. To prove part 5, suppose $a_U = 0$, and extend $\ker(A_U)$ to an A, B, C, D-invariant subspace $T_0 \subset \mathbb{W}$. Note that $\ker(A_U)$ is B_{U+}-invariant by the 0-momentum argument above. Hence, $T_0 \cap W^U_{U-} = 0$. Taking the direct sum of T_0 with $\mathbb{W}^{U'}$ for $U' \neq U$, we obtain an A, B, C, D-invariant subspace $T \subset \mathbb{W}$ containing $\mathrm{im}(a_{U'})$ for all $U' \neq U$. The (ν) condition forces $T = \mathbb{W}$, proving the first statement of 5. If $b_U = 0$, then the argument above implies $\ker(A_U)$ is B_{U+}-invariant. By (S1), $\ker(A_U) = 0$, and A_U is injective. It follows that $d^U_{U-} \geq d^U_{U+}$. The converse will be proven in part 6.

Lastly, we prove part 6. Let $T_0 \subset W_{U-}$ be spanned by vectors of the form $B^k_U(a_U(1))$ for $k \geq 0$ and $T'_0 = A_U^{-1}(T_0) \subset W_{U+}$. From the 0-momentum condition, we have the relation $A_U B_{U+} - a_U b_U = B_{U-}A_U$. This relation implies that $\mathrm{im}(A_U) + T_0$ is B_{U-}-invariant. The (S2) condition implies that $W_{U-} = \mathrm{im}A_U + T_0$. Hence, A_U induces an isomorphism $W_{U+}/T'_0 \to W_{U-}/T_0$. Recall that if $U' \neq U$, then $A_{U'}$ is invertible on $\mathbb{W}^U$. We may extend $T_0 \oplus T'_0$ to an A, A^{-1}, B, C, D-invariant subspace $T_1 \subset \mathbb{W}$ by acting by all available maps. Let $T = \bigoplus_{U' \neq U} \mathbb{W}^{U'}$. The subspace T satisfies the hypotheses of the (ν) condition, so $\mathbb{W} = T$. This proves the first statement of part 6, which will be used throughout the remainder of the proof.

To prove the second statement, first consider the case where $d^U_{U-} \geq d^U_{U+}$. By Lemma 3.1.8, A_U is injective. Since A_U preserves weights, it follows that all $\mathbb{T}$-weight spaces of W^U_{U+} are 1-dimensional. Moreover, W_{U-} does not have $u + \hbar$ as a weight, so W_{U+} cannot have $u + \hbar$ as a weight either. Part 4 implies that $b_U = 0$. By the 0-momentum argument above, A_U commutes with the B-maps. Since B maps lower the $\hbar$-weight, the lowest $\hbar$-weight of W^U_{U-} must be the same as the that of W^U_{U+}. The 0-momentum condition also implies that B_{U+} is nonzero on each $\mathbb{T}$-weight space of W^U_{U+} except the lowest. Hence, the highest $\hbar$-weight of W^U_{U+} is $d^U_{U+} - d^U_{U-}$, and W^U_{U+} is generated by any highest $\hbar$-weight vector as a $\mathbb{C}[B_{U+}]$-module.

Next, we consider the case $d^U_{U^-} < d^U_{U^+}$. In this case, A_U is surjective. Let the subspace $S_0 \subset W_{U^+}$ be the portion of $\ker(A_U)$ with weight $u + k\hbar$ for $k \leq 0$. By part 3, $b_U(S_0) = 0$. Applying the 0-momentum argument above yields the B_{U^+}-invariance of S_0. We have $S_0 = 0$ by (S1), so A_U restricted to the $(u + k\hbar)$ weight spaces for $k \leq 0$ is an isomorphism onto $W^U_{U^-}$. It follows that all such weight spaces are 1-dimensional. Denote the direct sum of these weight spaces by S. We will now show that the $(u + k\hbar)$-weight space of W_{U^+} is 1-dimensional for all $k > 0$, and that B_{U^+} is nonzero on each $\mathbb{T}$-weight space of $W^U_{U^+}$ except the lowest one.

We have shown in part 5 that $b_U \neq 0$. Let $w_1 \in W_{U^+}$ be a vector of weight $u + \hbar$ such that $b_U(w_1) = 1$. Suppose that $w_1 \in \ker(B_{U^+})$. Then, the 0-momentum condition implies $a(1) = 0$, because A_U vanishes on the $(u + \hbar)$-weight space. By part 5, $d^U_{U^-} = 0$ and $S = 0$. Hence, B_{U^+} vanishes on the $(u + \hbar)$-weight space. The (S1) condition implies that the $(u + \hbar)$-weight space of W_{U^+} is 1-dimensional, since otherwise, it would intersect the kernel of b_U and B_{U^+}. Suppose $w_1 \notin \ker(B_{U^+})$. If the $(u + \hbar)$-weight space of W_{U^+} had dimension greater than 1, then there would be a nonzero vector $w_1' \in \ker(b_U)$ of weight $u + \hbar$. By the 0-momentum condition, we have $A_U B_{U^+}(w_1') = 0$. Since $B_{U^+}(w_1') \in S$, and A_U is an isomorphism on S, $w_1' \in \ker(B_{U^+})$. This contradicts (S1), so again we have that the $(u + \hbar)$-weight space of W_{U^+} is 1-dimensional. The restriction of B_{U^+} to the $(u + k\hbar)$-weight space for each $k > 1$ must have zero kernel, due to (S1). It follows by induction on k that all such weight spaces are 1-dimensional and connected by B_{U^+}. The remainder of the proof is the same as in the previous case.

Finally, we show that all $\hbar$-weight spaces of $\mathbb{W}$ are 1-dimensional. Extend $T_0 = W^U_{U^-} \oplus W^U_{U^+}$ to a A, A^{-1}, B, C-invariant subspace $T_1 \subset \mathbb{W}$. Let $T = T_0 \oplus \bigoplus_{U' \neq U} \mathbb{W}^{U'}$. Due to (ν), $\mathbb{W} = T$. It follows that $\mathbb{W}^U$ can be generated from T_0 by acting by all available maps. Any two compositions of maps starting and ending in the same weight spaces are equal up to sign, due to the 0-momentum condition. Since the weight spaces of T_0 are 1-dimensional, all weight spaces are 1-dimensional. $\square$

By representing $\mathbb{C}_U$ and the $\mathbb{T}$-weight spaces of $\mathbb{W}^U$ by vertices and A, B, a, b, D, C maps by directed edges, we obtain the butterfly centered on U with dimension vector $d^U = (\dim(W^U_X))_{X \text{ D5}}$. The fact that d^U is a butterfly dimension vector follows from the various steps of the proof of Lemma 3.2.3. The shape of the butterfly and the signs on B and b follow from the 0-momentum condition. Thus, we obtain

Theorem 3.2.4. *Let $\mathcal{D}$ be a brane diagram. There are natural bijections between the following objects:*

- *$\mathbb{T}$-fixed points of $\mathcal{C}(\mathcal{D})$,*
- *tie diagrams on $\mathcal{D}$,*
- *BCTs with margins and separating line determined by $\mathcal{D}$,*
- *butterfly diagrams on $\mathcal{D}$.*

3.2.3 Fixed Point Restrictions of Tautological Bundles

Recall that there is a tautological rank d_X bundle $\xi_X \to \mathcal{C}(\mathcal{D})$ associated to each segment X of a brane diagram $\mathcal{D}$. Let n be the number of D5 branes in $\mathcal{D}$. In this section, we will study the *localization maps*

$$\begin{aligned}\mathrm{Loc}^K : K^0_{\mathbb{T}}(\mathcal{C}(\mathcal{D})) \to \prod_{f\in\mathcal{C}(\mathcal{D})^{\mathbb{T}}} K^0_{\mathbb{T}}(f) = \prod_{f\in\mathcal{C}(\mathcal{D})^{\mathbb{T}}} \mathbb{C}[\mathbf{u}_1^{\pm 1},...,\mathbf{u}_n^{\pm 1},\mathbf{h}^{\pm 1}],\\ \mathrm{Loc} : H^*_{\mathbb{T}}(\mathcal{C}(\mathcal{D})) \to \prod_{f\in\mathcal{C}(\mathcal{D})^{\mathbb{T}}} H^*_{\mathbb{T}}(f) = \prod_{f\in\mathcal{C}(\mathcal{D})^{\mathbb{T}}} \mathbb{C}[u_1,...,u_n,\hbar].\end{aligned}$$

These maps are defined component-wise by *restriction homomorphisms*

$$\begin{aligned}\mathrm{Loc}^K_f : K^0_{\mathbb{T}}(\mathcal{C}(\mathcal{D})) \to K^0_{\mathbb{T}}(f) = \mathbb{C}[\mathbf{u}_1^{\pm 1},...,\mathbf{u}_n^{\pm 1},\mathbf{h}^{\pm 1}],\\ \mathrm{Loc}_f : H^*_{\mathbb{T}}(\mathcal{C}(\mathcal{D})) \to H^*_{\mathbb{T}}(f) = \mathbb{C}[u_1,...,u_n,\hbar],\end{aligned}$$

induced by the inclusion of $\mathbb{T}$-fixed points f into $\mathcal{C}(\mathcal{D})$. In other words, the K-theoretic restriction homomorphisms applied to a bundle λ gives the sum of the characters of the $\mathbb{T}$-representation $\lambda|_f$, and the cohomological restriction homomorphism applied to $e_{\mathbb{T}}(\lambda)$ gives the product of the weights of $\lambda|_f$. When $\lambda = \xi_X$, these characters and weights can be read from the butterfly diagram of f (see Lemma 3.2.3).

For each butterfly, we introduce a notion of *height* for each nonframing vertex. Note that if both $a_U, b_U = 0$, then $d^U = 0$, and the butterfly centered on U has no nonframing vertices.

Definition 3.2.5. Let w be a nonframing vertex of the butterfly centered on U. Define the *height* $y(w)$ by taking the target of the a_U edge to have height 0 if $d^U_{U^-} \neq 0$ and the source of the b_U edge

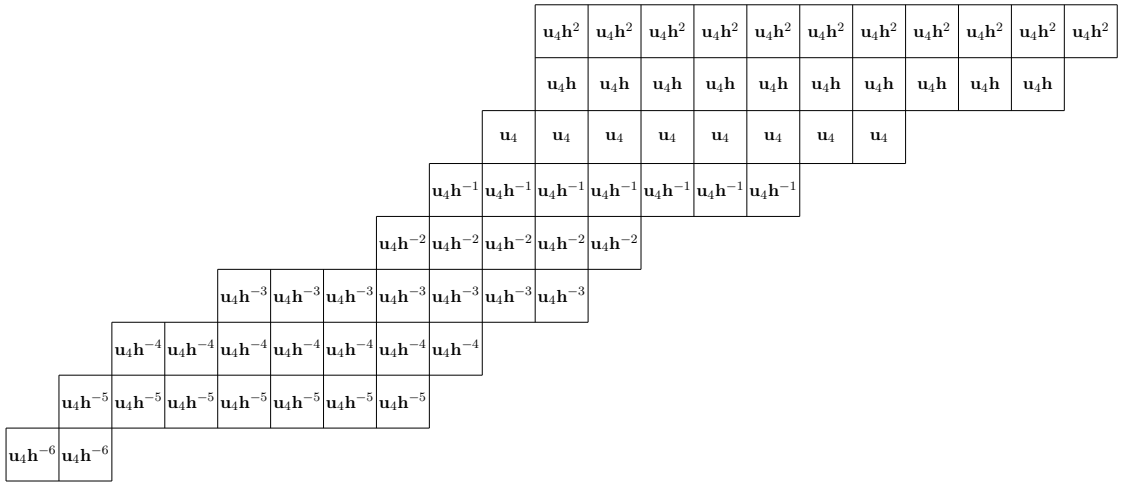

Figure 3.4: The monomials associated to the nonframing vertices of the butterfly in Figure 3.2.

to have height 1 if $d^U_{U^-} = 0$. The height of all other nonframing vertices is their vertical position relative to these two vertices.

Theorem 3.2.6. *Let $f \in \mathcal{C}(\mathcal{D})^{\mathbb{T}}$ and X be a segment in $\mathcal{D}$. We have*

$$\mathrm{Loc}^K_f(\xi_X) = \sum_U \sum_{D5} \sum_w \mathbf{uh}^{y(w)},$$
$$\mathrm{Loc}_f(\xi_X) = \prod_U \prod_{D5} \prod_w (u + y(w)\hbar),$$

where w ranges over all nonframing vertices below X of the butterfly centered on U.

We may also think of decorating each nonframing vertex w of the butterfly centered on U with the monomial $\mathbf{uh}^{y(w)}$. Then the Grothendieck roots (K-theoretic Chern roots) of $\xi_X|_f$ are precisely the monomials below X. See Figure 3.4 for an example. By taking "logarithms", $\mathbf{uh}^{y(w)} \mapsto u + y(w)\hbar$, we obtain the (cohomological) Chern roots.

Example 3.2.7. Continuing Example 3.1.7, consider the two tie diagrams

.

The corresponding decorated butterfly diagrams are $\boxed{\mathbf{u}_1}\boxed{\mathbf{u}_1}\boxed{\mathbf{u}_1}$ and $\boxed{\mathbf{u}_2}\boxed{\mathbf{u}_2}\boxed{\mathbf{u}_2}$. Therefore,

for the restriction maps in K theory we have

$$\xi_{X_1} \mapsto \mathbf{u}_1, \xi_{X_2} \mapsto \mathbf{u}_1, \xi_{X_3} \mapsto \mathbf{u}_1, \qquad \text{and} \qquad \xi_{X_1} \mapsto \mathbf{u}_2, \xi_{X_2} \mapsto \mathbf{u}_2, \xi_{X_3} \mapsto \mathbf{u}_2.$$

Making these substitutions into the formula for $T(\mathcal{C}(\mathcal{D}))$ (see Example 3.1.19) we find the tangent spaces at the two fixed points to be

$$\frac{\mathbf{u}_1}{\mathbf{u}_2} + \frac{\mathbf{u}_2}{\mathbf{u}_1}\mathbf{h} \qquad \text{and} \qquad \frac{\mathbf{u}_2}{\mathbf{u}_1} + \frac{\mathbf{u}_1}{\mathbf{u}_2}\mathbf{h}.$$

Example 3.2.8. Consider the two HW equivalent cobalanced and separated tie diagrams of Example 2.4.2. The decorated butterflies of the cobalanced form are

$\mathbf{u}_3$	$\mathbf{u}_3$	$\mathbf{u}_3$	$\mathbf{u}_3$	$\mathbf{u}_3$

$\mathbf{u}_4$	$\mathbf{u}_4$	$\mathbf{u}_4$	$\mathbf{u}_4$	$\mathbf{u}_4$

.

Note that all tautological bundles restrict to $\mathbf{u}_3 + \mathbf{u}_4$ at this fixed point. Indeed, all A maps are isomorphisms, so all tautological bundles are isomorphic. The formula for the tangent bundle is

$$\begin{aligned}\mathbf{h}(&\mathrm{Hom}(\xi, \mathbf{u}_1) \oplus \mathrm{Hom}(\xi, \mathbf{u}_2) \oplus \mathrm{Hom}(\xi, \mathbf{u}_3) \oplus \mathrm{Hom}(\xi, \mathbf{u}_4) \ominus \mathrm{End}(\xi)) \\ &\oplus \mathrm{Hom}(\mathbf{u}_1, \xi) \oplus \mathrm{Hom}(\mathbf{u}_2, \xi) \oplus \mathrm{Hom}(\mathbf{u}_3, \xi) \oplus \mathrm{Hom}(\mathbf{u}_4, \xi) \ominus \mathrm{End}(\xi),\end{aligned}$$

where we have identified all tautological bundles with ξ. Its image under the restriction homomorphism is

$$\begin{aligned}\mathbf{h}\left(\frac{\mathbf{u}_1}{\mathbf{u}_3} + \frac{\mathbf{u}_2}{\mathbf{u}_3} + \frac{\mathbf{u}_1}{\mathbf{u}_4} + \frac{\mathbf{u}_2}{\mathbf{u}_4}\right) \\ + \frac{\mathbf{u}_3}{\mathbf{u}_1} + \frac{\mathbf{u}_3}{\mathbf{u}_2} + \frac{\mathbf{u}_4}{\mathbf{u}_1} + \frac{\mathbf{u}_4}{\mathbf{u}_2}.\end{aligned}$$

In Section 3.3, we will see that this bow variety is $T^*\mathrm{Gr}(2,4)$, and this fixed point is given by the span of the 3rd and 4th standard basis vectors in $\mathbb{C}^4$. The bundle ξ is, in fact, the pull-back of the rank 2 tautological bundle on $\mathrm{Gr}(2,4)$ under the canonical projection of the cotangent bundle. Note that $\mathbb{C}^4 = \mathbf{u}_1 \oplus \mathbf{u}_2 \oplus \mathbf{u}_3 \oplus \mathbf{u}_4$ as equivariant bundles ($\mathbb{C}^4$ denotes the trivial rank 4 bundle over

$T^*\mathrm{Gr}(2,4)$). Hence, the tangent bundle can be rewritten as

$$\mathbf{h}(\mathrm{Hom}(\xi,\mathbb{C}^4)\ominus\mathrm{Hom}(\xi,\xi))\oplus\mathrm{Hom}(\mathbb{C}^4,\xi)\ominus\mathrm{Hom}(\xi,\xi)=\mathbf{h}\mathrm{Hom}(\xi,\mathbb{C}^4\ominus\xi)\oplus\mathrm{Hom}(\mathbb{C}^4\ominus\xi,\xi).$$

Ignoring the $\hbar$-action, this is the classical description of the tangent bundle of $T^*\mathrm{Gr}(2,4)$.

The decorated butterflies of the separated form are

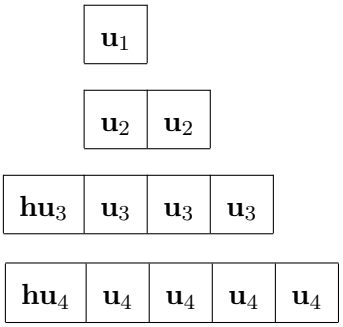

The fact that all A maps are injective is reflected in the nesting of the sets of Grothendieck roots in the last three columns. The restriction of the tangent bundle to this fixed point is the same as before, consistent with the fact that HW transitions are equivariant isomorphisms with respect to the reparametrizations of the torus described in Section 3.1.4.

Remark 3.2.9. Note that while the formulas for the tangent bundle in Example 3.2.7 and Example 3.2.8 contain negative signs, the fixed point restrictions do not. Indeed, the tangent bundle is an honest (rather than virtual) bundle, so its fixed point restrictions are honest $\mathbb{T}$-representations. The phenomenon that the fixed point restrictions of the tangent bundle are Laurent polynomials with positive coefficients is general, and a good sanity check for calculations.

3.2.4 Fixed Points Under Hanany-Witten Transition

In Section 2.4, we defined a natural action of Hanany-Witten transitions on tie diagrams and BCTs. In this section, we will show that this action is consistent with the action of HW transitions on the corresponding $\mathbb{T}$-fixed points. The first step is to describe the HW transition on butterflies.

Let $\mathcal{D}$ be a tie diagram, and let $f\in\mathcal{C}(\mathcal{D})^{\mathbb{T}}$. Fix an NS5 brane U such that $V=U^{\ddagger}$ is an NS5 brane. Adopt the notation of Section 3.1.4. Namely, let $\tilde{\mathcal{D}}$ be the tie diagram obtained by switching U and V by HW transition, and denote U and V in their new positions by $\tilde{U}$ and $\tilde{V}$. Let $X_1=U^-,X_2=U^+,X_3=V^+$ and $\tilde{X}_1=\tilde{V}^-,\tilde{X}_2=\tilde{V}^+,\tilde{X}_3=\tilde{U}^+$. Geometrically, the HW transition gives an isomorphism $\mathcal{C}(\mathcal{D})\to\mathcal{C}(\tilde{\mathcal{D}})$ (Section 3.1.4). Let $\tilde{f}\in\mathcal{C}(\tilde{\mathcal{D}})^{\mathbb{T}}$ be the image of f

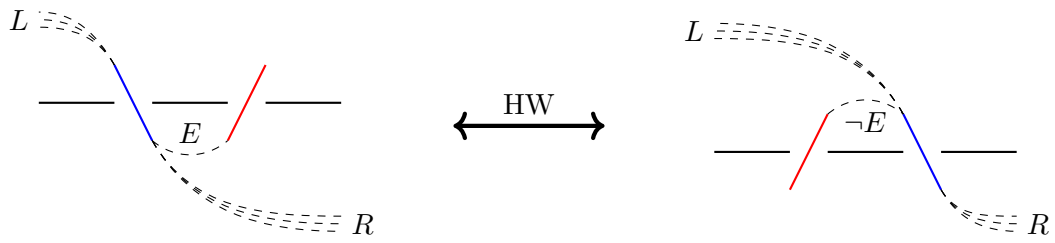

Figure 3.5: Change in the ties attached to U under Hanany-Witten transition. The notation $\neg E$ means that if tie E is in $\mathcal{D}$, then tie $\neg E$ is not in $\tilde{\mathcal{D}}$ and vice-versa.

under the HW transition. We will now examine the relationship between the butterfly centered on U in the butterfly diagram for f and the butterfly centered on $\tilde{U}$ in the butterfly diagram for $\tilde{f}$.

Let L be the number of ties attached to U extending to the left and R be the number of ties attached to U extending to the right past V. Let E denote a tie between U and V or between $\tilde{U}$ and $\tilde{V}$. See Figure 3.5 for an illustration of how these ties are changed by the HW transition. Let

$$\delta(E) = \begin{cases} 1 & \text{if } E \text{ is in } \mathcal{D}, \\ 0 & \text{otherwise.} \end{cases}$$

Then, we have

$$\begin{aligned} d^U_{X_1} &= L & , \quad d^U_{X_2} &= R + \delta(E) \\ d^{\tilde{U}}_{\tilde{X}_2} &= L + (1 - \delta(E)) & , \quad d^{\tilde{U}}_{\tilde{X}_3} &= R. \end{aligned}$$

If $d^U_{X_1} < d^U_{X_2}$, then it is easy to see that $d^{\tilde{U}}_{\tilde{X}_2} \leq d^{\tilde{U}}_{\tilde{X}_3}$. On the other hand, if $d^U_{X_1} \geq d^U_{X_2}$, then $d^{\tilde{U}}_{\tilde{X}_2} \geq d^{\tilde{U}}_{\tilde{X}_3}$.

Consider the case where $d^U_{X_1} < d^U_{X_2}$. The butterfly centered on U has the form

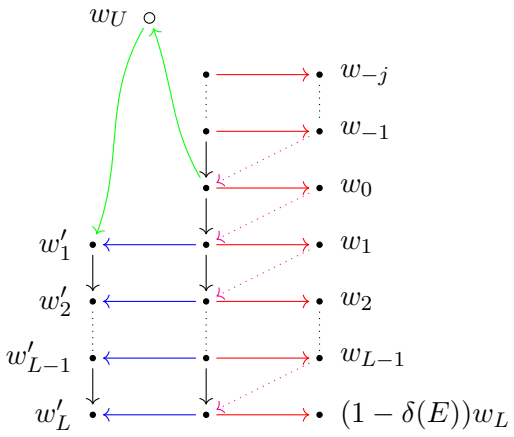

below X_1, X_2, X_3, where $j = R - L + \delta(E) - 1$. By $(1-\delta(E))w_L$, we mean the vertex w_L (and any incident edges) is present if and only if $\delta(E) = 0$. The effect of the HW transition on this butterfly is constrained to the A, B, a, b, C, D maps in this picture. From Section 3.1.4, we have $W^{\tilde{U}}_{\tilde{X}_2} = \operatorname{coker}(\alpha^U)$, where $\alpha^U : W^U_{X_2} \to W^U_{X_1} \oplus W^U_{X_3} \oplus \mathbb{C}_U$ is defined by $(A^U, D^U, b^U)^t$, and the superscript U denotes restriction to the $\mathbb{A}$-weight space $\mathbb{W}^U$ of $\mathbb{W}$. In $W^{\tilde{U}}_{\tilde{X}_2}$, we have the identifications

$$w'_L = (\delta(E)-1)w_L \quad , \quad w'_i = -w_i \text{ for } 0 < i < L \quad , \quad w_0 = w_U \quad , \quad w_i = 0 \text{ for } i < 0.$$

Hence, $W^{\tilde{U}}_{\tilde{X}_2}$ may be identified with the span of $\{w_i \mid 0 \le i \le L - \delta(E)\}$. We also have $W^{\tilde{U}}_{\tilde{X}_1} = W^U_{X_1} = \mathbb{C}\{w'_i \mid 1 \le i \le L\}$ and $W^{\tilde{U}}_{\tilde{X}_3} = W^U_{X_3} = \mathbb{C}\{w_i \mid -j \le i \le L - \delta(E)\}$. The maps $A_{\tilde{U}}$ and $a_{\tilde{U}}$ are induced by inclusion. Therefore, we have

$$A_{\tilde{U}}(w_i) = \begin{cases} w_i & \text{if } i \ge 0, \\ 0 & \text{if } i < 0, \end{cases}$$

and $a_U(w_{\tilde{U}}) = w_U = w_0$, where $w_{\tilde{U}}$ is a basis vector for $\mathbb{C}_{\tilde{U}}$. The map $D_{\tilde{V}}$ is the negative of the map induced by inclusion. Therefore, $D_{\tilde{V}}(w'_i) = -w'_i = w_i$ for $i \ge 1$. The map $C_{\tilde{V}}$ is induced by

$(B_{X_1}, A_U C_V, a_U)$. Hence, we have

$$C_{\tilde{V}}(w_i) = \begin{cases} w'_{i+1} & \text{if } i \geq 0, \\ 0 & \text{if } i < 0. \end{cases}$$

Finally, $b_{\tilde{U}} = b_U C_V$. If $j = 0$, then $b_{\tilde{U}} = 0$. Otherwise, $b_{\tilde{U}}$ maps w_{-1} to $-w_{\tilde{U}}$ and vanishes on w_i for $i \neq -1$. The $B_{\tilde{X}_2}, B_{\tilde{X}_3}$ maps are determined by the other maps and the 0-momentum condition. Diagramatically, these new maps can be represented by

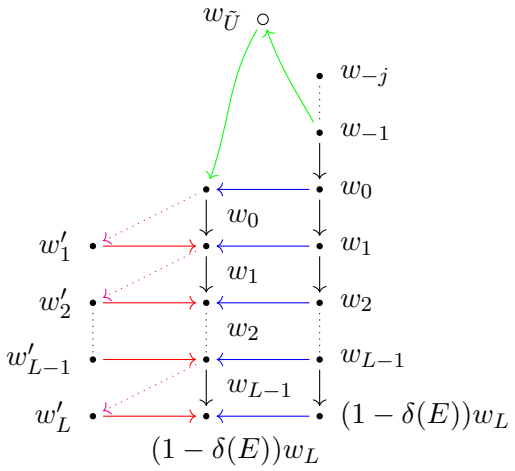

,

where a negative sign is attached to the black downward edges and the green upward edge. This is precisely the butterfly with dimension vector $d^{\tilde{U}}$. A similar argument applies in the case where $d^U_{X_1} \geq d^U_{X_2}$.

Now we examine the action of the HW transition on the butterfly centered on U' for $U' \neq U$. Suppose there are no ties joining U' with V. Then, the HW transition does not change any ties attached to U', so $d^{U'} = d^{\tilde{U}'}$. Moreover, $d^{U'}_{X_1} = d^{U'}_{X_2} = d^{U'}_{X_3} =: k$. The HW transition acting on the relevant maps is depicted by

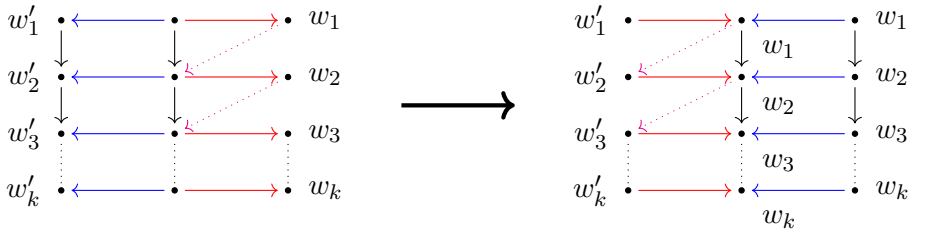

,

as can be verified using the reasoning above. This is consistent with the combinatorics of the HW transition.

Assuming there is a tie joining U' with V, and U' is left of U, we know that $d^{U'}_{X_2} - d^{U'}_{X_3} = 1$. After interchanging U and V, the tie joining U' with V no longer covers $\tilde{X}_2$, so $d^{U'}_{\tilde{X}_2} = d^{U'}_{X_3} =: k$. Acting on the relavant maps by the HW transition, we have

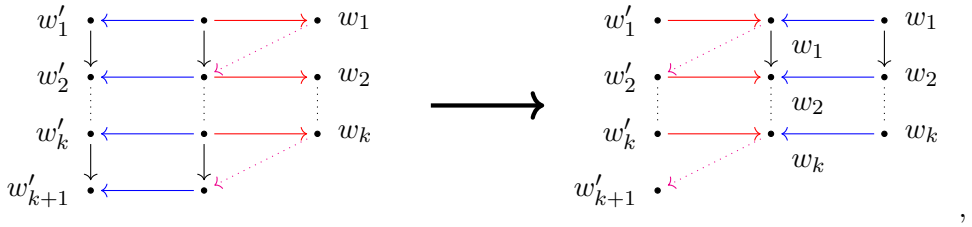

as desired. The case where U' is right of U is similar.

Theorem 3.2.10. *The action of Hanany-Witten transitions on tie diagrams and BCTs is consistent with the action of Hanany-Witten transitions on $\mathbb{T}$-fixed points with respect to the bijection of Theorem 3.2.4.*

3.3 Cobalanced Bow Varieties and Nakajima Quiver Varieties

When $\mathcal{D}$ is (co)balanced, we call $\mathcal{C}(\mathcal{D})$ a *(co)balanced bow variety*. In [NT, Section 2.6], it is shown that all cobalanced bow varieties are naturally isomorphic to a type A quiver variety. The construction of the isomorphism is an extrapolation of the argument in Example 3.1.7. We will begin by recalling the definition of quiver varieties, and then we will construct this isomorphism explicitly. Finally, the relationship between torus fixed points, butterfly diagrams, and partitions will be analyzed.

3.3.1 Quiver Varieties

A (framed) type A quiver is a graph with two kinds of vertices, circular "non-framing" vertices and square "framing" vertices, of the shape

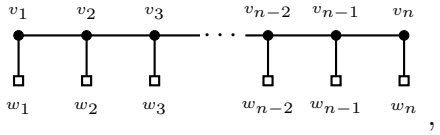

,

where the non-framing and framing vertices are decorated with numbers $v_i \in \mathbb{N}$ and $w_i \in \mathbb{N}$, respectively. The corresponding vectors $v, w \in \mathbb{N}^n$ are called the "dimension vectors" of the quiver. Denote this quiver by $Q = Q(v, w)$. These are the combinatorial objects parametrizing type A quiver varieties [N1]. Define

$$R = \bigoplus_{i=1}^{n-1} \mathrm{Hom}(\mathbb{C}^{v_i}, \mathbb{C}^{v_{i+1}}) \oplus \bigoplus_{i=1}^{n} \mathrm{Hom}(\mathbb{C}^{v_i}, \mathbb{C}^{w_i}).$$

Denote elements of $T^*R = R \oplus R^\vee$ by (D, b, C, a), where

$$D_i \in \mathrm{Hom}(\mathbb{C}^{v_i}, \mathbb{C}^{v_i+1}), b_i = \mathrm{Hom}(\mathbb{C}^{v_i}, \mathbb{C}^{w_i}), C_i = \mathrm{Hom}(\mathbb{C}^{v_i+1}, \mathbb{C}^{v_i}), a_i = \mathrm{Hom}(\mathbb{C}^{w_i}, \mathbb{C}^{v_i}).$$

Let $\mathcal{G}_v = \prod_{i=1}^n \mathrm{GL}(\mathbb{C}^{v_i})$ act on M by conjugation. The cotangent bundle possesses a canonical symplectic form and Hamiltonian action of $\mathcal{G}_v$. The moment map

$$\mu : T^*R \to \bigoplus_{i=1}^{n} \mathrm{End}(\mathbb{C}^{v_i})$$

is given by $\mu = [D, C] - ab$. The quiver variety $\mathcal{N}(Q) = \mathcal{N}(Q(v, w)) = \mathcal{N}(v, w)$ is defined to be

$$\mu^{-1}(0)^s \Big/ \prod_{i=1}^{n} \mathrm{GL}(\mathbb{C}^{v_i}),$$

where an element (D, b, C, a) is stable if $\mathrm{im}(a)$ generates $\bigoplus_{i=1}^n \mathbb{C}^{v_i}$ as a $\mathbb{C}[C, D]$-module, under our choice of GIT stability condition. Define a symplectic torus action of

$$\mathbb{A} = \prod_{i=1}^{n} (\mathbb{C}^\times)^{w_i} \quad \text{by} \quad u.(D, b, C, a) = (D, ub, C, au^{-1}).$$

Define an additional $\mathbb{C}^\times_\hbar$-action by scaling $R^\vee$. This action scales the symplectic form. Quiver varieties are smooth with the following additional structures:

- holomorphic symplectic structure,
- tautological bundle $\xi_i \to \mathcal{N}(Q)$ associated with $\mathbb{C}^{v_i}$,
- action of the torus $\mathbb{T} = \mathbb{A} \times \mathbb{C}^\times_\hbar$.

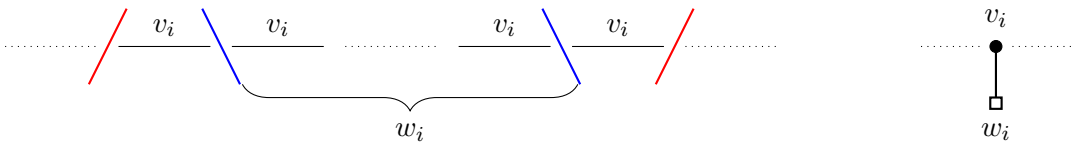

Figure 3.6: Local illustration of $\mathcal{D}$ and $Q(\mathcal{D})$.

Remark 3.3.1. Several similar definitions of quiver varieties exist that differ only by a reparametrization of $\mathbb{T}$ and the symplectic form, e.g. the definition of [RSVZ1]. The various parametrizations of the torus and symplectic forms can be encoded by giving Q an orientation. Implicitly, we have oriented all horizontal edges right and all vertical edges down.

3.3.2 Isomorphism Between Cobalanced Bow Varieties and Quiver Varieties

Let $\mathcal{D}$ be a cobalaned brane diagram, and consider the *intervals* between consecutive NS5 branes. All segments appearing in an interval I have the same multiplicty, say d_I. Listing the intervals $I_1, ..., I_n$ from left to right, define dimension vectors

$$v_i = d_{I_i} \quad , \quad w_i = \#\{\text{D5 branes in } I_i\}.$$

Let $Q(\mathcal{D}) = Q(v, w)$, and $\mathcal{N}(\mathcal{D}) = \mathcal{N}(Q(\mathcal{D}))$. We will now define a map $\mathcal{C}(\mathcal{D}) \to \mathcal{N}(\mathcal{D})$.

Let $p = (A, B, a, b, C, D) \in \widetilde{\mathcal{M}}^s$. Since $\mathcal{D}$ is cobalanced, the A maps are isomorphisms by Lemma 3.1.8. Given $1 \leq i \leq n$, let $U_{i,1}, ..., U_{i,w_i}$ be the D5 branes in I_i, $X_{i,1}, ..., X_{i,w_i+1}$ be the segments in I_i, and let I^- and I^+ be the NS5 branes on the left and right ends, respectively, of I. Define vector spaces

$$\mathcal{V}_i = W_{X_{i,1}} \quad , \quad \mathcal{W}_i = \bigoplus_{j=1}^{w_i} \mathbb{C}_{U_{i,j}},$$

and make identifications $\mathbb{C}^{v_i} = \mathcal{V}_i$ and $\mathbb{C}^{w_i} = \mathcal{W}_i$. Define $p_{\mathcal{N}} = (C, a, D, b) \in T^*R$ by

$$a_i = \sum_{j=1}^{w_i} a_{i,j}, \text{ where } a_{i,j} = A_{U_{i,1}} \cdots A_{U_{i,j-1}} a_{U_{i,j}},$$

$$b_i = -\sum_{j=1}^{w_i} b_{i,j}, \text{ where } b_{i,j} = b_{U_{i,j}} A^{-1}_{U_{i,j}} \cdots A^{-1}_{U_{i,1}},$$

$$C_i = A_{U_{i,1}} \cdots A_{U_{i,w_i}} C_{I^+},$$

$$D_i = -D_{I^+} A^{-1}_{U_{i,w_i}} \cdots A^{-1}_{U_{i,1}}.$$

One can check that $\mu(p) = 0$ implies $\mu(p_{\mathcal{N}}) = 0$, and that the GIT stability of p implies the GIT stability of $p_{\mathcal{N}}$. There is a natural identification of the torus acting on $\mathcal{C}(\mathcal{D})$ with the torus acting on $\mathcal{N}(\mathcal{D})$ coming from the splitting of the framing spaces $\mathcal{W}_i$ into $\mathbb{C}_U$ spaces.

Theorem 3.3.2 ([NT, Theorem 2.15])**.** *The map $p \mapsto p_{\mathcal{N}}$ induces a $\mathbb{T}$-equivariant symplectomorphism $\mathcal{C}(\mathcal{D}) \to \mathcal{N}(\mathcal{D})$. This map induces an equivariant isomorphism of tautological bundles up to a reparametrization of $\mathbb{T}$.*

Proof. First, we show that $p_{\mathcal{N}} \in \mu^{-1}(0)^s$. It is easy to see that the (ν) condition implies the stability of $p_{\mathcal{N}}$. Repeatedly applying the 0-momentum condition on p yields the sequence of equalities

$$\begin{aligned}
B_{U^+_{i,w_i}} &= -C_{I_i^+} D_{I_i^+} \\
B_{U^-_{i,w_i}} &= -A_{U_{i,w_i}} C_{I_i^+} D_{I_i^+} A^{-1}_{U_{i,w_i}} - a_{U_{i,w_i}} b_{U_{i,w_i}} A^{-1}_{U_{i,w_i}} \\
B_{U^-_{i,w_i-1}} &= -A_{U_{i,w_i-1}} A_{U_{i,w_i}} C_{I_i^+} D_{I_i^+} A^{-1}_{U_{i,w_i}} A^{-1}_{U_{i,w_i-1}} - A_{U_{i,w_i-1}} a_{U_{i,w_i}} b_{U_{i,w_i}} A^{-1}_{U_{i,w_i}} A^{-1}_{U_{i,w_i-1}} \\
&\quad -a_{U_{i,w_i-1}} b_{U_{i,w_i-1}} A^{-1}_{U_{i,w_i-1}} \\
&\quad \vdots \\
B_{U^-_{i,1}} &= -A_{U_{i,1}} \cdots A_{U_{i,w_i}} C_{I_i^+} D_{I_i^+} A^{-1}_{U_{i,w_i}} \cdots A^{-1}_{U_{i,1}} - A_{U_{i,1}} \cdots A_{U_{i,w_i-1}} a_{U_{i,w_i}} b_{U_{i,w_i}} A^{-1}_{U_{i,w_i}} \cdots A^{-1}_{U_{i,1}} \\
&\quad -A_{U_{i,1}} \cdots A_{U_{i,w_i-2}} a_{U_{i,w_2}} b_{U_{i,w_2}} A^{-1}_{U_{i,w_i-1}} \cdots A^{-1}_{U_{i,1}} \\
&\quad -\cdots - a_{U_{i,1}} b_{U_{i,1}} A^{-1}_{U_{i,1}} \\
B_{U^-_{i,1}} &= -D_{I_i^-} C_{I_i^-},
\end{aligned}$$

Combining the last two equalities gives $\mu(p_{\mathcal{N}}) = 0$. Second, define a map $\rho : \mathcal{G} \to \mathcal{G}_v$ by projecting onto the factors corresponding to the leftmost segments of each interval. The defining equations of $p_{\mathcal{N}}$ are visibly ρ-equivariant and $\mathbb{T}$-equivariant up to the reparametrization $\mathbf{u} \mapsto \mathbf{hu}$ of the torus acting on $\mathcal{N}(\mathcal{D})$, so we get an induced $\mathbb{T}$-equivariant map $\mathcal{C}(\mathcal{D}) \to \mathcal{N}(\mathcal{D})$. The fact that the symplectic form is preserved can be verified using the formulas of [NT, Section 3] and [N1, Section 2]. Finally, we construct an inverse map.

Identify the jth coordinate subspace of $\mathbb{C}^{w_i}$ with $\mathbb{C}_{U_{i,j}}$. Identify W_X with $\mathbb{C}^{v_i}$ for all segments

X in I_i. Let $p_{\mathcal{N}} \in \mathcal{N}(\mathcal{D})$ and define $p \in \mathcal{C}(\mathcal{D})$ by

$$\begin{aligned}
A_{U_{i,j}} &= \mathrm{id}_{\mathbb{C}^{v_i}}, \text{ for } j = 1, ..., w_i, \\
a_{U_{i,j}} &= a_i|_{\mathbb{C}_{U_{i,j}}}, \\
b_{U_{i,j}} &= -b_i^j, \text{ where } b_i^j \text{ is the projection of } b_i \text{ onto the } j\text{th coordinate}, \\
C_{I^+} &= C_i, \\
D_{I^+} &= -D_i,
\end{aligned}$$

and defining B maps according to the sequence of equalities above. The map $p_{\mathcal{N}} \mapsto p$ induces a map $\mathcal{N}(\mathcal{D}) \to \mathcal{C}(\mathcal{D})$. Given $p = (A, B, a, b, C, D) \in \widetilde{\mathcal{M}}^s$, it is always possible to change the A maps to identity maps through the action of $\ker(\rho)$. It follows that $\mathcal{C}(\mathcal{D}) \to \mathcal{N}(\mathcal{D})$ and $\mathcal{N}(\mathcal{D}) \to \mathcal{C}(\mathcal{D})$ are inverses. □

Remark 3.3.3. The reparametrization of the torus described in the proof of Theorem 3.3.2 can be absorbed into the $\mathcal{G}_v$-action. Hence, it does not change the action of $\mathbb{T}$ on $\mathcal{N}(\mathcal{D})$. It does, however, change the action of $\mathbb{T}$ on the tautological bundles.

Example 3.3.4.

$\mathcal{N}\Big($ 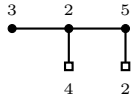

$\Big) \quad = \quad \mathcal{C}(/3/2\backslash 2\backslash 2\backslash 2/5\backslash 5\backslash 5/).$

Let $\mathcal{D}$ be the brane diagram such that $\mathcal{C}(\mathcal{D}) = \mathcal{N}(v, w)$. The margin vectors of $\mathcal{D}$ are

$$r = \left(v_i - v_{i-1} + \sum_{j=1}^{i-1} w_j \right)_{i=1,...,n+1}, \quad c = (n^{w_1}, (n-1)^{w_2}, (n-2)^{w_3}, ..., 1^{w_n}), \tag{3.2}$$

where $v_0 = v_{n+1} = 0$ by convention, and the notation a^b means b copies of a. Since the Euler characteristic of a quiver variety is the number of $\mathbb{T}$-fixed points, we may calculate $\chi(\mathcal{N}(v, w))$ by counting BCTs.

Corollary 3.3.5. *For $v, w \in \mathbb{N}^n$, we have*

$$\chi(\mathcal{N}(v, w)) = \#\mathrm{BCT}\left(\left(v_i - v_{i-1} + \sum_{j=1}^{i-1} w_j \right)_{i=1,...,n+1}, (n^{w_1}, (n-1)^{w_2}, (n-2)^{w_3}, \ldots, 1^{w_n}) \right).$$

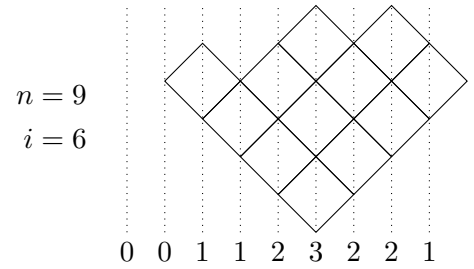

Figure 3.7: An illustration of the bijection between partition dimension vectors and Young diagrams.

Formulas and various generating functions are known for some special cases of r, c. For example, according to Corollary 3.3.5 and [St, Corollary 5.5.11] we have

$$\sum_{n=0}^{\infty} \chi\left(\mathcal{N}\left(\begin{array}{ccccccc} \bullet & \bullet & \bullet & & \bullet & \bullet \\ 2 & 4 & 6 & \cdots & 2n-2 & n-1 \\ & & & & & \bullet \\ & & & & & n+1 \end{array}\right)\right) \frac{x^n}{(n!)^2} = \sum_{n=0}^{\infty} \#\mathrm{BCT}((2^n),(2^n)) \frac{x^n}{(n!)^2} = \frac{e^{-\frac{x}{2}}}{\sqrt{1-x}}.$$

3.3.3 Fixed Points, Butterfly Diagrams, and Partitions

In the cobalanced case, butterflies collapse into Young diagrams, recovering classical results for the torus fixed points of a Nakajima quiver variety. To make this phenomenon explicit, we will describe partitions by integer vectors.

Definition 3.3.6. Given $n \in \mathbb{N}$ and $1 \leq i \leq n$, a vector $d^i = (d^i_1, ..., d^i_n) \in \mathbb{N}^n$ is called a *partition dimension vector with mode i* if

1. $d^i_1 \leq \cdots \leq d^i_i \geq \cdots \geq d^i_n$ (i.e. d^i is unimodal with mode i),

2. $\forall 0 \leq j \leq n \;\; |d^i_{j+1} - d^i_j| \leq 1$, where $d^i_0 = d^i_{n+1} = 0$ by convention.

Classically, partition dimension vectors are put in bijection with Young diagrams by tilting the Young diagram 45° and counting the number of boxes appearing in each vertical column. See Figure 3.7 for an illustrative example.

Proposition 3.3.7. *For fixed $n \in \mathbb{N}$ and index $1 \leq i \leq n$. Partition dimension vectors $d^i \in \mathbb{N}^n$ with mode i are in bijection with Young diagrams fitting within a $(n-i+1) \times i$ rectangle.*

Let $\mathcal{D}$ be a cobalanced tie diagram, and let U be a D5 brane in the ith interval I_i of $\mathcal{D}$. Since $\mathcal{D}$ is cobalanced, $d^U_{U^-} = d^U_{U^+}$. Indeed, we have $d_{U^-} = d_{U^+}$, and any tie not connected to U, i.e. any tie not counted by d^U, must cover both U^- and U^+ or neither. For all D5 branes $U' \neq U$, we have

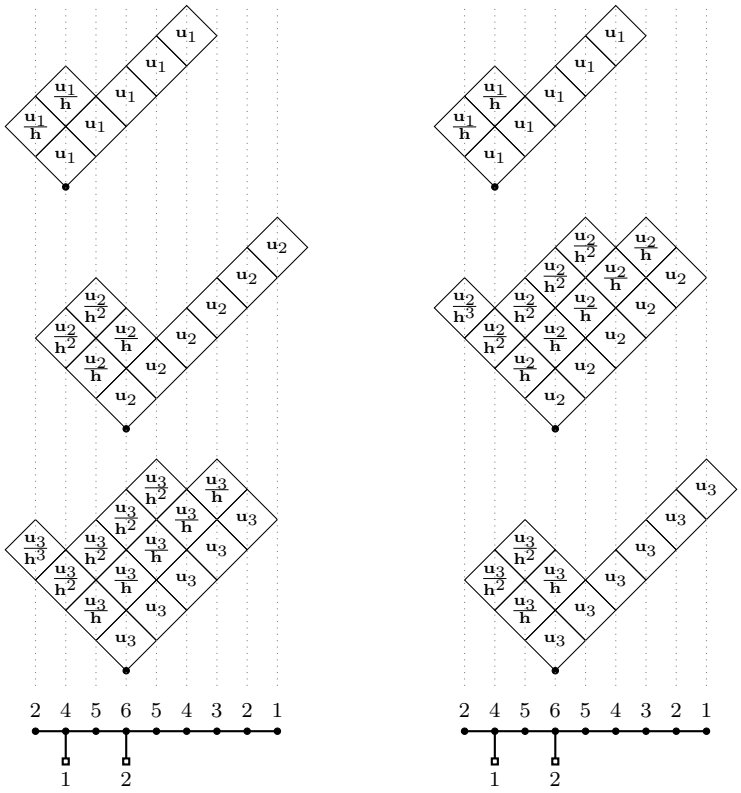

Figure 3.8: The combinatorial code for two of the 3,150 fixed points of the quiver variety $\mathcal{N}((2,4,5,6,5,4,3,2,1),(0,1,0,2,0,0,0,0,0,0))$, with partitions ordered from top to bottom.

$d^{U'}_{U'-} = d^{U'}_{U'+}$ by Definition 3.2.1. It follows that d^U_X takes a common value for all segments X in an interval I. Thus, we may collapse the butterfly dimension vector d^U to obtain a partition dimension vector d^i, where the common value of d^U_X for X in the jth interval I_j is d^i_j. The fact that d^i is a partition dimension vector with mode i follows immediately by comparing Definition 3.2.1 with Definition 3.3.6. This collapsing has a geometric significance as well.

When collapsing a butterfly dimension vector, one may also think about collapsing the columns of the corresponding butterfly that are separated by a D5 brane. Geometrically speaking, this collapsing is the action of the isomorphism $\mathcal{C}(\mathcal{D}) \to \mathcal{N}(\mathcal{D})$ of Theorem 3.3.2 on the fixed point represented by the butterfly diagram. Since the A maps in a cobalanced bow variety are isomorphisms, the tautological bundles ξ_X for all X in I_j are isomorphic. Indeed, they are isomorphic to the tautological bundle ξ_j on $\mathcal{N}(\mathcal{D})$. It follows that we may also collapse the butterfly decorated with fixed point restrictions of the tautological bundles, yielding a (skewed) Young diagram filled with Grothendieck roots of the fixed point restrictions of the tautological bundles on $\mathcal{N}(\mathcal{D})$. See Figure 3.9 for an

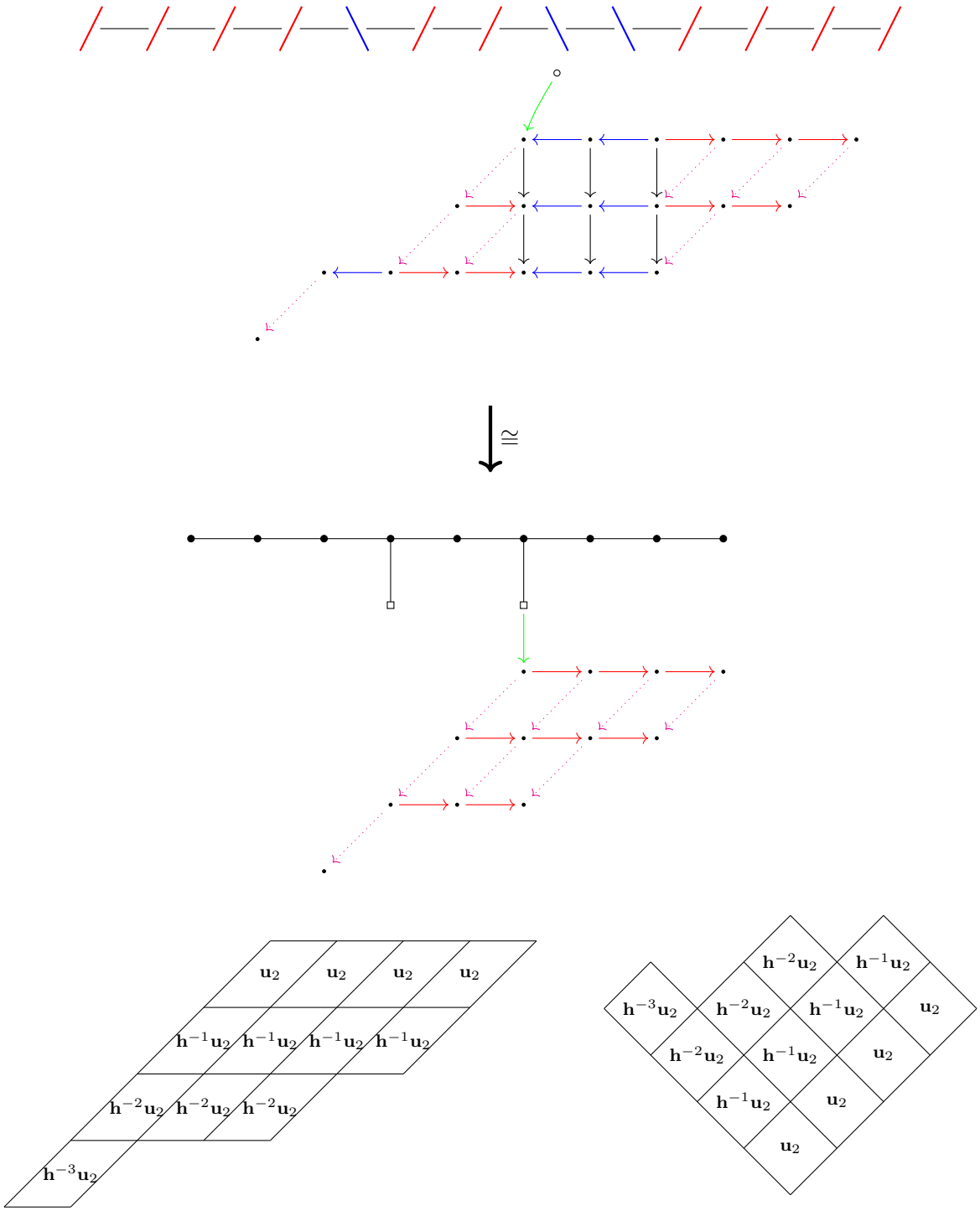

Figure 3.9: Cobalanced butterflies are collapsed along blue edges by the isomorphism $\mathcal{C}(\mathcal{D}) \to \mathcal{N}(\mathcal{D})$. Butterflies decorated with fixed point restrictions collapse to filled Young diagrams.

illustration of this collapsing procedure. This recovers the well known characterization of the $\mathbb{T}$-fixed points of a quiver variety in terms of tuples of partitions, and the fixed point restrictions of the tautological bundles as fillings of the Young diagrams by monomials in the equivariant parameters.

Let $v, w \in \mathbb{N}^n$. Then, the $\mathbb{T}$-fixed points of $\mathcal{N}(v, w)$ are in bijection with tuples $(d^{i,j})$ where

1. $d^{i,j} \in \mathbb{N}^n$ is a partition dimension vector with mode i for all $1 \leq i \leq n, 1 \leq j \leq w_i$,
2. $\sum_{i,j} d^{i,j} = v$.

Alternatively, one can think of a tuple of w_i Young diagrams "growing" out of the ith vertex of $Q(v, w)$ at a 45° degree angle (as in Figure 3.8) for each $1 \leq i \leq n$, such that the total number of boxes among all Young diagrams above the ith vertex is v_i for each $1 \leq i \leq n$. Filling each Young diagram as shown in Figure 3.8, 3.9, the Grothendieck roots of ξ_i are precisely the monomials that appear above the ith vertex. See Section 4.2.1 for additional examples.

Remark 3.3.8. The isomorphism of Theorem 3.3.2 involves a reparametrization of the torus that changes the $\hbar$-action on the tautological bundles. Hence, our Young diagram fillings may differ slightly from other conventions.

Example 3.3.9. The quiver variety of Example 3.3.4 has no fixed points. Indeed, any fixed point corresponds to a tuple of Young diagrams over the 2nd and 3rd vertices with 3 boxes over the 1st vertex, 2 boxes over the 2nd, and 5 boxes over the 3rd. This is impossible, since having 3 boxes over the 1st vertex forces at least 3 boxes over the 2nd. This can also be verified by a similar argument using tie diagrams.

3.4 Invariant Curves

Invariant curves play an important role in the study of equivariant characteristic classes. By an *invariant curve*, we mean an embedding of $\mathbb{P}^1$ into $\mathcal{C}(\mathcal{D})$ with $\mathbb{T}$-invariant image. We will construct such curves by constructing embeddings $\gamma : \mathbb{C} \to \widetilde{\mathcal{M}}^s$ with the property that $\lim_{t\to\infty} \gamma(t)$ converges to an element of $\widetilde{\mathcal{M}}^s$. These embeddings are associated with combinatorial operations on pairs of butterflies called *butterfly surgeries*. The invariant curves contructed this way will always have $\mathbb{T}$-fixed points at $t = 0$ and $t = \infty$. We call these fixed points the *poles* of the invariant curve—we can think of $\mathbb{P}^1$ as a sphere and the fixed points as the north and south poles. Note that there may not be a unique curve with specified poles; no such curve may exist, or there might be a pencil of curves joining the fixed points.

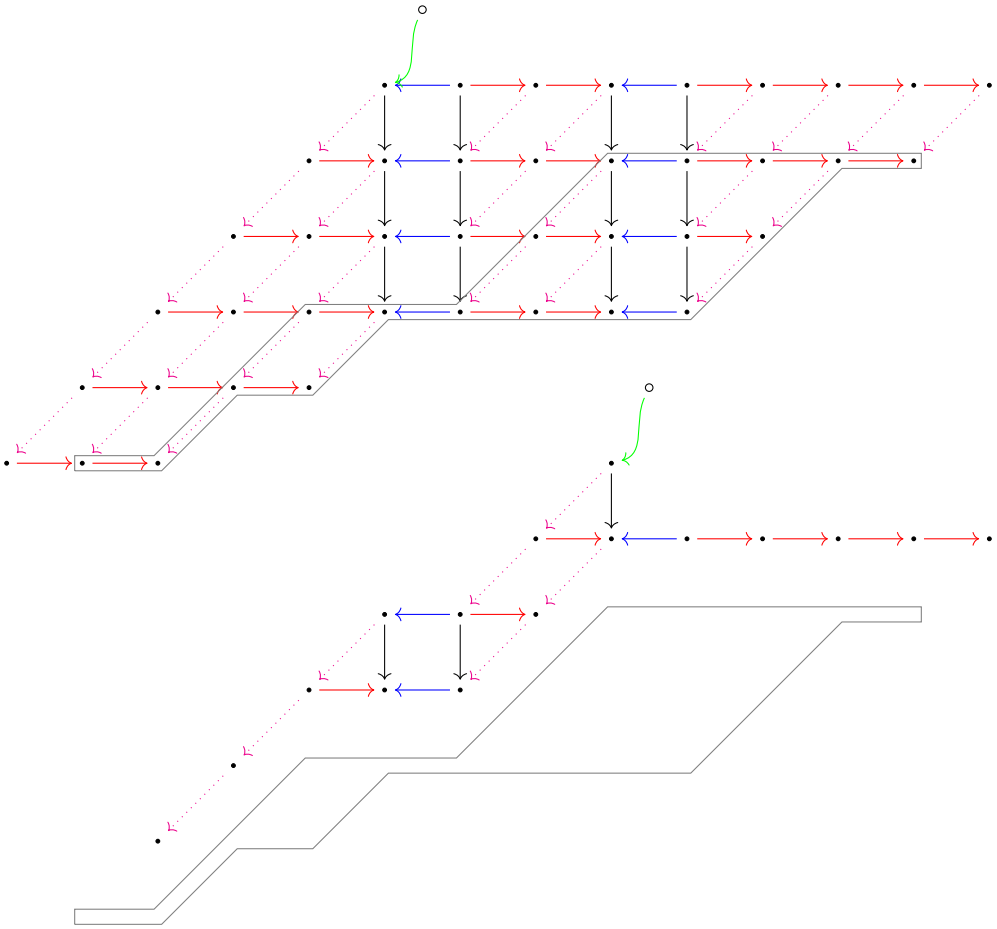

Figure 3.10: Fixed point with the site of a butterfly surgery outlined.

3.4.1 Butterfly Surgery

A fixed point $f_1 \in \mathcal{C}(\mathcal{D})^{\mathbb{T}}$ corresponds to a butterfly diagram (Theorem 3.2.4), that is, a collection of butterflies, one centered on each D5 brane. We stack the butterflies on top of each other, so that the centers of the butterflies listed from top to bottom go from left to right in $\mathcal{D}$. Fix two butterflies $\mathfrak{b}_1$ and $\mathfrak{b}_1'$ with centers U and U', respectively. Suppose that there is a (possibly disconnected) subgraph $\mathfrak{s}$ of $\mathfrak{b}_1$, such that stacking $\mathfrak{s}$ below $\mathfrak{b}_1'$ and creating new edges between $\mathfrak{b}_1'$ and $\mathfrak{s}$ according to the rules of Section 3.2.1 results in a butterfly $\mathfrak{b}_2'$. The subgraph $\mathfrak{s}$, called the *site* of the surgery, must be translated vertically without any lateral movement, rotation, or deformation, and we no not create new edges within $\mathfrak{s}$. The 0-momentum condition forces such an $\mathfrak{s}$ is to be A, A^{-1}, B, C, D-invariant. In other words, all edges in $\mathfrak{b}_1$ adjacent to $\mathfrak{s}$ are directed into $\mathfrak{s}$, and $\mathfrak{s}$ contains all adjacent blue A edges. Let $\mathfrak{b}_2$ be obtained by deleting $\mathfrak{s}$ and all adjacent edges from $\mathfrak{b}_1$, and assume that $\mathfrak{b}_2$ is also a butterfly. The operation of replacing $\mathfrak{b}_1$ with $\mathfrak{b}_2$ and $\mathfrak{b}_1'$ with $\mathfrak{b}_2'$ is

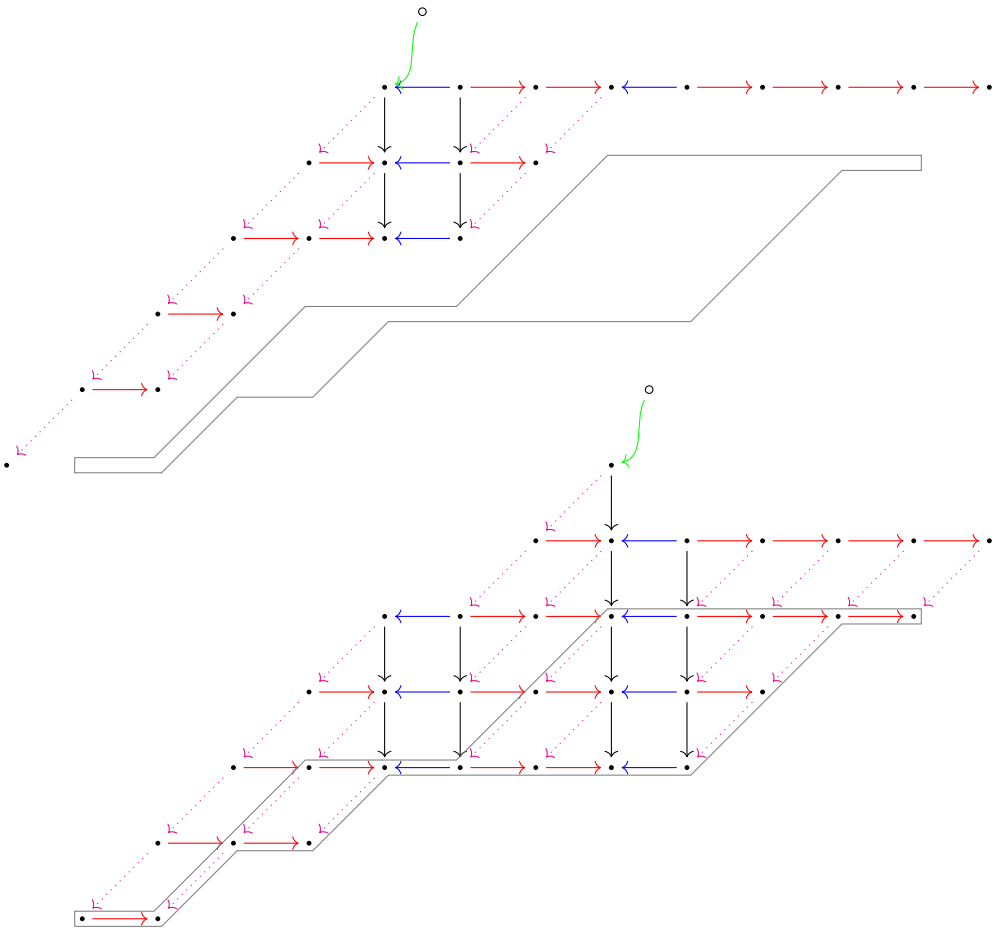

Figure 3.11: New fixed point resulting from butterfly surgery.

called a *butterfly surgery*. It transforms the butterfly diagram for f_1 into the butterfly diagram for another fixed point $f_2 \in \mathcal{C}(\mathcal{D})^{\mathbb{T}}$

We can construct an invariant curve as follows. Consider the newly created edges, i.e. $\mathfrak{b}_2' \setminus \mathfrak{b}_1'$, in the butterfly diagram for f_2. Each edge starts in $\mathfrak{b}_1'$ and ends in the translated copy of $\mathfrak{s}$, which we will call $\mathfrak{s}'$. Create the corresponding edges starting in $\mathfrak{b}_1'$ and ending in $\mathfrak{s} \subset \mathfrak{b}_1$ in the butterfly diagram for f_1 with weighting $t \in \mathbb{C}$. Interpreting these new edges as multiplication by t, the resulting graph gives an element $\gamma(t) \in \widetilde{\mathcal{M}}^s$. The 0-momentum condition can be verified pictorially (see Figure 3.12). Adding new edges expands $\mathrm{im}(A), \mathrm{im}(B), \mathrm{im}(a), \mathrm{im}(C), \mathrm{im}(D)$ and shrinks $\ker(A), \ker(b)$. Moreover, adding edges does not result in new invariant subspaces of $\mathbb{W}$. In fact, some invariant subspaces may lose their invariance. Thus, (S1),(S2),(ν) for $\gamma(t)$ follows for all t from (S1),(S2),(ν) for f_1.

By compactifying γ, we obtain a $\mathbb{T}$-invariant curve with poles f_1 and f_2. Clearly, $\gamma(0) = f_1$. To

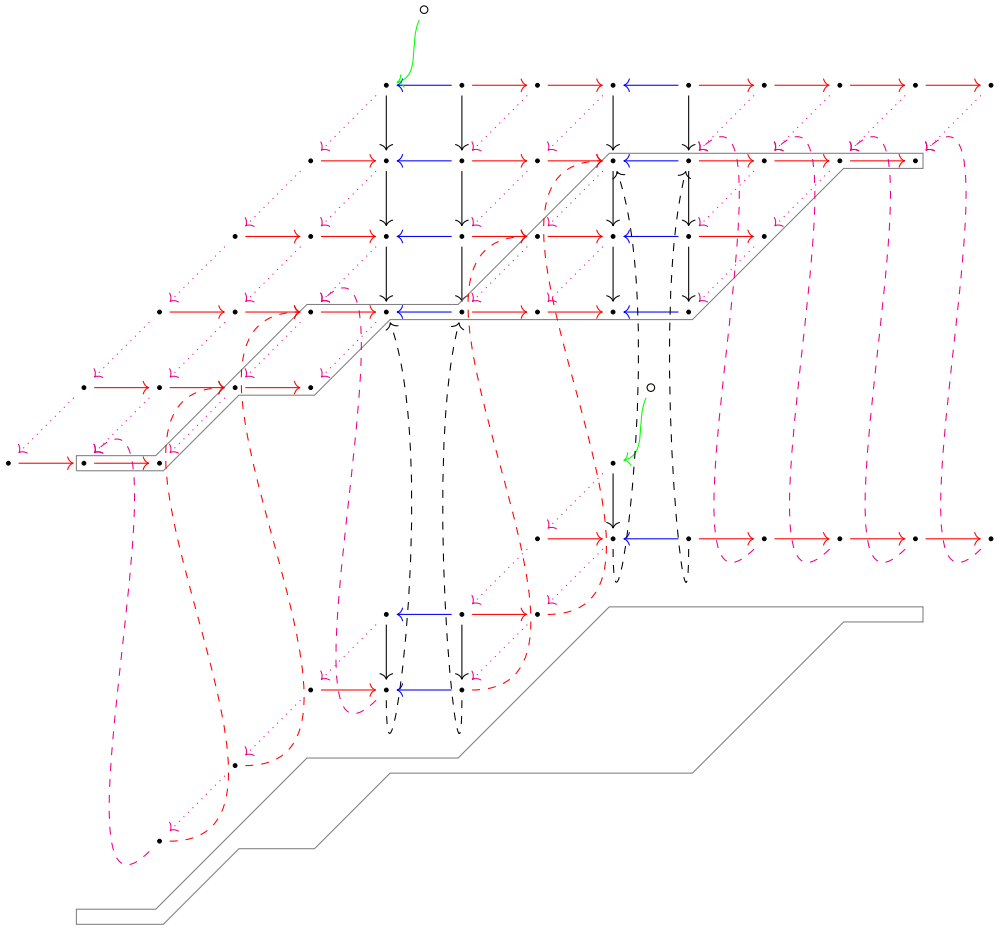

Figure 3.12: Explicit invariant curve corresponding to butterfly surgery. The dashed lines represent multiplication by t. The curve has tangent weight $\pm(u_1 - u_2 + \hbar)$ at its poles.

take the $t \to \infty$ limit, act on each vertex of $\mathfrak{s}$ by $1/t$. Since all adjacent edges to $\mathfrak{s}$ in $\mathfrak{b}_1 \setminus \mathfrak{s}$ point into $\mathfrak{s}$, these edges are acted upon by $1/t$. The new edges from $\mathfrak{b}_1'$ to $\mathfrak{s}$, which originally represented multiplication by t, become multiplication by 1. Since $\mathfrak{s}$ is A, B, C, D-invariant, all other edges remain fixed. Taking the limit as $t \to \infty$ kills the edges in $\mathfrak{b}_1 \setminus \mathfrak{s}$ adjacent to $\mathfrak{s}$, so $\lim_{t\to\infty} \gamma(t) = f_2$. The $\mathbb{T}$-invariance of this curve can be verified pictorially (see Figure 3.12).

The tangent weight of this curve at f_1 can be read from any of the edges weighted by t. If the edge represents a C or B map, it is the weight of the target minus the weight of the source plus $\hbar$. If the edge represents an A or D map, it is simply the weight of the target minus the weight of the source. The tangent weight of the curve at f_2 is the negation of the tangent weight at f_1. In other

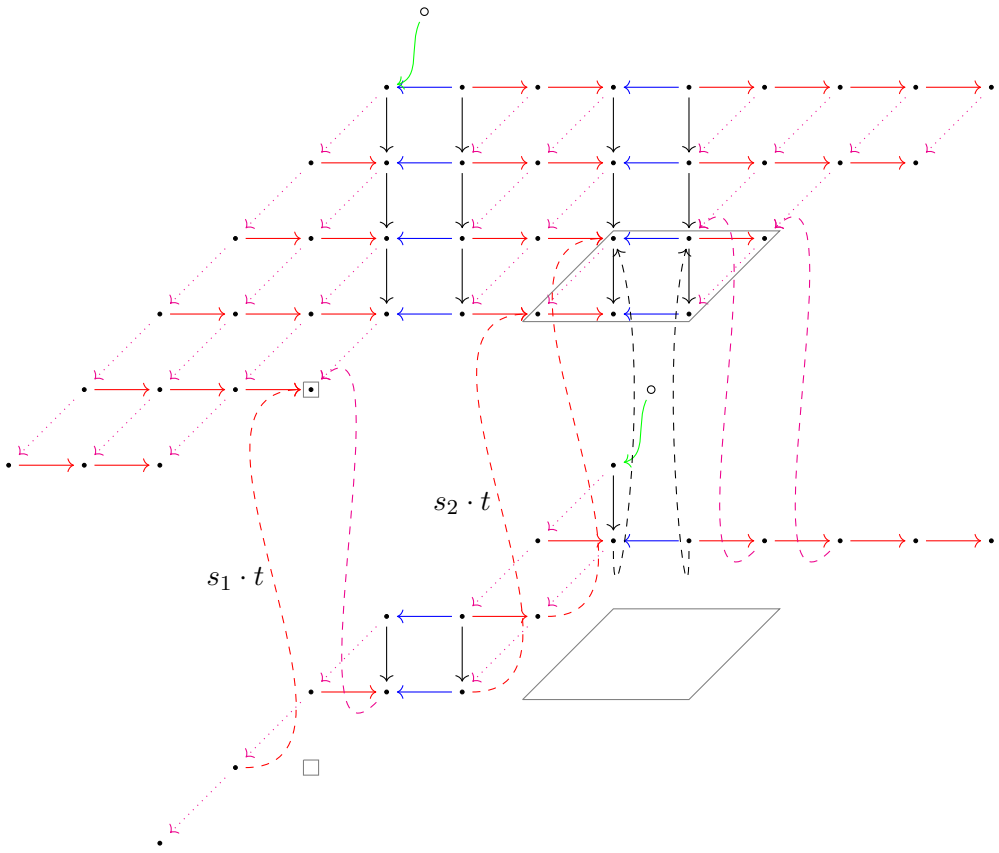

Figure 3.13: Explicit 2-dimensional pencil of invariant curves with tangent weight $\pm(u_1 - u_2)$ at its poles.

words, we have

$$e_{\mathbb{T}}(T_{f_1}\gamma) = -e_{\mathbb{T}}(T_{f_2}\gamma) = u - u' + \hbar^{y(\mathfrak{s})-y(\mathfrak{s}')} \in H^*_{\mathbb{T}}(\mathrm{pt}),$$

where $y(\mathfrak{s})$ is the maximum height (Definition 3.2.5) of the vertices of $\mathfrak{s}$ measured in $\mathfrak{b}_1$, and $y(\mathfrak{s}')$ is the maximum height of the vertices of $\mathfrak{s}'$ measured in $\mathfrak{b}'_2$. The tangent weight encodes which butterflies are involved in the butterfly surgery and the displacement in the position of the surgery site within each of these butterflies.

Suppose $\mathfrak{s}$ has $r > 1$ connected components. By replacing the curve parameter t in the ith component by $s_i \cdot t$, where $s_i \in \mathbb{C}^\times$, we obtain an r-parameter family of $\mathbb{T}$-invariant curves with poles f_1 and f_2. We may projectivize to obtain an r-dimensional pencil $(\mathbb{C}^\times)^{r-1} \times \mathbb{P}^1 \to \mathcal{C}(\mathcal{D})$ of $\mathbb{T}$-invariant curves with poles f_1, f_2. Consider partial butterfly surgeries obtained by restricting the surgery to a subset of the r connected components of $\mathfrak{s}$. There is a natural poset structure on the set of fixed points arising from these partial surgeries.

Definition 3.4.1. Let $f_1, f_2 \in \mathcal{C}(\mathcal{D})^{\mathbb{T}}$. If there is no butterfly surgery relating f_1 and f_2, then define $\mathfrak{S}(f_1, f_2) = \emptyset$. Otherwise, let $\mathfrak{s}$ be the site of the unique butterfly surgery relating f_1 to f_2. Let $\mathfrak{S}(f_1, f_2) \subset \mathcal{C}(\mathcal{D})^{\mathbb{T}}$ consist of the fixed points $\tilde{f}$ obtained from f_1 by restricting the butterfly surgery to some of the connected components of $\mathfrak{s}$. For $\tilde{f} \in \mathfrak{S}(f_1, f_2)$, let $\tilde{\mathfrak{s}}$ be the site of the surgery relating f_1 to $\tilde{f}$. Define a partial order on $\mathfrak{S}(f_1, f_2)$ by

$$\tilde{f}_1 \leq \tilde{f}_2 \Leftrightarrow \tilde{\mathfrak{s}}_1 \subset \tilde{\mathfrak{s}}_2.$$

It is easy to verify that this relation is a partial order with smallest element f_1 and largest element f_2. Suppose we have $\tilde{f}_1 \leq \tilde{f}_2 \in \mathfrak{S}(f_1, f_2)$. Fix $t \in \mathbb{C}^\times$, and take the limit as the s_i's associated with $\mathfrak{s} \setminus \tilde{\mathfrak{s}}_2$ approach 0, and the s_i's associated with $\tilde{\mathfrak{s}}_1$ approach ∞. This limit converges to the pencil of invariant curves with poles $\tilde{f}_1, \tilde{f}_2$ obtained from butterfly surgery. The results of this section are summarized by

Theorem 3.4.2. *Let $f_1, f_2 \in \mathcal{C}(\mathcal{D})^{\mathbb{T}}$.*

1. *If $\mathfrak{S}(f_1, f_2) \neq \emptyset$, then $|\mathfrak{S}(f_1, f_2)| = 2^r$ for some $r \in \mathbb{N}$, and there is an r-dimensional pencil of invariant curves with poles f_1, f_2. The tangent weights of each curve γ in this pencil are given by*

$$e_{\mathbb{T}}(T_{f_1}\gamma) = -e_{\mathbb{T}}(T_{f_2}\gamma) = u - u' + (y(\mathfrak{s}) - y(\mathfrak{s}'))\hbar \in H^*_{\mathbb{T}}(\mathrm{pt}),$$

   where $\mathfrak{s}$ is the site of the butterfly surgery sending f_1 to f_2, and U is the D5 brane whose butterfly contains $\mathfrak{s}$.

2. *For each $\tilde{f}_1, \tilde{f}_2 \in \mathfrak{S}(f_1, f_2)$, we have $\mathfrak{S}(\tilde{f}_1, \tilde{f}_2) = [\tilde{f}_1, \tilde{f}_2] \subset \mathfrak{S}(f_1, f_2)$. Moreover, the pencil of invariant curves associated with $\mathfrak{S}(\tilde{f}_1, \tilde{f}_2)$ (if there is one) is in the closure of the pencil of invariant curves associated with $\mathfrak{S}(f_1, f_2)$.*

Remark 3.4.3. One may also consider pencils of curves arising from disjoint independent butterfly surgeries on the same pair of butterflies. The curves in such pencils will be $\mathbb{A}$-invariant but not $\mathbb{T}$-invariant. Generalizing further to disjoint independent butterfly surgeries on different pairs of butterflies, we obtain $\mathbb{T}$-invariant pencils of curves. However, the individual curves in these pencils are not invariant with respect to $\mathbb{A}$ or $\mathbb{T}$.

Bow varieties are noncompact in general. Thus, there may be noncompact $\mathbb{T}$-invariant curves. By this, we mean an embedding $\gamma : \mathbb{C} \to \mathcal{C}(\mathcal{D})$ such that $\gamma(0) \in \mathcal{C}(\mathcal{D})^{\mathbb{T}}$ and $\lim_{t\to\infty} \gamma(t)$ diverges. Such curves are not captured by butterfly surgery. We suspect, however, that butterfly surgery does capture all compact invariant curves, that is, those that join pairs of fixed points.

Conjecture 3.4.4. *All pencils of $\mathbb{T}$-invariant curves joining pairs of $\mathbb{T}$-fixed points of $\mathcal{C}(\mathcal{D})$ can be obtained from butterfly surgery.*

Example 3.4.5. In Section 4.2.1, we will show that $\mathcal{C}(/2\backslash 2\backslash 2\backslash 2\backslash 2/) \cong T^*\mathrm{Gr}(2,4)$. The butterfly diagrams and butterfly surgeries relating them are indicated in Figure 3.14. Ignoring the framing vertex and green edges, each butterfly diagram has 2 butteflies of the form $\cdot \leftarrow \cdot \leftarrow \cdot \leftarrow \cdot \leftarrow \cdot$ and 2 empty butterflies. Suppose that the two nonempty butterflies have centers U_i, U_j. Then, the corresponding fixed point is given by the span of $\{\epsilon_i, \epsilon_j\}$ in $\mathbb{C}^4$, where ϵ_i is the ith standard basis vector. A butterfly surgery simply exchanges one of the nonempty butterflies with one of the empty ones. These surgeries give an invariant curve between $\mathbb{C}\{\epsilon_i, \epsilon_j\}$ and $\mathbb{C}\{\epsilon_i, \epsilon_k\}$ whenever $k \neq i, j$, with tangent weight $\pm(u_j - u_k)$. This accounts for all compact invariant curves and recovers the well known moment graph of $\mathrm{Gr}(2,4)$. Coordinate lines in the cotangent fibres over fixed points give noncompact invariant curves in $T^*\mathrm{Gr}(2,4)$, which are not obtained through butterfly surgery. Note that there are no higher dimensional pencils of invariant curves. In fact, $T^*\mathrm{Gr}(2,4)$ is a GKM variety [GKM].

Example 3.4.6. Consider the variety $\mathcal{C}(\backslash 2/2/2/2/2\backslash)$ corresponding to the dual brane diagram (Section 2.3) to Example 3.4.5. It is HW equivalent to a cobalanced bow variety, and from Section 3.3 we see that it is isomorphic to the Nakajima quiver variety $\mathcal{N}\left(\begin{array}{ccccc} 1 & & 2 & & 1 \\ \bullet & - & \bullet & - & \bullet \\ & & \square & & \\ & & 2 & & \end{array}\right)$. The butterfly diagrams and butterfly surgeries relating them are indicated in Figure 3.15. There is a natural bijection between the fixed points of this dual variety and those of $T^*\mathrm{Gr}(2,4)$ given by dualizing tie diagrams. The fixed point of a butterfly diagram in Figure 3.15 corresponds to the fixed point of the butterfly diagram in the same position in Figure 3.14 under this bijection. Note that while there were no higher dimensional pencils of invariant curves in $T^*\mathrm{Gr}(2,4)$, there is a 2-dimensional pencil in the dual.

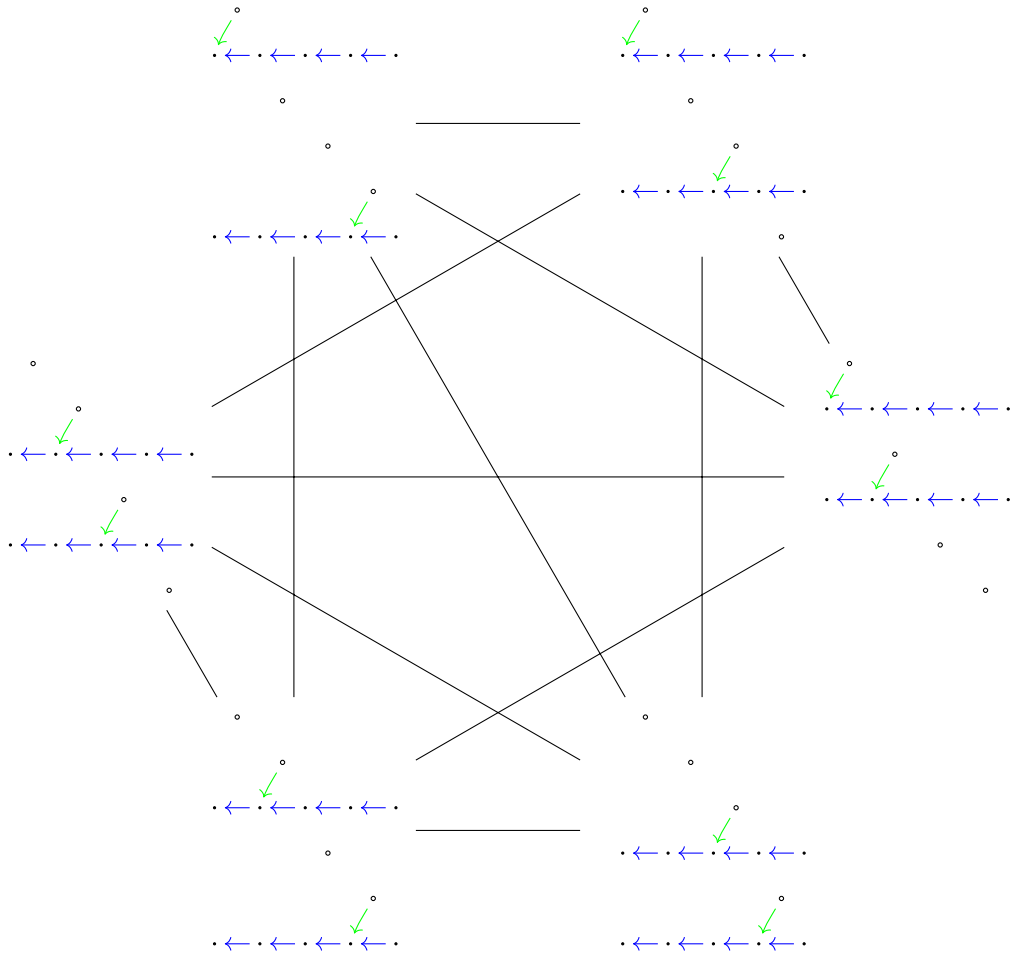

Figure 3.14: Butterfly diagrams for $\mathcal{C}(/2\backslash 2\backslash 2\backslash 2\backslash 2/) \cong T^*\mathrm{Gr}(2,4)$ with $\mathbb{T}$-invariant curves arising from butterfly surgery.

3.4.2 Tie Diagram Surgery for Separated Bow Varieties

In general, the combinatorics of butterfly surgeries is quite subtle. In this section, we will analyze butterfly surgeries in the special case where $\mathcal{D}$ is separated. Let m be the number of NS5 branes and n be the number of D5 branes in $\mathcal{D}$. Then, the number of segments is $s = m + n - 1$. From the structure of $\mathcal{D}$ (see Figure 2.14), we see that the site of any butterfly surgery cannot cross below the segments $X_m, ..., X_{m+n-1}$ on the right. Hence, the action of any butterfly butterfly surgery is constrained to below the segments $X_1, ..., X_{m-1}$ on the left. This and the fact that butterfly surgeries only affect two butterflies at a time, allow us to assume without loss of generality that $n = 2$. We denote the two D5 branes by U, U'. Consider a tie diagram on $\mathcal{D}$. Draw the ties as semicircular arcs. Then, the longer ties attached to a D5 brane enclose the smaller ones. Abusing

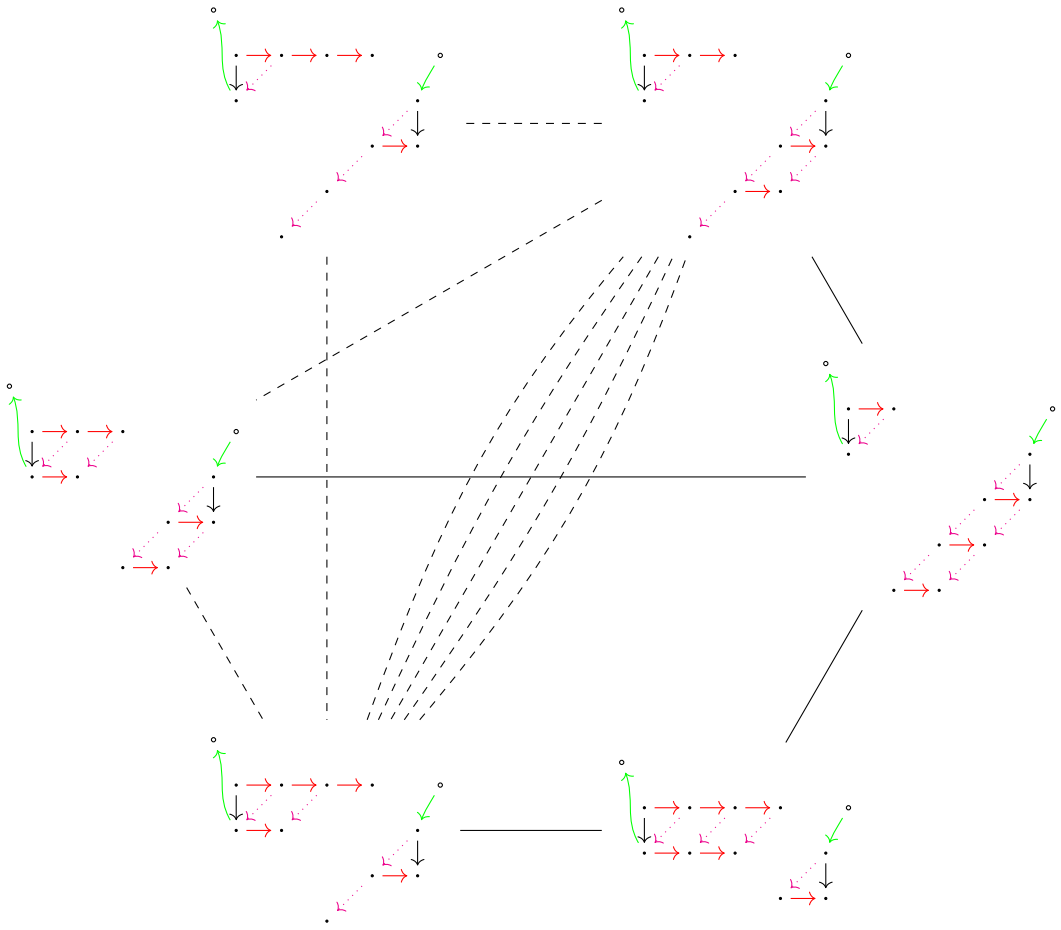

Figure 3.15: Butterfly diagrams for $\mathcal{C}(\backslash 2/2/2/2/2\backslash)$ with $\mathbb{T}$-invariant curves arising from butterfly surgery. The dashed curves are in the closure of the dashed pencil.

notation, let $\mathfrak{s}$ be a subset of the NS5 branes attached to U by a tie and $\mathfrak{s}'$ be a subset of the NS5 branes attached to U'. There is at most one tie joining each pair of 5-branes, so we may equivalently think of $\mathfrak{s}, \mathfrak{s}'$ as sets of ties.

Definition 3.4.7. Assume $|\mathfrak{s}| = |\mathfrak{s}'|$. Consider the operation of

- severing the ties of $\mathfrak{s}$ at the NS5 branes and reattaching them to the NS5 branes of $\mathfrak{s}'$, so that no ties attached to U pass through each other and
- severing the ties of $\mathfrak{s}'$ at the NS5 branes and reattaching them to the NS5 branes of $\mathfrak{s}$, so that no ties attached to U' pass through each other.

We further require that all ties of $\mathfrak{s}$ are reattached to NS5 branes either all to the left or all to the

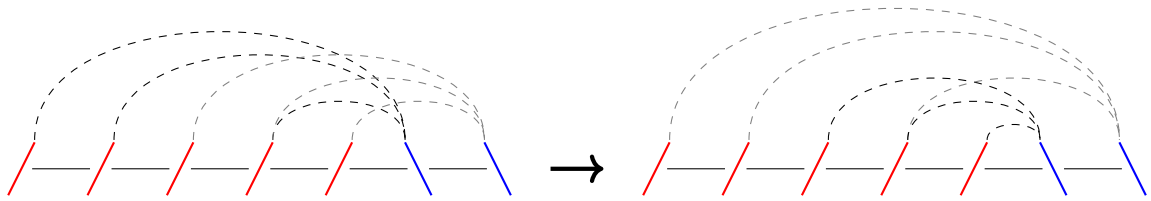

Figure 3.16: An example of an indecomposable tie diagram surgery involving all ties. Such surgeries give rise to invariant curves with tangent weights $\pm(u-u')$.

right of their original NS5 branes. This operation is a *tie diagram surgery* if it results in another tie diagram for $\mathcal{D}$. We refer to $\mathfrak{s}$ as the *site* of the surgery.

It follows from the conditions of Definition 3.4.7 that $\mathfrak{s}$ determines $\mathfrak{s}'$ up to whether the surgery reattaches ties to the left or the right. If for instance, $\mathfrak{s}$ is on the left, then $\mathfrak{s}'$ must contain the first $|\mathfrak{s}|$ NS5 branes attached to U' that are to the right of (or equal to) the leftmost NS5 brane in $\mathfrak{s}$.

Theorem 3.4.8. *When $\mathcal{D}$ is separated, tie diagram surgeries correspond to butterfly surgeries. The tangent weights of the corresponding invariant curves are*

$$\pm(u-u'-(y-y')\hbar), \tag{3.3}$$

where y is the number of ties attached to U enclosing $\mathfrak{s}\cup\mathfrak{s}'$, and y' is number of ties attached to U' enclosing $\mathfrak{s}\cup\mathfrak{s}'$. If $\mathfrak{s}$ is left of $\mathfrak{s}'$, then the sign in (3.3) is positive,and it is negative otherwise. If the tie diagram surgery can be decomposed into r independent surgeries with the same tangent weight, then it corresponds to a butterfly surgery on a site with r connected components.

Proof. We will show that any tie diagram surgery gives rise to a butterfly surgery. One can obtain an inverse using similar reasoning. Fix a tie diagram surgery with site $\mathfrak{s}$ that transforms the fixed point f_1 to f_2. Assume that $\mathfrak{s}$ is left of $\mathfrak{s}'$. Without loss of generality, we may assume that no ties attach to the left of $\mathfrak{s}$. Such ties simply add higher layers to the butterflies that play no role in any potential butterfly surgeries sending f_1 to f_2. Similarly, we may assume that there are no ties attaching to the right of $\mathfrak{s}'$. We will make a final simplification by assuming that the tie diagram surgery cannot be decomposed into independent surgeries on smaller sites. Such indecomposable surgeries will give rise to connected butterfly surgeries. Performing independent tie diagram surgeries simultaneously gives rise to pencils of invariant curves.

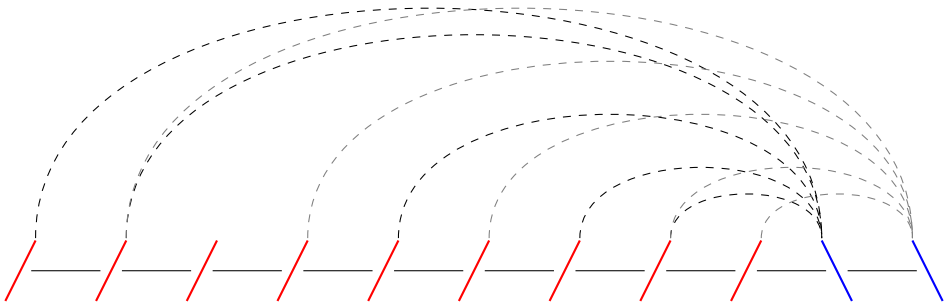

Figure 3.17: Performing surgery on all ties in this diagram gives rise to a 3-dimensional pencil of invariant curves with tangent weights $\pm(u - u')$.

From our simplifying assumptions, we may conclude that $\mathfrak{s}$ contains all ties attached to U, and consequently $\mathfrak{s}'$ contains all ties attached to U'. Indeed, suppose there is a tie attached to U not in $\mathfrak{s}$. We assumed that it does not attach to the left of $\mathfrak{s}$ or the right of $\mathfrak{s}'$, so it must attach somewhere in between. It obviously cannot attach to any NS5 brane in $\mathfrak{s}$, since all NS5 branes of $\mathfrak{s}$ are attached to U as well. Similarly, if it attaches to an NS5 brane in $\mathfrak{s}'$, then the surgery does not result in a tie diagram. Since ties attached to U and U' cannot pass through each other during surgery, this tie would split the surgery into two independent surgeries. We also assumed that this does not happen.

It follows that the desired butterfly surgery moves the bottom $d_X^U - d_X^{U'}$ vertices below X of the butterfly centered on U to the butterfly centered on U'. Removing these vertices from the U butterfly leaves $d_X^{U'}$ vertices below X. However, $d^{U'}$ is a butterfly dimension vector. Therefore, the remaining vertices form a butterfly. In particular, they form the portion of the butterfly centered on U' to the left of U. It follows that the deleted portion of the U butterfly has the correct shape to fit below the U' butterfly. Hence, we have obtained a butterfly surgery. Moreover, the tangent weight of the resulting invariant curve at f_1 is $u - u'$. Enclosing $\mathfrak{s} \cup \mathfrak{s}'$ with ties adds horizontal layers to the butterflies, causing a shift in weights. □

Example 3.4.9. We will use tie diagram surgeries to recover a part of Figure 4.5. Consider the tie diagram

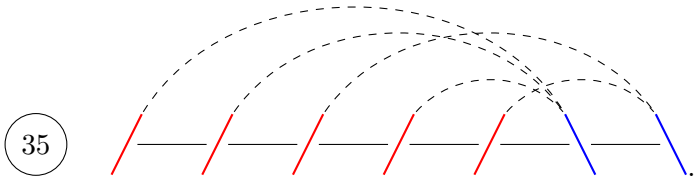

Two independent surgeries can be performed. Taking the convention that $\mathfrak{s}$ is left of $\mathfrak{s}'$, these two surgeries have sites $\mathfrak{s}_1 = \{V_2\}, \mathfrak{s}_2 = \{V_4\}$. Performing partial surgery on $\mathfrak{s}_1$ and $\mathfrak{s}_2$ yields

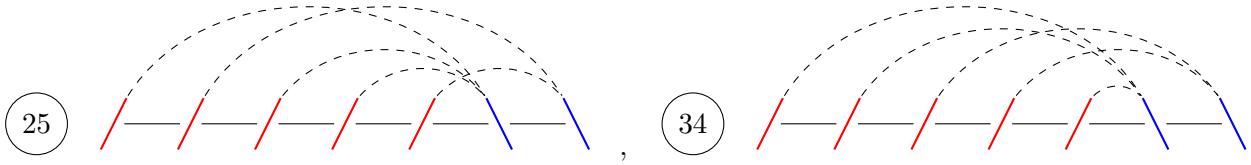

respectively. Performing the full surgery on $\mathfrak{s}_1 \cup \mathfrak{s}_2$ yields

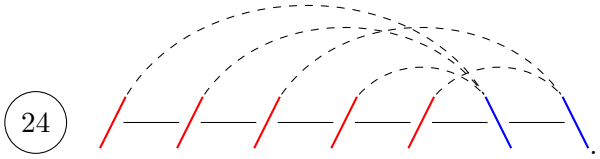

There is one enclosing tie, which is attached to U_1, so the resulting 2-dimensional pencil of curves has tangent weight $u_1 - u_2 - \hbar$ at 35. The poset $\mathfrak{S}(35, 24)$ (and corresponding invariant curves) is illustrated in Figure 4.5 along with the other sugery posets for this brane diagram.

CHAPTER 4

Characteristic Classes

In this chapter, we will begin with an overview of characteristic classes for partial flag varieties in (equivariant) cohomology, K-theory, and elliptic cohomology. Elliptic characteristic classes lead to a notion of 3d (N=4) mirror symmetry for partial flag varieties. Existing results for full flag varieties [RSVZ2, RW2] and Grassmannians [RSVZ1] will be summarized. Finally, we will take the first steps toward generalizing such results to bow varieties by creating and analyzing conjectural formulas for cohomological stable envelopes for bow varieties.

4.1 Partial Flag Varieties and Schubert Calculus

Important motivating ideas for the study of the bow varieties in this work come from the study of characteristic classes in the cohomology, K-theory, and elliptic cohomology of partial flag varieties. This section aims to give a brief overview of this area of mathematics, and show why it naturally leads to the study of bow varieties.

4.1.1 Partial Flag Varieties

Given $v_1, ..., v_n \in \mathbb{N}$, let $M = \mathcal{F}_{v_1,...,v_{n+1}}$ be the partial flag variety parametrizing nested sequences of subspaces

$$0 \subset \mathcal{V}_1 \subset \cdots \subset \mathcal{V}_n \subset \mathbb{C}^{v_{n+1}},$$

where $\dim(\mathcal{V}_i) = v_i$. Partial flag varieties are smooth with a natural action of the torus $\mathbb{A} = (\mathbb{C}^\times)^{v_{n+1}}$. Let $\underline{v}_i = v_i - v_{i-1}$ for $1 \leq i \leq n+1$, where $v_0 = 0$ by convention. Denote a partition of the set $\{1, ..., v_{n+1}\}$ into a tuple of sets $I_1, ..., I_{n+1}$ of size $\underline{v}_1, ..., \underline{v}_{n+1}$ by

$$I = \{I_1|\cdots|I_n\} = \{i_{1,1}, ..., i_{1,\underline{v}_1}|i_{2,1}, ..., i_{2,\underline{v}_2}|\cdots|i_{n,1}, ..., i_{n,\underline{v}_n}\},$$

where the set of size $\underline{v}_{n+1}$ is not listed (it is just the complement of the listed sets). Let $\mathcal{I}$ be the set of all such partitions. These tuples are in bijection with the $\mathbb{A}$-fixed points of M. Namely, I corresponds to the flag f_I given by $\mathcal{V}_j = \mathbb{C}\{\epsilon_i \mid i \in I_1 \cup \cdots \cup I_j\}$, where ϵ_j is the jth standard

basis vector in $\mathbb{C}^{v_{n+1}}$. Partial flag varieties admit a canonical CW structure called the "Bruhat decomposition". The cells of the Bruhat decomposition are called "Schubert cells", and the cell closures are called "Schubert varieties". There is one such cell associated to each fixed point. The Schubert cell Ω_I is the Borel (upper triangular invertible matrices) orbit of the fixed point f_I. There is an induced partial order on $M^{\mathbb{A}}$, the "Bruhat order", given by

$$f_I \leq f_J \Leftrightarrow \Omega_I \subset \overline{\Omega_J}.$$

The Bruhat order can also be described combinatorially as a partial order on $\mathcal{I}$. For $I = \{I_1|\cdots|I_n\}, J = \{J_1|\cdots|J_n\} \in \mathcal{I}$, let

$$I_1 \cup \cdots \cup I_k = \{i_1^k, ..., i_{v_k}^k\} \quad , \quad J_1 \cup \cdots \cup J_k = \{j_1^k, ..., j_{v_k}^k\},$$

where $i_1^k < \cdots < i_{v_k}^k$ and $j_1^k < \cdots < j_{v_k}^k$ for all $1 \leq k \leq n$. The Bruhat order is given by

$$I \leq J \Leftrightarrow i_l^k \leq j_l^k \text{ for all } 1 \leq k \leq n \text{ and } 1 \leq l \leq v_k.$$

An important area of mathematics involves associating characteristic classes to Schubert cells and varieties.

4.1.2 Schubert Calculus

The study of ($\mathbb{A}$-equivariant) characteristic classes of flag varieties falls under the umbrella of "Schubert calculus". Classically, the cohomological and K-theoretic fundamental classes $[\Omega_I]$ of Schubert varieties were studied. These form bases for the cohomology and K-theory rings of the variety, and questions of change of basis (e.g. Schubert/Grothendieck polynomials), and structure constants (e.g. Schubert problems and Littlewood-Richardson numbers) were explored. More recently, deformations of the fundamental class—the Chern-Schwarz-MacPherson class [M, Oh1, Oh2, Sch, W1] in cohomology and motivic Chern class [BSY, FRW1] in K-theory— gave rise to $\hbar$-deformed Schubert calculus. See [Ri] for a summary and [AMSS1, AMSS2, FR, RTV1, RTV2] for results.

Let M be a smooth complex algebraic variety. Both the Chern-Schwarz-MacPherson (CSM) and motivic Chern (mC) class can be defined axiomatically as the unique characteristic class associating

an element of H^*M or $K^0M[y^{\pm 1}]$, respectively, to each constructible subset $Z \subset M$ satisfying

1. additivity: if $Y, Z \subset M$ are disjoint, then the class of $Y \cup Z$ is the sum of the class of Y and the class of Z,

2. functoriality: if Y is smooth and $\phi : M \to N$ is a proper morphism, then the pushforward of the class of $Z \subset X$ is the class of $\phi(Z) \subset Y$,

3. normalization: the class of M itself is the total Chern class of TM.

We adopt the convention of using

$$\Lambda_y(\eta) = \sum_i y^i \bigwedge^i \eta^\vee$$

as the K-theoretic total Chern class of a vector bundle ξ. Such characteristic classes are referred to as "motivic". There is, for instance, a motivic version of the Hirzebruch class [BSY, W2], where in the normalization axiom, the total Chern class is replaced by the Hirzebruch class. Equivariant versions of these characteristic classes exist and are defined the same way. Note that while a fundamental class is associated to all closed subvarieties of M, the CSM and mC classes are defined for all subvarieties of M. Moreover, it is easy to see from the axioms that for any subvariety $Z \subset M$, the lowest degree term of the CSM class of Z is the fundamental class of $\overline{Z}$. A similar property holds for the mC class with $y = 0$. Hence, these classes deform the fundamental class.

When $M = \mathcal{F}_{v_1,\ldots,v_{n+1}}$, the deformation property implies that the CSM classes and mC classes of both Schubert cells and Schubert varieties form bases for H^*M and $K^0M[y^{\pm 1}]$, respectively. Hence, both give reasonable notions of deformed Schubert classes. For our purposes, the classes associated to Schubert cells will be more natural. The CSM and mC classes

$$\mathrm{c}^{\mathrm{sm}}(\Omega_I) \in H^*M \quad , \quad \mathrm{mC}(\Omega_I) \in K^0M[y^{\pm 1}],$$

are called "deformed Schubert classes". The change of basis relating the classical Schubert classes to the deformed Schubert classes is studied in [AM1, AM2, AMSS1, AMSS2].

Example 4.1.1. The simplest nontrivial example is $M = \mathcal{F}_{1,2} = \mathbb{P}^1$. The two Schubert cells are

$$\Omega_{\{1\}} = \{[1:0]\} \quad , \quad \Omega_{\{2\}} = \{[z:1] \mid z \in \mathbb{C}\} = \mathbb{P}^1 \setminus \Omega_{\{1\}}.$$

It follows immediately from the defining axioms that

$$\begin{aligned} \mathrm{c}^{\mathrm{sm}}(\Omega_{\{1\}}) &= [\Omega_{\{1\}}] \quad , \quad \mathrm{mC}(\Omega_{\{1\}}) = [\Omega_{\{1\}}] \quad , \\ \mathrm{c}^{\mathrm{sm}}(\Omega_{\{2\}}) &= c^*(T\mathbb{P}^1) - [\Omega_{\{1\}}] \quad , \quad \mathrm{mC}(\Omega_{\{2\}}) = \Lambda_y(T\mathbb{P}^1) - [\Omega_{\{1\}}] \quad . \end{aligned}$$

Remark 4.1.2. The simplicity of Example 4.1.1 is due to the fact that all Schubert varieties in $\mathbb{P}^1$ are smooth. Hence, we may compute the CSM and mC class of a Schubert variety by pushing forward the total Chern classes of its tangent bundle through the inclusion map. The deformed Schubert classes can then be obtained by subtracting the class of its boundary, which is another Schubert variety. In all partial flag varieties that are not projective spaces, there will be singular Schubert varieties. However, the same approach can be carried out replacing inclusion maps of Schubert varieties with Bott-Samuelson resolutions and using inclusion-exclusion to delete the boundaries of the Schubert varieties.

4.1.3 Stable Envelopes

The previous approach applies to both the equivariant and nonequivariant settings. In the $\mathbb{A}$-equivariant setting, there is an alternative approach to deformed Schubert classes called "stable envelopes" [MO, O]. Instead of the partial flag variety $\mathcal{F}_{v_1,\ldots,v_{n+1}}$, we consider the cotangent bundle $M = T^*\mathcal{F}_{v_1,\ldots,v_{n+1}}$, with additional $\mathbb{C}^\times_\hbar$-action given by scaling the fibres by $\mathbf{h}^{-1}$, where $\mathbf{h}$ is the coordinate of $\mathbb{C}^\times_\hbar$. Let $\mathbb{T} = \mathbb{A} \times \mathbb{C}^\times_\hbar$. Cotangent bundles of partial flag varieties are examples of GKM varieties [GKM]. Hence, the cohomological and K-theoretic localization maps

$$\mathrm{Loc}^K : K^0_{\mathbb{T}}(M) \to \bigoplus_{I\in\mathcal{I}} K^0_{\mathbb{T}}(f_I) \quad , \quad \mathrm{Loc} : H^*_{\mathbb{T}}(M) \to \bigoplus_{I\in\mathcal{I}} H^*_{\mathbb{T}}(f_I),$$

defined component-wise by fixed point restrictions, as in Section 3.2.3, are injective with image determined by GKM conditions. The GKM conditions are related to $\mathbb{T}$-invariant curves in M (see Section 3.4). GKM varieties have no higher dimensional pencils of invariant curves, and each invariant curve places a condition on its poles. Namely, the difference of the fixed point restrictions at the poles f_I, f_J of each invariant curve γ must be divisible by $e_{\mathbb{T}}(T\gamma)|_{f_I}$ (or equivalently by $e_{\mathbb{T}}(T\gamma)|_{f_J}$). The stable envelope classes

$$\mathrm{Stab}(f) \in H^*_{\mathbb{T}}(M) \quad , \quad \mathrm{Stab}^K(f) \in K^0_{\mathbb{T}}(M),$$

are axiomatically defined characteristic classes associated with the $\mathbb{T}$-fixed points f of T^*M. These fixed points are precisely the image of the $\mathbb{A}$-fixed points of $\mathcal{F}_{v_1,...,v_{n+1}}$ under the 0-section. Before listing the axioms, we need a few preliminary constructions.

We begin by describing $\mathbb{T}$-equivariant virtual bundles over M and each fixed point $f \in M^{\mathbb{T}}$. The *canonical polarization bundle* of M is

$$T^{1/2}M = \pi^*(T\mathcal{F}_{v_1,...,v_{n+1}}),$$

where $\pi : M = T^*\mathcal{F}_{v_1,...,v_{n+1}} \to \mathcal{F}_{v_1,...,v_{n+1}}$ is the cotangent bundle projection. Observe that

$$T^{1/2}M \oplus \mathbf{h}^{-1}(T^{1/2}M)^\vee = TM.$$

Denote the coordinates of $\mathbb{A}$ by $\mathbf{u}_1, ..., \mathbf{u}_{v_{n+1}}$ and the coordinate of $\mathbb{C}^\times_\hbar$ by $\mathbf{h}$. For each $f \in M^{\mathbb{T}}$, the $\mathbb{T}$-representation T_fM can expressed as a sum of Grothendieck roots of the form $\mathbf{h}^k\mathbf{u}_i/\mathbf{u}_j$, where $k \in \mathbb{Z}$. Define $T^-_f M$ to be the sum of all Grothendieck roots with $i > j$, and $T^+_f M$ to be the sum of all Grothendieck roots with $i < j$. We have

$$T^-_f M \oplus T^+_f M = T_fM.$$

This definition extends to any equivariant subbundle of T_fM. Next, we recall the definition of Newton polytope.

Definition 4.1.3. Given a Laurent polynomial $\rho \in \mathbb{Z}[\mathbf{h}^\pm][\mathbf{u}_1^\pm, ..., \mathbf{u}_{v_{n+1}}^\pm]$, its Newton polytope $\Delta(\rho) \subset \mathbb{R}^{v_{n+1}}$ is the convex hull of all points $(k_1, ..., k_{v_{n+1}}) \in \mathbb{Z}^{v_{n+1}}$ for which the coefficient of $\mathbf{u}_1^{k_1} \cdots \mathbf{u}_{v_{n+1}}^{k_{v_{n+1}}}$ in ρ is nonzero.

We are now ready to state the stable envelope axioms.

Definition 4.1.4. For each $f \in M^{\mathbb{T}}$, the *cohomological stable envelope class* $\mathrm{Stab}(f)$ is the unique homogeneous degree $\dim_{\mathbb{C}}(M)/2$ element of $H^*_{\mathbb{T}}(M)$ satisfying

- (support-1) $\mathrm{Stab}(f_I)|_{f_J} = 0$ unless $J \leq I$,
- (support-2) $\mathrm{Stab}(f_I)|_{f_J}$ is divisible by $e_{\mathbb{T}}(T^-_{f_J}\pi^{-1}(f_J))$,

- (normalization) $\mathrm{Stab}(f)|_f = P_f e_{\mathbb{T}}(T_f^- M)$, where $P_f = \frac{e_{\mathbb{A}}(T_f^{1/2} M)}{e_{\mathbb{A}}(T_f^- M)}$,
- (boundary) $\mathrm{Stab}(f_I)|_{f_J}$ is divisible by $\hbar$ whenever $I \neq J$.

Definition 4.1.5. For each $f \in M^{\mathbb{T}}$, the *K-theoretic stable envelope class* $\mathrm{Stab}^K(f)$ is the unique element of $K^0_{\mathbb{T}}(M)$ satisfying

- (support-1) $\mathrm{Stab}^K(f_I)|_{f_J} = 0$ unless $J \leq I$,
- (support-2) $\mathrm{Stab}^K(f_I)|_{f_J}$ is divisible by $e_{\mathbb{T}}(T^-_{f_J} \pi^{-1}(f_J))$,
- (normalization) $\mathrm{Stab}^K(f)|_f = P_f e_{\mathbb{T}}(T_f^- M)$, where $P_f = \frac{e_{\mathbb{A}}(T_f^{1/2} M)}{e_{\mathbb{A}}(T_f^- M)}$,
- (boundary) $\Delta(\mathrm{Stab}^K(f_I)|_{f_J}) \subset \Delta(\mathrm{Stab}^K(f_I)|_{f_I}) \setminus \{0\}$ whenever $I \neq J$.

We use $e(\eta) = \Lambda_{-1}(\eta)$ as the K-theoretic Euler class of a vector bundle η.

Remark 4.1.6. The support-1 axiom follows from the rest, but it is an important feature of stable envelopes, so we list it anyways. Support-2 is a local version of the global support axiom in [MO]. Consider conormal bundles $C\Omega_I \subset M$ of Schubert cells in the partial flag variety, and define $\mathrm{Slope}(f_I) = \bigcup_{J \leq I} C\Omega_J$. The global support condition may be phrased as $\mathrm{Stab}(f_I)$ and $\mathrm{Stab}^K(f_I)$ being in the kernel of the map in cohomology or K-theory, respectively, induced by the inclusion $M \setminus \mathrm{Slope}(f_I) \hookrightarrow M$. The fact that the global and local conditions are equivalent can be proven using the Gysin sequence and a Meyer-Vietoris induction [RTV2, Section 5.25].

By extending the Bruhat order on $M^{\mathbb{T}}$ to a linear order $f_1 \leq \cdots \leq f_r$, we may list the fixed point restrictions of the stable envelope classes in an $r \times r$ matrix. Define

$$\mathrm{Stab} = (\mathrm{Stab}(f_i)|_{f_j})_{1 \leq i,j \leq r} \quad \text{and} \quad \mathrm{Stab}^K = (\mathrm{Stab}^K(f_i)|_{f_j})_{1 \leq i,j \leq r}.$$

Each column corresponds to a fixed point and each row contains the fixed point restrictions of a stable envelope class. The stable envelope axioms may be rephrased in terms of these matrices. The normalization axiom fixes the diagonal, and the support-1 axiom translates to lower triangularity. In cohomology, support-2 translates to each entry below a diagonal entry being divisible by the terms of the diagonal entry with $\hbar$. The boundary axiom can also be phrased as a relationship between a diagonal entry the terms below it. In the cohomology case, the entries below a diagonal

entry must be divisible by $\hbar$. In the K-theory case, the Newton polytope of each entry below a diagonal entry must be contained in the Newton polytope of the diagonal entry minus the origin. Let us consider an example.

Example 4.1.7. The simplest nontrivial example is $M = T^*\mathbb{P}^1 = T^*\mathcal{F}_{1,2}$. There are two fixed points $\{1\} = [1:0] \leq \{2\} = [0:1]$. Consider the matrices of fixed point restrictions

$H^*_{\mathbb{T}}M$	$\{1\}$	$\{2\}$
$\mathrm{Stab}(f_{\{1\}})$	$u_2 - u_1$	0
$\mathrm{Stab}(f_{\{2\}})$	$\hbar$	$u_1 - u_2 + \hbar$

,

$K^0_{\mathbb{T}}M$	$\{1\}$	$\{2\}$
$\mathrm{Stab}(f_{\{1\}})$	$1 - \frac{\mathbf{u}_1}{\mathbf{u}_2}$	0
$\mathrm{Stab}(f_{\{2\}})$	$(\mathbf{h}-1)\frac{\mathbf{u}_1}{\mathbf{u}_2}$	$\mathbf{h} - \frac{\mathbf{u}_2}{\mathbf{u}_1}$

.

The stable envelope axioms are easy to verify. However, we must also check that these restrictions are in the image of the localization maps, i.e. the restrictions come from an element of $H^*_{\mathbb{T}}M$ or $K^0_{\mathbb{T}}M$. Let $S \to M$ be the pull-back of the tautological line bundle on $\mathbb{P}^1$ under the cotangent bundle projection. The fixed point restrictions of S are

$$S|_{f_{\{1\}}} = \mathbf{u}_1 \quad , \quad S|_{f_{\{2\}}} = \mathbf{u}_2.$$

Hence, we see that

$$\begin{aligned} \mathrm{Stab}(f_{\{1\}}) &= e_{\mathbb{T}}(\mathbf{u}_2/S) \quad , \quad \mathrm{Stab}^K(f_{\{1\}}) = e_{\mathbb{T}}(\mathbf{u}_2/S) \quad , \\ \mathrm{Stab}(f_{\{2\}}) &= e_{\mathbb{T}}(\mathbf{h}\mathbf{u}_1/S) \quad , \quad \mathrm{Stab}^K(f_{\{2\}}) = (\mathbf{h}S/\mathbf{u}_2) \cdot e_{\mathbb{T}}(\mathbf{h}\mathbf{u}_1/S) \quad . \end{aligned}$$

Alternatively, one can check the GKM conditions. There is an invariant curve, the 0-section, joining the two fixed points, with tangent weights $\pm(u_1 - u_2)$ at its poles. Thus, the GKM conditions state that the two columns in each table agree upon setting $u_1 = u_2$ and $\mathbf{u}_1 = \mathbf{u}_2$.

Various approaches exist for computing the matrices of fixed point restrictions for stable envelopes. The conjectural formulas of Section 4.3.6 are generalizations of the weight functions of [RTV1, RTV2]. Note that the conventions of [RTV1, RTV2] differ slightly from our conventions, so the fixed point restrictions may differ slightly.

Table 4.1: Comparison of deformed Schubert classes with stable envelope classes.

Equivariant CSM and mC classes	Stable envelopes
$\mathcal{F}_{v_1,\dots,v_{n+1}}$	$T^*\mathcal{F}_{v_1,\dots,v_{n+1}}$
Permutation in $S_{v_{n+1}}$/Schubert frame	Chamber in Lie($\mathbb{T}$)
Schubert cell Ω_I	Attracting set of f_I
$\mathrm{c}^{\mathrm{sm}}(\Omega_I)$ and $\mathrm{mC}(\Omega_I)$	$\mathrm{Stab}(f_I)$ and $\mathrm{Stab}^K(f_I)$

4.1.4 Relating Deformed Schubert Classes to Stable Envelopes

Performing the calculation of Example 4.1.1 equivariantly, we obtain the following fixed point restrictions:

$H^*_{\mathbb{T}}M$	$\{1\}$	$\{2\}$
$\mathrm{c}^{\mathrm{sm}}(\Omega_{\{1\}})$	u_2-u_1	0
$\mathrm{c}^{\mathrm{sm}}(\Omega_{\{2\}})$	1	u_1-u_2+1

,

$K^0_{\mathbb{T}}M$	$\{1\}$	$\{2\}$
$\mathrm{mC}(\Omega_{\{1\}})$	$1-\frac{\mathbf{u}_1}{\mathbf{u}_2}$	0
$\mathrm{mC}(\Omega_{\{2\}})$	$(1+y)\frac{\mathbf{u}_1}{\mathbf{u}_2}$	$1+y\frac{\mathbf{u}_2}{\mathbf{u}_1}$

.

Indeed, the first row of each matrix gives the fixed point restrictions of the fundamental class of the point $[1:0]$, and adding the two rows yields the fixed point restrictions of the total Chern class of $T\mathbb{P}^1$. Observe that the CSM classes agree with the cohomological stable envelope classes computed in Example 4.1.7 after setting $\hbar \mapsto 1$. Moreover, the mC classes agree with the K-theoretic stable envelope classes after setting $y \mapsto -\mathbf{h}^{-1}$ and multiplying the second row by $\mathbf{h} = \mathbf{h}^{\dim(\Omega_{\{2\}})}$. These relationships hold in general. Those familiar with the generalities of CSM and mC classes and stable envelopes for partial flag varieties may use Table 4.1 for comparisons (see [FRW2] for details).

4.1.5 Elliptic Schubert Classes

The two approaches to deformed Schubert classes in Section 4.1.2, 4.1.3 can be lifted to elliptic cohomology. Since we do not study elliptic characteristic classes for bow varieties in this work, we will not give any precise definitions. Instead, we will highlight key features of elliptic characteristic classes related to 3d mirror symmetry.

In this section, we will work with extended equivariant elliptic cohomology only. Like in cohomology and K-theory, every elliptic cohomology class is determined by its fixed point restrictions. Rather than explain what the extended equivariant elliptic cohomology is in general, we will only explain how to construct the extended equivariant elliptic cohomology of a point.

The extended $\mathbb{A}$-equivariant elliptic cohomology of a point $f \in \mathcal{F}^{\mathbb{A}}_{v_1,\dots,v_{n+1}}$ is the space of sections

of certain line bundles over the abelian variety $E^{v_{n+1}+(n+1)}$, where $E = \mathbb{C}^\times/\langle q\rangle,\ 0 < |q| < 1$ is a fixed elliptic curve. Here many different choices involving which line bundles we consider and what kind of sections we consider can be made. We will not go into details regarding these choices. Denoting the coordinates of this abelian variety by $\mathbf{u}_1, ..., \mathbf{u}_{v_{n+1}}, \mathbf{v}_1, ..., \mathbf{v}_{n+1}$, such sections can be described by quasiperiodic meromorphic functions in $\mathbf{u}_1, ..., \mathbf{u}_{v_{n+1}}, \mathbf{v}_1, ..., \mathbf{v}_{n+1}$. The quasiperiod in each coordinate determines which line bundle the section belongs to. We call $\mathbf{u}_1, ..., \mathbf{u}_{v_{n+1}}$ the *equivariant parameters* and $\mathbf{v}_1, ..., \mathbf{v}_{n+1}$ the *Kähler* or *dynamical* parameters. The new Kähler parameters are an important aspect of this theory. As we did for mC classes, we adjoin a formal parameter y as well. In this context, this means adding another factor of E with coordinate y to the Cartesian product. In terms of quasiperiodic functions, we allow for quasiperiodic meromorphic depence on y. Denote the extended elliptic cohomology with formal parameter by $Ell_{\mathbb{A}}$.

The CSM and mC classes are lifted to $Ell_{\mathbb{A}}$ by the Borisov-Libgober elliptic class $\mathcal{E}\ell\ell$ of [BL]. The additivity axiom no longer holds in the elliptic setting, but there is a normalization and functoriality property. BGG style recursions for the fixed point restrictions of $\mathcal{E}\ell\ell(\Omega_I)$ are obtained from Bott-Samuelson resolutions in [RW1, KRW]. Stable envelopes can also be lifted to elliptic cohomology.

Like before, in order to define stable envelopes, we pass to the cotangent bundle with additional $\mathbb{C}_\hbar^\times$-action on the fibres. The extended $\mathbb{T} = \mathbb{A} \times \mathbb{C}_\hbar^\times$-equivariant cohomology of a point $f \in T^*\mathcal{F}^{\mathbb{T}}_{v_1,...,v_{n+1}}$ is the space of sections of certain line bundles over the abelian variety $E^{v_{n+1}+(n+1)+1}$. Denote the coordinates of this abelian variety by $\mathbf{u}_1, ..., \mathbf{u}_{v_{n+1}}, \mathbf{v}_1, ..., \mathbf{v}_{n+1}, \mathbf{h}$. Like before, $\mathbf{u}_1, ..., \mathbf{u}_{v_{n+1}}$ are the equivariant parameters, and $\mathbf{v}_1, ..., \mathbf{v}_{n+1}$ are the Kähler or dynamical parameters. Sections can be described as quasiperiodic meromorphic functions in these parameters. Denote the extended $\mathbb{T}$-equivariant elliptic cohomology by $Ell_{\mathbb{T}}$.

Elliptic stable envelope classes $\mathrm{Stab}^{Ell}(f) \in Ell_{\mathbb{T}}(T^*\mathcal{F}_{v_1,...,v_n})$ are defined axiomatically in [AO]. They are related to $\mathcal{E}\ell\ell$ by the substitution $y \mapsto \mathbf{h}^{-1}$ and a renormalization. The fixed point restrictions can be expressed in terms of Jacobi theta functions

$$\theta(x) = \theta(x, q) = x^{1/2}(1 - x^{-1}) \prod_{j\geq 1}(1 - q^j x)(1 - q^j/x).$$

Weight function formulas for the elliptic stable envelope are given in [RTV3]. See Table 4.2 for the

Table 4.2: The restriction matrices of the elliptic stable envelope of $T^*\mathbb{P}^1$ with respect to the Bruhat order and reverse Bruhat order.

$Ell_{\mathbb{T}}(T^*\mathbb{P}^1)$	$\{1\}$	$\{2\}$
$\mathrm{Stab}^{Ell}(f_{\{1\}})$	$\theta(\frac{\mathbf{u}_2}{\mathbf{u}_1})\theta(\frac{\mathbf{h}\mathbf{v}_2}{\mathbf{v}_1})$	0
$\mathrm{Stab}^{Ell}(f_{\{2\}})$	$\theta(\mathbf{h})\theta(\frac{\mathbf{u}_2\mathbf{v}_2}{\mathbf{u}_1\mathbf{v}_1})$	$\theta(\frac{\mathbf{h}\mathbf{u}_1}{\mathbf{u}_2})\theta(\frac{\mathbf{v}_2}{\mathbf{v}_1})$

$Ell_{\mathbb{T}}(T^*\mathbb{P}^1)$	$\{2\}$	$\{1\}$
$\mathrm{Stab}^{Ell}(f_{\{2\}})$	$\theta(\frac{\mathbf{h}\mathbf{u}_1}{\mathbf{u}_2})\theta(\frac{\mathbf{v}_2}{\mathbf{v}_1})$	$\theta(\mathbf{h})\theta(\frac{\mathbf{u}_2\mathbf{v}_2}{\mathbf{u}_1\mathbf{v}_1})$
$\mathrm{Stab}^{Ell}(f_{\{1\}})$	0	$\theta(\frac{\mathbf{u}_2}{\mathbf{u}_1})\theta(\frac{\mathbf{h}\mathbf{v}_2}{\mathbf{v}_1})$

elliptic stable envelope of $T^*\mathbb{P}^1$.

Remark 4.1.8. The Borisov-Libgober class and elliptic stable envelope are elliptic versions of the deformed Schubert classes in cohomology and K-theory. However, it is incorrect to say that they are themselves deformations. For technical reasons, there is no well-defined notion of elliptic fundamental class. Indeed, twisting by the Kähler and $y = \mathbf{h}^{-1}$ parameters is essential for defining elliptic characteristic classes of singular subvarieties. See [Ri] for an intuitive introduction to elliptic cohomology and the necessity of extending by additional parameters.

4.1.6 3d Mirror Symmetry for Full Flag Varieties

Compare the two matrices in Table 4.2. The matrix on the left is the restriction matrix for the elliptic stable envelope of $T^*\mathbb{P}^1$. The matrix on the right is the same matrix with the order of the rows and columns reversed. Using the fact that $\theta(x^{-1}) = -\theta(x)$, we find that the first matrix is related to the second by

1. transposing,
2. switching equivariant and Kähler paramenters, $\mathbf{u}_i \mapsto \mathbf{v}_i$,
3. substituting $\mathbf{h} \mapsto \mathbf{h}^{-1}$,
4. and multiplying by -1.

This is an incarnation of the phenomenon of 3d mirror symmetry.

Motivated by ideas from physics [BFN, BDGH, GW, GMMS, IS], we expect certain holomorphic symplectic $\mathbb{T}$-manifolds (with some additional structures) to come in dual pairs (M, M'). One aspect of this notion of duality is a relationship between the elliptic stable envelopes of M and M'. Namely, we want a natural bijection $M^{\mathbb{T}} \leftrightarrow {M'}^{\mathbb{T}}$ between the torus fixed points under which the restriction

matrices of the elliptic stable envelopes "match". This "matching" is given by transposition, followed by interchanging equivariant and Kähler parameters, substituting $\mathbf{h} \leftrightarrow \mathbf{h}^{-1}$, and inserting signs.

Definition 4.1.9. Let M be a holomorphic symplectic $\mathbb{T}$-manifold and M' be a holomorphic symplectic $\mathbb{T}'$-manifold (with some additional requirements). Let $\mathbf{u}_1, ..., \mathbf{u}_n$ and $\mathbf{v}_1, ..., \mathbf{v}_m$ be the equivariant and Kähler parameters, respectively, on M. Let $\mathbf{u}'_1, ..., \mathbf{u}'_m$ and $\mathbf{v}'_1, ..., \mathbf{v}'_n$ be the equivariant and Kähler parameters, respectively, on M'. The pair (M, M') are said to exhibit *3d mirror symmetry for characteristic classes* if there is a bijection $\mathrm{bj} : M^{\mathbb{T}} \to M'^{\mathbb{T}'}$ such that for all $f_1, f_2 \in M^{\mathbb{T}}$,

$$\mathrm{Stab}^{Ell}(f_1)|_{f_2} = \pm \mathrm{Stab}^{Ell}(\mathrm{bj}(f_2))|_{\mathrm{bj}(f_1)} \quad \text{with substitutions} \quad \mathbf{u}_i \leftrightarrow \mathbf{v}'_i, \mathbf{v}_i \leftrightarrow \mathbf{u}'_i, \mathbf{h} \leftrightarrow \mathbf{h}^{-1}. \quad (4.1)$$

In the case of full flag varieties, it is shown in [RSVZ1, RW2] that the self-dual pair

$$M = T^*\mathcal{F}_{1,2,...,n+1} = M'$$

exhibits 3d mirror symmetry for characteristic classes. The torus fixed points of M are in bijection with permutations of $\{1, ..., n+1\}$, and there is a natural automorphism of the fixed point locus given by reversing the permutation. Under this automorphism the restriction matrix matches with itself. The matching shown for $T^*\mathbb{P}^1$ above is a special case of this result. This notion of duality gives a geometric meaning to the seemingly artificial Kähler parameters in elliptic Schubert calculus: they are the equivariant parameters on the dual.

Remark 4.1.10. In [RW2, Section 5], it is shown that a full flag variety of any simply connected semisimple linear group is 3d mirror dual to the full flag variety of the Langlands dual group. The self-duality of the type A full flag varieties considered in this work follows from this more general result.

An important part of the elliptic Schubert calculus program is extending 3d mirror symmetry for characteristic classes to all partial flag varieties. However, one encounters an immediate problem. The dual of a partial flag variety need not be a partial flag variety. It is believed that they will in fact be bow varieties of the type considered in this work. Further evidence for this belief may be found in [RSVZ2], where it is shown that the dual to $T^*\mathrm{Gr}(k, n)$ where $n \geq 2k$ is a Nakajima quiver

variety (cobalanced bow variety). Moreover, as we will show in the following sections, there is reason to believe that bow varieties are the most natural setting for the study of 3d mirror symmetry.

Remark 4.1.11. Known results on elliptic stable envelopes and 3d mirror symmetry include the following:

- elliptic stable envelopes are defined for Nakajima quiver varieties and hypertoric varieties, and so-called abelianization formulas are known for them [AO], [RSVZ1, Section 5], [RTV3], [Sm];
- using those abelianization formulas, 3d mirror symmetry is proven for $T^*\mathrm{Gr}(k,n)$ and its dual for $n \geq 2k$ [RSVZ1];
- 3d mirror symmetry is proven for the full flag variety and its 3d dual (which is the Langland dual full flag variety) in [RSVZ2, RW2].
- 3d mirror symmetry is proven for hypertoric varieties in [SZ] and also [KS].

4.2 3d Mirror Symmetry for Partial Flag Varieties

As shown in Example 3.1.7, there is an ismorphism $M = T^*\mathbb{P}^1 \cong \mathcal{C}(\mathcal{D})$ where $\mathcal{D} = /1\backslash 1\backslash 1/$. Taking the dual of $\mathcal{D}$ yields $\mathcal{D}' = \backslash 1/1/1\backslash$. This dual brane diagram is HW equivalent to $\mathcal{D}$, and the HW equivalence interchanges the two fixed points. Hence, we see that the self-duality of M in the sense of 3d mirror symmetry for characteristic classes (Definition 4.1.9) is reflected in the self-duality of its brane diagram up to HW transition. Motivated by such results and ideas from physics, we define bow varieties with dual brane diagrams to be 3d mirror dual.

Definition 4.2.1. Two bow varieties $\mathcal{C}(\mathcal{D}), \mathcal{C}(\mathcal{D}')$ are called *3d mirror dual* if $\mathcal{D}$ is dual to $\mathcal{D}'$ in the sense of Section 2.3.

In this section, we will analyze the 3d mirror duals to cotangent bundles of partial flag varieties. The first step will be to realize $T^*\mathcal{F}_v$ as a bow variety.

4.2.1 Cotangent Bundle of a Partial Flag Variety as a Bow Variety

One approach to Schubert calculus is to realize $M = T^*\mathcal{F}_{v_1,\ldots,v_{n+1}}$ as a quiver variety, and then take advantage of the abelianization formulas that exist for the stable envelopes of quiver varieties [AO, RSVZ1]. Let $v = (v_1, \ldots, v_n), w = (0, \ldots, 0, v_{n+1})$, and consider the quiver $Q = Q(v,w)$. Using a similar argument to Example 3.1.7, one can show

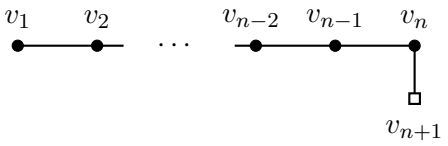

Figure 4.1: The quiver Q with $\mathcal{N}(Q) \cong T^*\mathcal{F}_{v_1,\dots,v_{n+1}}$.

Proposition 4.2.2. *With M and Q as above, we have $\mathcal{N}(Q) \cong M$.*

Proof. Take a point $(D, b, C, a) \in \mathcal{N}(Q)$. The stability condition implies that $\mathrm{im}(b_n)$ generates $\mathcal{V}$ as a $\mathbb{C}[C, D]$-module. From the 0-momentum condition, we have $D_iC_i = C_{i+1}D_{i+1}$ for $1 \leq i \leq n-2$, $D_{n-1}C_{n-1} = a_nb_n$, and $C_1D_1 = 0$. It follows from the stability condition that all C maps and a_n are surjective. Taking duals, we obtain injections $C_i^\vee$ for $1 \leq i \leq n-1$ and $a_n^\vee$. This gives a flag

$$0 \subset \mathrm{im}(C_1^\vee \cdots C_{n-1}^\vee a_n^\vee) \subset \mathrm{im}(C_2^\vee \cdots C_{n-1}^\vee a_n^\vee) \subset \cdots \subset \mathrm{im}(a_n^\vee) \subset \mathbb{C}^{v_n+1}.$$

Moreover, the 0-momentum condition implies that the D and $b_n^\vee$ maps can be pulled back to a well-defined endomorphism $\mathbb{C}^{v_{n+1}} \to \mathbb{C}^{v_{n+1}}$ that sends each step of the flag into the next lower step. This is precisely the classical description of M. □

Remark 4.2.3. Since the isomorphism in Proposition 4.2.2 involves dualizing, the torus action is inverted. Moreover, the $\hbar$-action on the tautological bundles is nonstandard. This explains the discrepancies in Example 3.1.19, 3.2.8.

Recall that $\underline{v}_i = v_i - v_{i-1}$ for $1 \leq i \leq n+1$, where $v_0 = 0$ by convention. As an immediate corollary of Proposition 4.2.2 and Theorem 3.3.2, we have

Corollary 4.2.4. *For all $v_1, \dots, v_{n+1} \in \mathbb{N}$, we have $T^*\mathcal{F}_{v_1,\dots,v_{n+1}} \cong \mathcal{C}(\mathcal{D})$, where*

$$\mathcal{D} = /v_1/v_2/\cdots/v_n\underbrace{\backslash v_n\backslash\cdots\backslash}_{n+1}v_n/.$$

The margin vectors are $r = \underline{v}$ and $c = (1, \dots, 1)$.

Example 4.2.5.

$$T^*\mathrm{Gr}(2,5) = \mathcal{N}\Big(\begin{array}{c}\bullet^{2}\\ \vert\\ \square_{5}\end{array}\Big) = \mathcal{C}(/2\backslash 2\backslash 2\backslash 2\backslash 2\backslash 2/),$$

$$T^*\mathcal{F}_{1,2,4,6} = \mathcal{N}\Big(\begin{array}{ccccc}\overset{1}{\bullet} & - & \overset{2}{\bullet} & - & \overset{4}{\bullet}\\ & & & & \vert\\ & & & & \square_{6}\end{array}\Big) = \mathcal{C}(/1/2/4\backslash 4\backslash 4\backslash 4\backslash 4\backslash 4\backslash 4/).$$

As a consequence of Corollary 4.2.4 and Corollary 3.3.5 we recover the trivial equality

$$\chi(T^*\mathcal{F}_v) = \#\mathrm{BCT}(\underline{v}, (1^{n+1})) = |\mathcal{I}| = \binom{v_{n+1}}{\underline{v}_1, \underline{v}_2, ..., \underline{v}_{n+1}}.$$

Moreover, from Corollary 2.5.2 we have

Corollary 4.2.6. *The 3d mirror dual of $T^*\mathcal{F}_v$ is HW equivalent to a quiver variety if and only if $\underline{v}$ is weakly increasing.*

4.2.2 3d Mirror Symmetry for Quiver Varieties

Consider a quiver variety (i.e. cobalanced bow variety) and its brane diagram $\mathcal{D}$. The dual brane diagram $\mathcal{D}''$ is generally not cobalanced, so a priori, the associated bow variety is not a quiver variety. However, $\mathcal{D}'$ may be HW equivalent to a cobalanced brane diagram (see Corollary 4.2.6). In this case, we have found two quiver varieties that are 3d mirror dual to each other up to HW equivalence.

For example, let $M = T^*\mathrm{Gr}(2,5) = \mathcal{C}(/2\backslash 2\backslash 2\backslash 2\backslash 2\backslash 2/)$, and let $M'' = \mathcal{C}(\backslash 2/2/2/2/2/2\backslash)$ be the 3d mirror dual variety. Carrying out the sequence of HW transitions

$$/2\backslash 2\backslash 2\backslash 2\backslash 2\backslash 2/ \leftrightarrow \backslash 1/2\backslash 2\backslash 2\backslash 2\backslash 2/ \leftrightarrow \backslash 1\backslash 2/2\backslash 2\backslash 2\backslash 2/ \leftrightarrow \backslash 1\backslash 2/2\backslash 2\backslash 2/1\backslash \leftrightarrow \backslash 1\backslash 2/2\backslash 2/2\backslash 1\backslash,$$

we obtain a cobalanced bow variety $M' = \mathcal{C}(\backslash 1\backslash 2/2\backslash 2/2\backslash 1\backslash)$ isomorphic to M''. Namely, we have

$\mathcal{N}\Big(\begin{array}{c}\bullet^{2}\\ \vert\\ \square_{5}\end{array}\Big)$ is 3d mirror dual to $\mathcal{N}\Big(\begin{array}{ccccc}\overset{1}{\bullet} & - & \overset{2}{\bullet} & - & \overset{2}{\bullet} & - & \overset{1}{\bullet}\\ & & \vert & & \vert & & \\ & & \square_{1} & & \square_{1} & & \end{array}\Big)$

up to HW transition.

More generally for Grassmannians, take the 3d mirror dual $M'' = \mathcal{C}(\backslash k \underbrace{/k\cdots k/}_{n} k\backslash)$ to $M = T^*\mathrm{Gr}(k,n)$, where $2k \leq n$. Using HW transitions to move U_1 to the right k times and U_2 to the left k

times yields $\mathcal{C}(/1/2\cdots/k\backslash k\underbrace{/k\cdots k/}_{n-2k}k\backslash k/k-1\cdots 1/)$. Hence, we have that $T^*\mathrm{Gr}(k,n)=\mathcal{N}\left(\begin{smallmatrix}\bullet^{k}\\ \square_{n}\end{smallmatrix}\right)$ is 3d mirror dual—up to HW isomorphism—to $M'=\mathcal{N}(v,w)$, where

$$v=(1,2,\ldots,k-1,k^{n-2k+1},k-1,\ldots,2,1),\qquad w=\epsilon_k+\epsilon_{n-k}.$$

Here ϵ_i is the ith standard basis vector in $\mathbb{N}^{n-1}$ and a^b means a repeated b times. This pair of 3d mirror symmetric varieties is explored in terms of elliptic stable envelopes in [RSVZ1]. We restate one of the main results in bow variety language.

Theorem 4.2.7 ([RSVZ1, Corollary 2])**.** *There is a bijection* $\mathrm{bj}: M^{\mathbb{T}}\to {M'}^{\mathbb{T}'}$ *given by dualizing and performing HW transitions on tie diagrams. The pair* (M,M') *exhibits 3d mirror symmetry for characteristic classes (Definition 4.1.9) with respect to* bj.

Example 4.2.8 (3d mirror symmetry for $T^*\mathbb{P}^2$). Let $M=T^*\mathbb{P}^2$. The restriction matrices for M and M' are given in Table 4.3. Here we set $f_i=f_{\{i\}}$ and $f_i'=\mathrm{bj}(f_i)$. Using the relation $\theta(x^{-1})=-\theta(x)$, it is straightforward to verify

$$\mathrm{Stab}_{kl}\overset{\substack{\mathbf{h}\leftrightarrow\mathbf{h}^{-1}\\ \mathbf{u}_i\leftrightarrow\mathbf{v}_i'\\ \mathbf{v}_j\leftrightarrow\mathbf{u}_j'}}{=\!=\!=}(-1)^{k+l+1}\mathrm{Stab}'_{lk}.$$

Table 4.3: The elliptic stable envelopes of $T^*\mathbb{P}^2$ and its 3d mirror dual.

	f_1	f_2	f_3
f_1	$\theta(\frac{\mathbf{u}_1}{\mathbf{u}_2})\theta(\frac{\mathbf{u}_1}{\mathbf{u}_3})\theta(\frac{\mathbf{v}_2}{\mathbf{v}_1}\mathbf{h}^4)$	0	0
f_2	$\theta(\mathbf{h})\theta(\frac{\mathbf{u}_1}{\mathbf{u}_3})\theta(\frac{\mathbf{u}_2\mathbf{v}_2}{\mathbf{u}_1\mathbf{v}_1}\mathbf{h}^3)$	$\theta(\frac{\mathbf{u}_1}{\mathbf{u}_2}\mathbf{h})\theta(\frac{\mathbf{u}_2}{\mathbf{u}_3})\theta(\frac{\mathbf{v}_2}{\mathbf{v}_1}\mathbf{h}^3)$	0
f_3	$\theta(\mathbf{h})\theta(\frac{\mathbf{u}_2}{\mathbf{u}_1}\mathbf{h})\theta(\frac{\mathbf{u}_3\mathbf{v}_2}{\mathbf{u}_1\mathbf{v}_1}\mathbf{h}^2)$	$\theta(\mathbf{h})\theta(\frac{\mathbf{u}_1}{\mathbf{u}_2}\mathbf{h})\theta(\frac{\mathbf{u}_3\mathbf{v}_2}{\mathbf{u}_2\mathbf{v}_1}\mathbf{h}^2)$	$\theta(\frac{\mathbf{u}_2}{\mathbf{u}_3}\mathbf{h})\theta(\frac{\mathbf{u}_1}{\mathbf{u}_3}\mathbf{h})\theta(\frac{\mathbf{v}_2}{\mathbf{v}_1}\mathbf{h}^2)$

	f_1'	f_2'	f_3'
f_1'	$\theta(\frac{\mathbf{u}_1'}{\mathbf{u}_2'}\mathbf{h}^4)\theta(\frac{\mathbf{v}_2'}{\mathbf{v}_1'})\theta(\frac{\mathbf{v}_3'}{\mathbf{v}_1'})$	$\theta(\mathbf{h})\theta(\frac{\mathbf{v}_3'}{\mathbf{v}_1'})\theta(\frac{\mathbf{v}_2'\mathbf{u}_2'}{\mathbf{v}_1'\mathbf{u}_1'}\mathbf{h}^{-3})$	$\theta(\mathbf{h})\theta(\frac{\mathbf{v}_2'}{\mathbf{v}_1'}\mathbf{h}^{-1})\theta(\frac{\mathbf{v}_3'\mathbf{u}_2'}{\mathbf{v}_1'\mathbf{u}_1'}\mathbf{h}^{-2})$
f_2'	0	$\theta(\frac{\mathbf{u}_1'}{\mathbf{u}_2'}\mathbf{h}^3)\theta(\frac{\mathbf{v}_2'}{\mathbf{v}_1'}\mathbf{h})\theta(\frac{\mathbf{v}_3'}{\mathbf{v}_2'})$	$\theta(\mathbf{h})\theta(\frac{\mathbf{v}_2'}{\mathbf{v}_1'}\mathbf{h})\theta(\frac{\mathbf{v}_3'\mathbf{u}_2'}{\mathbf{v}_2'\mathbf{u}_1'}\mathbf{h}^{-2})$
f_3'	0	0	$\theta(\frac{\mathbf{u}_1'}{\mathbf{u}_2'}\mathbf{h}^2)\theta(\frac{\mathbf{v}_3'}{\mathbf{v}_2'}\mathbf{h})\theta(\frac{\mathbf{v}_3'}{\mathbf{v}_1'}\mathbf{h})$

Now, consider $M=T^*\mathcal{F}_{v_1,\ldots,v_{n+1}}$ where $\underline{v}$ is weakly increasing. In order to formulate a version

of Theorem 4.2.7 for M, we must find the cobalanced form M' of the 3d mirror dual M'' and the bijection $\mathrm{bj} : M^{\mathbb{T}} \to M'^{\mathbb{T}}$ given by dualizing and appyling HW transitions to tie diagrams. We will formulate these in quiver variety language. Define

$$\mu = (n^{\underline{v}_1}, (n-1)^{\underline{v}_2 - \underline{v}_1}, (n-2)^{\underline{v}_3 - \underline{v}_2}, \ldots, 1^{\underline{v}_n - \underline{v}_{n-1}}, 0^{\underline{v}_{n+1} - \underline{v}_n}, (-1)^{k-1})$$

where $k = \sum_{j=1}^{n+1} (\underline{v}_j - \underline{v}_{j-1})(n-j+1)$ (that is, the sum of the first $\underline{v}_{n+1}$ entries of μ). Define $v', w' \in \mathbb{N}^{v_{n+1}-1}$ by

$$v'_i = \sum_{j=1}^{i} \mu_j, \qquad w' = \epsilon_{\underline{v}_1} + \epsilon_{\underline{v}_2} + \ldots + \epsilon_{\underline{v}_{n+1}}, \tag{4.2}$$

and $M' = \mathcal{N}(v', w')$. The fixed points of quiver varieties can be described in terms of tuples of partitions "growing" from the framing vertices (see Section 3.3.3). A fixed point f of M corresponds to a tuple of v_{n+1} partitions consisting of $\underline{v}_j$ copies of (1^{n-j+1}) for $1 \le j \le n+1$. For $\lambda = (1^j)$ where $j \in \mathbb{N}$, let $\mathrm{pos}(\lambda) \in \mathbb{N}^{\underline{v}_{n-j+1}}$ record the positions of the copies of (1^j) in the tuple for f (see Figure 4.2). The fixed points of M' correspond to tuples of w'_i partitions with mode i for each $1 \le i \le v_{n+1} - 1$ such that the sum of their dimension vectors is v'.

Theorem 4.2.9. *The pair of quiver varieties M, M' are 3d mirror dual up to HW transition. Let $1 \le i \le v_{n+1} - 1$, and let $j_1 < \cdots < j_{w'_i}$ be the indices for which $\underline{v}_j = i$. Then, $\mathrm{bj}(f)$ corresponds to the tuple of partitions $(\mathrm{pos}((1^{n-j_k+1})) - (1, 2, ..., \underline{v}_i))_{k=1}^{w'_i}$ with mode i for each i.*

Proof. The cobalanced brane diagram $\mathcal{D}$ corresponding to M is

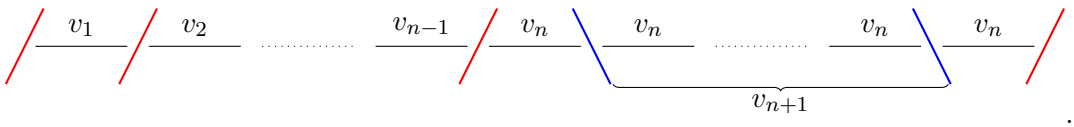

.

We begin by finding a sequence of Hanany-Witten transitions that turns the dual brane diagram, $\mathcal{D}''$,

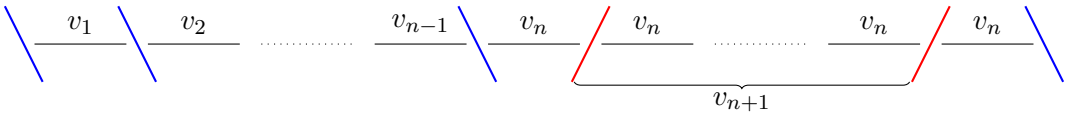

into a cobalanced brane diagram $\mathcal{D}'$. The first step is to move the group of n D5 branes on the left past the NS5 branes until each D5 brane U in this group reaches the "cobalanced state" $d_{U-} = d_{U+}$. We will rely on the relation

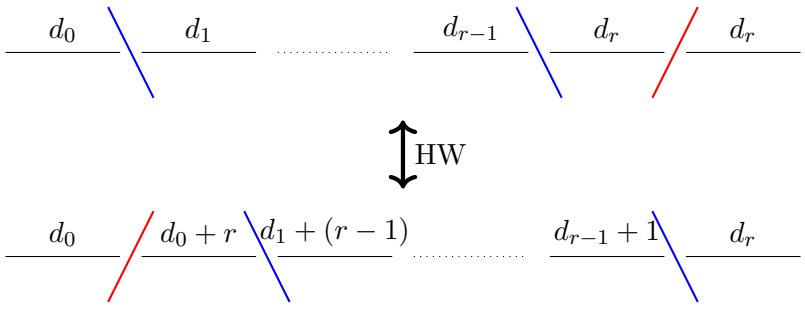

According to the relation, whenever the group of D5 branes is moved past an NS5 brane, the difference $d_{U+} - d_{U-}$ in D3 multiplicites to the right and left of each D5 brane U decreases by 1. This along with the fact that $\underline{v}$ is weakly increasing guarantees that the leftmost D5 brane will reach a cobalanced state after moving the group past sufficiently many NS5 branes. Namely, we have

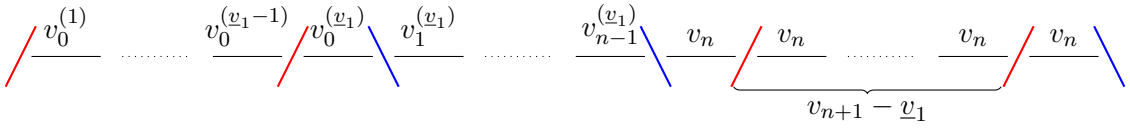

where $v_i^{(j)} = v_i + j(n-i)$. Note that $v_0^{(\underline{v}_1)} = v_1^{(\underline{v}_1)}$, and more generally $v_i^{(\underline{v}_{i+1})} = v_{i+1}^{(\underline{v}_{i+1})}$. Also, we have $v_n^{(j)} = v_n$. Continue moving the remaining non-cobalanced D5 branes to the right to bring the next into a cobalanced state, and so on. Repeating until all blue D5 branes reach a cobalanced state yields

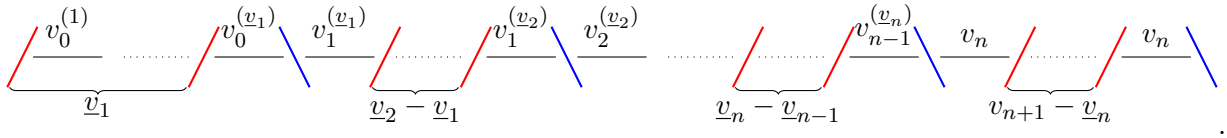

The second step is to move the lone D5 brane on the far right past the NS5 branes until it

becomes cobalanced. From $\underline{v}_{n+1} \geq \underline{v}_n$ it follows that $v_{n+1} - \underline{v}_n \geq v_n$. Moreover, we have the relation

It follows that the D5 brane will become cobalanced after passing through v_n many of the NS5 branes. Hence, the dual M'' is related by Hanany-Witten moves to the quiver variety M' given by the cobalanced brane diagram

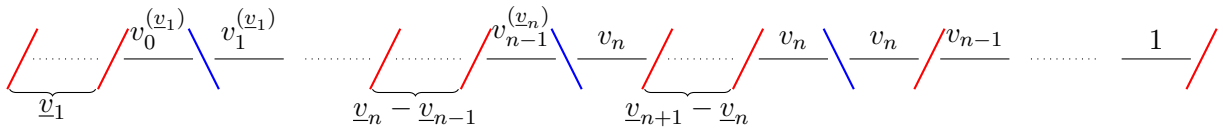

The dimension vectors of the corresponding quiver variety are precisely the v', w' vectors in (4.2).

Next, we will trace a fixed point through this sequence of Hanany-Witten transitions. Let $U'_{i,k}$ be the kth D5 brane in the ith interval of $\mathcal{D}'$. From the structure of $\mathcal{D}'$, we see that $i = \underline{v}_{j_1} = \cdots = \underline{v}_{j_{w'_i}}$ for some consecutive $j_1 < \cdots < j_{w'_i}$. Apply the inverse sequence of HW transitions and follow this D5 brane. We get U''_{j_k} in $\mathcal{D}''$. Dualizing, we get V_{j_k} in $\mathcal{D}$. Suppose $j_k < n+1$, and consider all ties attached to V_{j_k}. Let those ties be attached to the D5 branes U_{p_l} for $1 \leq l \leq \underline{v}_{j_k}$. Note that p is precisely $\mathrm{pos}((1^{n-j_k+1}))$. In $\mathcal{D}''$, the ties attaching to U''_{j_k} attach to V''_{p_l} at the other end for $1 \leq l \leq \underline{v}_{j_k}$. The sequence of HW transitions moves U''_{j_k} past the NS5 branes V''_l for $1 \leq l \leq \underline{v}_{j_k}$. Thus, the ties in $\mathcal{D}'$ attached to $U'_{i,k}$ attach to the NS5 branes V'_l for $l \in p'$, where

$$p' = ([1,i] \setminus (p \cap [1,i])) \cup (p \cap [i+1, v_{n+1}]).$$

Consider the corresponding partition dimension vector $d^{i,k}$. The entries of $d^{i,k}$ change precisely where the ties starting at $U^{i,k}$ end. Hence,

1. for each $l \in p \cap [1,i]$, we have $d^{i,k}_l - d^{i,k}_{l-1} = 0$, and
2. for each $l \in p \cap [i+1, v_{n+1}]$, we have $d^{i,k}_{l-1} - d^{i,k}_l = 1$,

where $d^{i,k}_0 = d^{i,k}_{n+1} = 0$ by convention. The indices l in 1 are the horizontal coordinates of the right side of each part of the partition that is contained to the left of the mode. The indices l in 2 are

the horizontal coordinates of the right side of each part of the partition that crosses over the mode. Hence, $p = \text{pos}((1^{n-j_k+1}))$ records the horizontal coordinates of the right end of each part of the partition. The left ends of the parts of the partition have horizontal coordinates $1, 2, ..., \underline{v}_i$, so the length of each part of the partition is given by $\text{pos}((1^{n-j_k+1})) - (1, 2, ..., \underline{v}_i)$.

Similarly, consider the case $j_k = n + 1$, i.e. $U' = U'_{i,k}$ is the rightmost D5 brane in $\mathcal{D}'$, and $i = \underline{v}_{n+1}$. Applying the inverse sequence of HW transitions and dualizing sends U' to the rightmost NS5 brane V in $\mathcal{D}$. Because $\mathcal{D}$ is cobalanced, we have $d^U_{U-} = d^U_{U+}$ for all D5 branes U. Since for each D5 brane in $\mathcal{D}$, V is the only NS5 brane to the right, the ties attached to V attach at the other end to all D5 branes except those that have no attached ties whatsoever. These are precisely the D5 branes whose butterflies collapse to the empty partition. Let these D5 branes be U_{p_l} for $1 \leq l \leq \underline{v}_{n+1}$. After dualizing and applying HW transitions,

1. the NS5 branes to the left of U' not joined to U' by a tie are precisely V'_l for $l \in p \cap [1, \underline{v}_{n+1}]$, and

2. the NS5 branes to the right of U' joined to U' by a tie are V'_l for $l \in p \cap [\underline{v}_{n+1} + 1, v_{n+1}]$.

Repeating the above argument finishes the proof. □

Alternatively, one can use the margin vector criterion (2.1) from Section 2.3. For $v, w \in \mathbb{N}^n$ define

$$r(v, w) = (v_i - v_{i-1} + \sum_{j=1}^{i-1} w_j)_{i=1,...,n+1}, \qquad c(v, w) = (n^{w_1}, (n-1)^{w_2}, \ldots, 2^{w_{n-1}}, 1^{w_n})$$

where we set $v_0 = v_{n+1} = 0$. These are the margin vectors of $\mathcal{N}(Q(v, w))$ as a bow variety.

Theorem 4.2.10. *Suppose $v, w \in \mathbb{N}^{a-1}$, $v', w' \in \mathbb{N}^{b-1}$ with $\sum w_i = b, \sum w'_i = a$. The quiver varieties $\mathcal{N}(Q(v, w))$ and $\mathcal{N}(Q(v', w'))$ are 3d mirror duals—up to HW isomorphism—if and only if*

$$r(v, w) + c(v', w') = (b^a), \qquad c(v, w) + r(v', w') = (a^b).$$

The first statement of Theorem 4.2.9 is a special case of Theorem 4.2.10. The second statement requires translating between BCTs and tuples of partitions. We do not carry out this translation in this work.

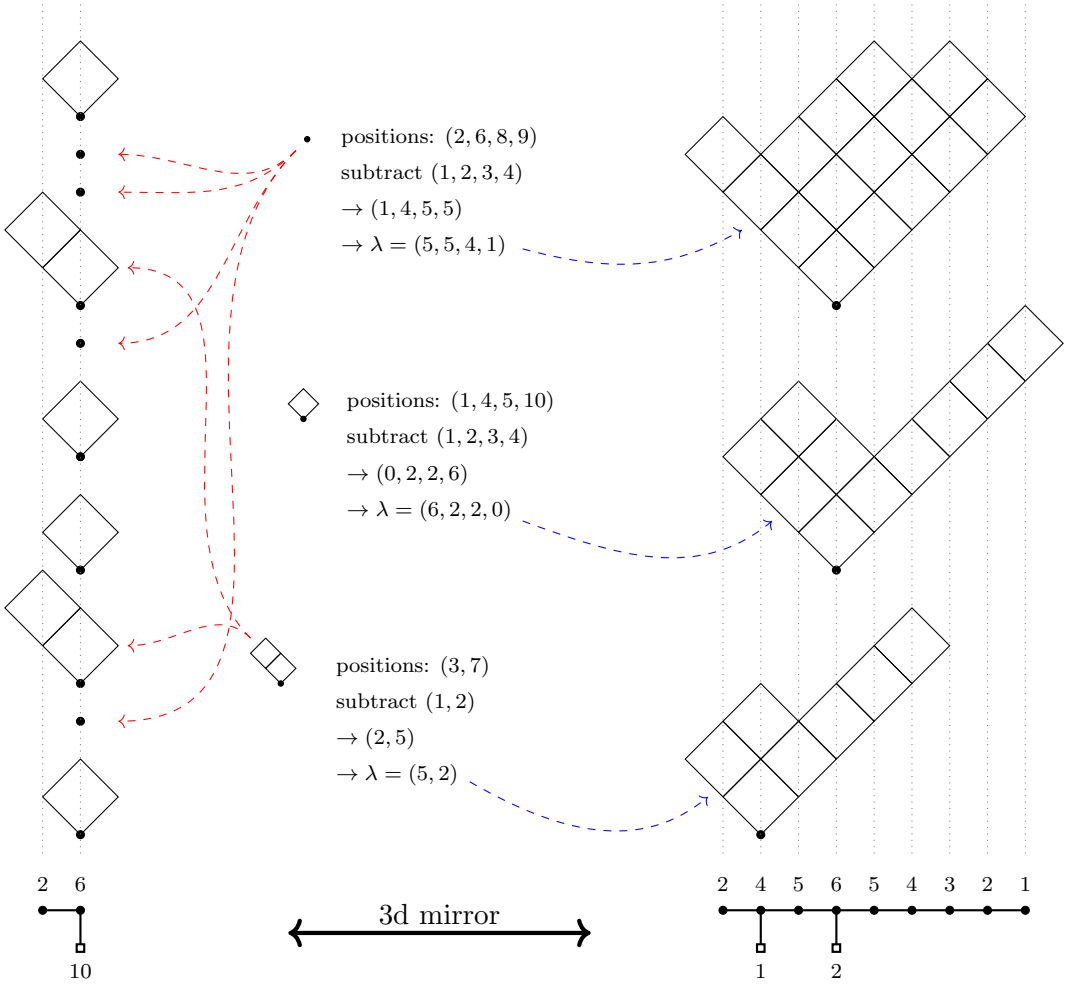

Figure 4.2: Combinatorial description of the bijection between the torus fixed points of $T^*\mathcal{F}_{2,4,4}$ and its 3d mirror dual. The tuples of partitions are ordered from bottom to top.

In the special case of full flag varieties, we find that the pair of quivers

are 3d mirror dual. The corresponding quiver varieties are both isomorphic to $T^*\mathcal{F}_{1,2,\ldots,n+1}$, but the action on the tautological bundles is different. This self-duality is explored in [RSVZ2, RW2].

4.2.3 3d Mirror Symmetry for Bow Varieties

In the case of $T^*\mathcal{F}_v$ where $\underline{v}$ is not weakly increasing, Corollary 4.2.6 implies that the 3d mirror dual is not a quiver variety. Hence, existing formulas for quiver varieties no longer apply. In the Grassmannian case, $\mathrm{Gr}(k,n)$ is isomorphic to $\mathrm{Gr}(n-k,n)$ via taking complements with respect to

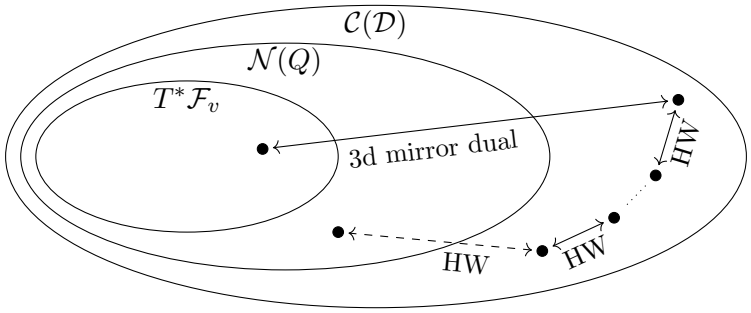

Figure 4.3: An illustration of the relationship between partial flag varieties, quiver varieties, and bow varieties. The dashed HW transition only exists when $\underline{v}$ is weakly increasing.

the standard dot product. Hence, the issue of nonincreasing $\underline{v}$ can be avoided. In general, however, the obvious approach of taking complements fails. One requires a Hermitian inner product, which is not complex algebraic (see Section 4.5 for further discussion).

The study of 3d mirror symmetry for general bow varieties is also interesting in its own right. Bow varieties possess features that make them a very natural setting for the study of 3d mirror symmetry for characteristic classes. The equivariant parameters are associated to D5 branes and the Kähler parameters are associated to NS5 branes. Dualizing the brane diagram corresponds to interchanging equivariant and Kähler parameters, as desired. Moreover, the sophisticated and technical proof in [RSVZ1] does not do justice to the simple elegance of the statement. The reason seems to be that in [RSVZ1] two quiver varieties are considered which are not 3d mirror duals of each other on the nose, but rather one is Hanany-Witten equivalent to the mirror dual of the other one. Relating characteristic class formulas for Hanany-Witten equivalent varieties is not expected to be simple, because HW equivalence involves difference bundles of tautological bundles (see part 2 of Theorem 3.1.21). Once elliptic stable envelopes are defined for bow varieties, and (say abelianization) formulas are know for them, the comparison between elliptic stable envelopes of 3d mirror dual varieties should be combinatorial, and the comparison between elliptic stable envelopes on the two sides of a single Hanany-Witten transition should be a theta-function identity. We plan to pursue this project in the future.

4.3 Characteristic Classes of Bow Varieties

Motivated by Section 4.1, we wish to associate characteristic classes to subvarieties of bow varieties. These characteristic classes can be considered in various extraordinary cohomology theories, typically (equivariant) cohomology, K-theory, or elliptic cohomology. While equivariant

elliptic cohomology is important to the study of 3d mirror symmetry, we will only consider ordinary equivariant cohomology in this work.

4.3.1 Cohomology, K-theory, and Localization

An effective method for studying equivariant cohomology and K-theory is equivariant localization. This tool usually has three steps of arguments (here we phrase them for $H^*_{\mathbb{T}}$):

1. Optimally, the (equivariant) characteristic classes of the tautological bundles over the space M generate $H^*_{\mathbb{T}}(M)$.

2. Optimally, the localization (restriction to the fixed points) map $\mathrm{Loc} : H^*_{\mathbb{T}}(M) \to H^*_{\mathbb{T}}(M^{\mathbb{T}})$ is injective.

3. Optimally, the image of the localization map is described by "simple" relations among its components $H^*_{\mathbb{T}}(M^{\mathbb{T}}) = \oplus H^*_{\mathbb{T}}(\text{connected components of } M^{\mathbb{T}})$.

The first step, under the name of "Kirwan surjectivity", is studied extensively: it generally holds for GIT quotients (and more), but may or may not hold for hyperkähler quotients. We do not know if it holds for our class of bow varieties or not, cf. [JKK, MG1, MG2].

The second step holds in very general topological circumstances, but only up to $H^*_{\mathbb{T}}(\mathrm{pt})$-torsion, and only under some (generalized, equivariant) compactness (or properness) assumptions, see e.g. [HHH, Thm 2.3]. Further studies are needed to verify whether bow varieties are covered.

The third step holds for so-called GKM spaces [GKM]. The assumptions that make a space a GKM space include that there is at most one torus invariant curve on M joining a given pair of fixed points. For GKM spaces, the image of the localization map is described by relations of the following flavor: pairs of components corresponding to poles of an invariant curve agree under some substitutions of variables. For non-GKM spaces these coincidences must hold not only for the components themselves, but also for *some of their higher derivatives* as well. Bow varieties are typically not GKM spaces (an example is in Figure 4.5), hence GKM theory does not apply. To circumvent some of the aforementioned obstacles, we make the following definitions.

Definition 4.3.1. In the algebra $H^*_{\mathbb{T}}(\mathcal{C}(\mathcal{D}))$ (over $H^*_{\mathbb{T}}(\mathrm{pt}) = \mathbb{C}[u_1, \ldots, u_n, \hbar]$) consider the subalgebra generated by the Chern classes of the tautological bundles. Define $\mathbb{H}_{\mathbb{T}}(\mathcal{C}(\mathcal{D}))$ to be the Loc-image of this subalgebra in $H^*_{\mathbb{T}}(\mathcal{C}(\mathcal{D})^{\mathbb{T}}) = \mathbb{C}[u_1, \ldots, u_n, \hbar]^N$, where N is the number of fixed points.

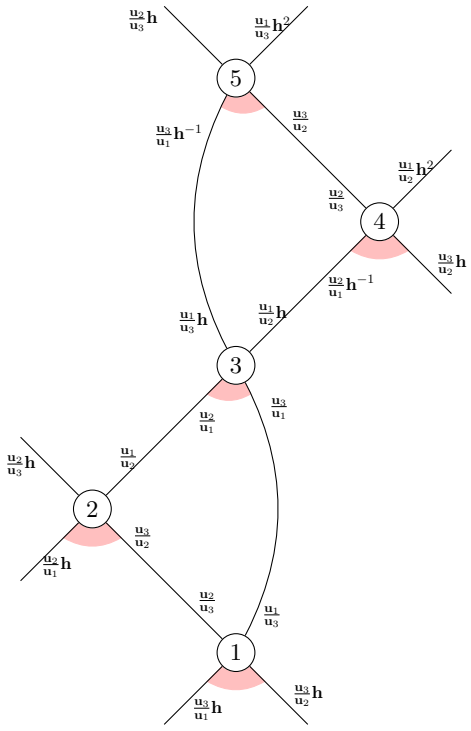

Figure 4.4: Illustration of $\mathbb{T}$ fixed points, invariant curves, poset structure, Leafs, Slopes, and N_f^+ spaces on $\mathcal{C}(/1\backslash 1/2\backslash 2\backslash 2/) = \mathcal{N}((1,2),(1,2))$. See Section 4.3.3.

Definition 4.3.2. In the algebra $K^0_{\mathbb{T}}(\mathcal{C}(\mathcal{D}))$ (over $K^0_{\mathbb{T}}(\mathrm{pt}) = \mathbb{C}[\mathbf{u}_1^{\pm 1}, \ldots, \mathbf{u}_n^{\pm 1}, \mathbf{h}^{\pm 1}]$) consider the subalgebra generated by the classes of the tautological bundles. Define $\mathbb{K}_{\mathbb{T}}(\mathcal{C}(\mathcal{D}))$ to be the Loc-image of this subalgebra in $K^*_{\mathbb{T}}(\mathcal{C}(\mathcal{D})^{\mathbb{T}}) = \mathbb{C}[\mathbf{u}_1^{\pm 1}, \ldots, \mathbf{u}_n^{\pm 1}, \mathbf{h}^{\pm 1}]^N$, where N is the number of fixed points.

The algebras $\mathbb{H}_{\mathbb{T}}(\mathcal{C}(\mathcal{D}))$ and $\mathbb{K}_{\mathbb{T}}(\mathcal{C}(\mathcal{D}))$ will be the home of our characteristic classes. If the first and second steps above hold, then these algebras are isomorphic to $H^*_{\mathbb{T}}(\mathcal{C}(D))$ and $K^0_{\mathbb{T}}(\mathcal{C}(\mathcal{D}))$, respectively.

4.3.2 Cohomological Stable Envelopes

Our goal is to associate a characteristic class to every fixed point on $\mathcal{C}(\mathcal{D})$, which generalizes the notion of stable envelope for quiver varieties, and in turn, the Chern-Schwartz-MacPherson class of Schubert varieties in partial flag varieties (which itself is a generalization of the Schubert class). Let $\sigma : \mathbb{C}^\times \to \mathbb{T} = \mathbb{A} \times \mathbb{C}^\times_\hbar$ be the one-parameter subgroup

$$\sigma(z) = (z, z^2, z^3, \ldots, z^n, 1). \tag{4.3}$$

Definition 4.3.3.

- For a fixed point $f \in \mathcal{C}(\mathcal{D})^{\mathbb{T}}$, define

$$\mathrm{Leaf}(f) = \{x \in \mathcal{C}(\mathcal{D}) : \lim_{z\to 0} \sigma(z).x = f\}.$$

- Define the partial order on $\mathcal{C}(\mathcal{D})^{\mathbb{T}}$ by

$$f' \leq f \qquad \text{if} \qquad f' \in \overline{\mathrm{Leaf}(f)}.$$

- Define the *slope* (alternatively, "stable leaf" or "full attracting set") of a fixed point f by

$$\mathrm{Slope}(f) = \bigcup_{f' \leq f} \mathrm{Leaf}(f').$$

- Let $N_f^+ \oplus N_f^-$ denote the $\mathbb{T}$ invariant decomposition of $T_f\mathcal{C}(\mathcal{D})$ to positive and negative σ weight spaces.

In simpler terms, $T_f\mathcal{C}(\mathcal{D})$ decomposes as a sum of Grothendieck roots of the form $\mathbf{h}^k\mathbf{u}_i/\mathbf{u}_j$, where $1 \leq i, j \leq n$ and $k \in \mathbb{Z}$. The $\mathbb{T}$-representation N_f^- is the sum of Grothendieck roots for which $i < j$, and N_f^+ is the sum of Grothendieck roots for which $i > j$. Each Leaf is a cell, and it follows that $T_f\mathrm{Leaf}(f) = N_f^+$.

At this point it is worth looking at examples, that is, Figures 4.4–4.6. In these figures the vertices represent fixed points. The edges represent (possibly noncompact) $\mathbb{T}$-invariant curves, and the decoration on an edge at a vertex is the $\mathbb{T}$-character on the tangent line of the curve at that fixed point. The compact invariant curves can be constructed using butterfly surgery (see Section 3.4.1). The tangent space of the Leaf at its own fixed point is indicated in the figures by the pink shading. The fixed points are positioned in such a way that the poset structure is illustrated the usual way: in the figures the vertexes are $\leq$-growing from bottom up. At each fixed point f, the characters of N_f^+ (respectively N_f^-) are the labels on the edges in the pink (respectively non-pink) region.

First let us recall the general axiomatic definition of cohomological stable envelopes of Maulik-Okounkov. Let the $\mathbb{T}$-manifold M be a symplectic resolution. Fix a cocharacter $\sigma : \mathbb{C}^\times \to \mathbb{A}$ and a virtual polarization bundle $T^{1/2}M$ such that $TM = T^{1/2}M + \mathbf{h}(T^{1/2}M)^\vee$. For $f \in M$, let $T_fM = N_f^- \oplus N_f^+$ be the decomposition into positive and negative weight spaces of σ.

Definition 4.3.4 ([MO])**.** Let $f \in M^{\mathbb{T}}$. The cohomology class $\mathrm{Stab}(f) \in H^*_{\mathbb{T}}(M)$ of homogeneous degree $\dim_{\mathbb{C}} M/2$ is called the stable envelope of f, if it satisfies the axioms:

- (support) it is supported on $\mathrm{Slope}(f)$,
- (normalization) $\mathrm{Stab}(f)|_f = P_f e_{\mathbb{T}}(N_f^-)$, where $P_f = \frac{e_{\mathbb{A}}(T_f^{1/2}M)}{e_{\mathbb{A}}(N_f^-)}$
- (boundary) $\mathrm{Stab}(f)|_{f'}$ is divisible by $\hbar$, for $f' \neq f$.

Since we are working with $\mathbb{H}_{\mathbb{T}}$ instead of $H^*_{\mathbb{T}}$, we need a local reformulation of the support condition. See Remark 4.1.6 for a discussion of local versus global support conditions in the context of partial flag varieties. For that, we need the notion of normal bundle of $\mathrm{Slope}(f)$ at f'.

Definition 4.3.5. We say that a $\mathbb{T}$-invariant line bundle ℓ "belongs to $T_{f'}(\mathrm{Slope}(f))$" either if it is tangent to an invariant curve connecting f' with f'', for an f'' satisfying $f' < f'' \leq f$, or, if $\ell \subset N^+_{f'}$. The span of these line bundles is called $T_{f'}(\mathrm{Slope}(f))$. A $\mathbb{T}$ invariant complement of $T_{f'}(\mathrm{Slope}(f))$ in $T_{f'}\mathcal{C}(\mathcal{D})$ is called $N_{f'}(\mathrm{Slope}(f))$.

Example 4.3.6. In Figure 4.4 let f be the fixed point denoted by 5. Then for $f' = 4$ we have that $N_{f'}(\mathrm{Slope}(f))$ is one-dimensional, with $\mathbb{T}$-weight $u_1 - u_2 + 2\hbar$. For $f' = 3$ we have that $N_{f'}(\mathrm{Slope}(f))$ is zero-dimensional. For $f' = 2$ we have that $N_{f'}(\mathrm{Slope}(f))$ is one-dimensional, with weight $u_2 - u_3 + \hbar$. For $f' = 1$ we have that $N_{f'}(\mathrm{Slope}(f))$ is zero dimensional.

We will now define a version of the stable envelope that lives in $\mathbb{H}_{\mathbb{T}}$. In our version, we will ignore the polarization entirely and consider only the cocharacter (4.3) given above. The polarization is relatively unimportant; it has the effect of multiplying certain stable envelope classes by -1. The choice of cocharacter, however, is important. In particular, the comparison of stable envelopes for different cocharacters endows $H^*_{\mathbb{T}}$ with the structure of a quantum group representation. See [AO, MO, O] for details.

Definition 4.3.7. Let $f \in \mathcal{C}(\mathcal{D})^{\mathbb{T}}$. The cohomology class $\mathrm{Stab}(f) \in \mathbb{H}_{\mathbb{T}}(\mathcal{C}(\mathcal{D}))$ of homogeneous degree $\dim_{\mathbb{C}} \mathcal{C}(\mathcal{D})/2$ is called the *stable envelope* of f, if it satisfies the axioms:

- (support-1) $\mathrm{Stab}(f)|_{f'} = 0$ if $f' \notin \mathrm{Slope}(f)$;
- (support-2) $\mathrm{Stab}(f)|_{f'}$ is divisible by $e_{\mathbb{T}}(N_{f'}(\mathrm{Slope}(f)))$.

- (normalization) $\mathrm{Stab}(f)|_f = e_{\mathbb{T}}(N_f^-)$;
- (boundary) $\mathrm{Stab}(f)|_{f'}$ is divisible by $\hbar$, for $f' \neq f$.

The relation between the global support condition in Definition 4.3.4 and the local support-2 condition is the well known argument combining the Gysin sequence argument and a Mayer-Vietoris induction, see eg. [RTV3, Section 5.25]. The local support-1 condition is in fact a corollary of the rest of the axioms. Nonetheless, we listed it for clarity. If a stable envelope exists, then it is unique, as the original proof [MO, Section 3.3.4] carries over to this case (see also [RTV2, Section 3.1], [RTV3, Section 7.8]). In the next three sections, we show examples of stable envelopes.

4.3.3 Stable envelopes for $\mathcal{C}(/1\backslash 1/2\backslash 2\backslash 2/) = \mathcal{N}((1,2),(1,2))$.

The "skeleton" of the $\dim_{\mathbb{C}} = 4$ bow variety $\mathcal{C}(/1\backslash 1/2\backslash 2\backslash 2/)$ is in Figure 4.4, where the fixed points named 1, 2, 3, 4, 5 are

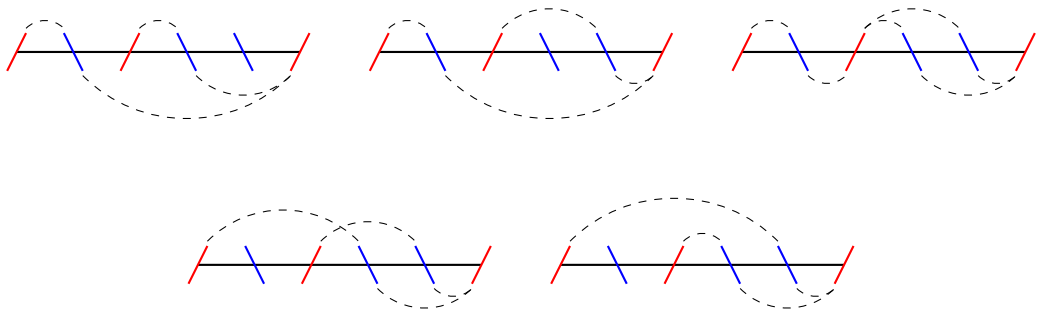

respectively. The stable envelopes are in the table (*)

	1	2	3	4	5
1	$(u_1-u_3)(u_2-u_3)$	0	0	0	0
2	$(u_1-u_3)\hbar$	$(u_1-u_2)(u_2-u_3+\hbar)$	0	0	0
3	$(u_3-u_2+\hbar)\hbar$	$(u_2-u_3+\hbar)\hbar$	$(u_1-u_3+\hbar)(u_1-u_2+\hbar)$	0	0
4	$\hbar^2$	$(u_2-u_3+\hbar)\hbar$	$(u_1-u_3+\hbar)\hbar$	$(u_2-u_3)(u_1-u_2+2\hbar)$	0
5	$(u_2-u_3)\hbar$	0	$(u_2-u_1)\hbar$	$(u_1-u_2+2\hbar)\hbar$	$(u_1-u_3+2\hbar)(u_2-u_3+\hbar)$

In this, and similar tables in the whole paper, each row contains the fixed point restrictions of the stable envelope of the corresponding fixed point.

To verify that this table is correct we need to verify that

(i) each row (as a five-tuple) is an element of $\mathbb{H}_{\mathbb{T}}(\mathcal{C}(\mathcal{D}))$; and that

(ii) the axioms of Definition 4.3.7 are satisfied.

Property (i) is proved by applying the five fixed point restriction homomorphisms $\mathrm{Loc}_1, \ldots, \mathrm{Loc}_5$ (as described in Section 3.2.3)

$$
\begin{array}{llllllll}
x_{11} \mapsto u_1 & x_{21} \mapsto u_1 & x_{31} \mapsto u_1 & x_{32} \mapsto u_2 & x_{41} \mapsto u_1 & x_{42} \mapsto u_2 & x_{51} \mapsto u_1 & x_{52} \mapsto u_2, \\
x_{11} \mapsto u_1 & x_{21} \mapsto u_1 & x_{31} \mapsto u_1 & x_{32} \mapsto u_3 & x_{41} \mapsto u_1 & x_{42} \mapsto u_3 & x_{51} \mapsto u_1 & x_{52} \mapsto u_3, \\
x_{11} \mapsto u_1 & x_{21} \mapsto u_1 & x_{31} \mapsto u_2 & x_{32} \mapsto u_3 & x_{41} \mapsto u_2 & x_{42} \mapsto u_3 & x_{51} \mapsto u_2 & x_{52} \mapsto u_3, \\
x_{11} \mapsto u_2 - \hbar & x_{21} \mapsto u_2 - \hbar & x_{31} \mapsto u_2 & x_{32} \mapsto u_3 & x_{41} \mapsto u_2 & x_{42} \mapsto u_3 & x_{51} \mapsto u_2 & x_{52} \mapsto u_3, \\
x_{11} \mapsto u_3 - \hbar & x_{21} \mapsto u_3 - \hbar & x_{31} \mapsto u_2 & x_{32} \mapsto u_3 & x_{41} \mapsto u_2 & x_{42} \mapsto u_3 & x_{51} \mapsto u_2 & x_{52} \mapsto u_3
\end{array}
$$

to the concrete formulas

$$
\begin{aligned}
F_1 =& (x_{31} - u_3)(x_{32} - u_3), \\
F_2 =& (x_{31} + x_{32} - u_2 - u_3)(u_1 + u_2 - x_{31} - x_{32} + \hbar), \\
F_3 =& (x_{11} - x_{31} - x_{32} + u_3 + \hbar)(x_{11} - x_{31} - x_{32} + u_2 + \hbar), \\
F_4 =& (u_1 - x_{11} + \hbar)(x_{11} - x_{31} - x_{32} + u_2 + \hbar), \\
F_5 =& (u_1 - x_{11} + \hbar)(-x_{11} + x_{31} + x_{32} - u_3),
\end{aligned}
\tag{4.4}
$$

where $x_{i1}, x_{i2}, \ldots, x_{i,d_{X_i}}$ are the Chern roots of the i'th tautological bundle.

Remark 4.3.8. The polynomials in (4.4) are not unique, they are only defined up to $\cap_i \ker(\mathrm{Loc}_i)$. We chose 'nice' representatives F_j, which in this case factor to linear factors. The existence of such nice representatives is not expected for more complicated brane diagrams. If $\mathcal{C}(\mathcal{D})$ is the cotangent bundle of a partial flag variety, then there are reasonably nice representatives of stable envelopes called "weight functions," see [RTV1, RTV2, RTV3, RV].

Remark 4.3.9. In fact we could argue differently to prove (i)—because this particular $\mathcal{C}(\mathcal{D})$ shares properties with GKM spaces. Namely, the five-tuple $(p_1, p_2, p_3, p_4, p_5)$ of polynomials in $\mathbb{C}[u_1, u_2, u_3, \hbar]$ is the $(\mathrm{Loc}_1, \ldots, \mathrm{Loc}_5)$-image of a polynomial

$$
F \in \mathbb{C}[u_1, u_2, u_3, \hbar][x_{11}, x_{21}, x_{31}, x_{32}, x_{41}, x_{42}, x_{51}, x_{52}]^{S_1 \times S_1 \times S_1 \times S_2 \times S_2 \times S_2},
$$

if and only if

$$\begin{aligned} &(p_1-p_2)|_{u_2=u_3}=0, && (p_1-p_3)|_{u_1=u_3}=0, && (p_2-p_3)|_{u_1=u_2}=0,\\ &(p_3-p_4)|_{u_2=u_1+\hbar}=0, && (p_3-p_5)|_{u_3=u_1+\hbar}=0, && (p_4-p_5)|_{u_2=u_3}=0 \end{aligned} \tag{4.5}$$

(these equations are read from the edges of the graph in Figure 4.4). To prove this statement consider a linear space $\mathbb{C}^{12}$ with coordinates

$$u_1, u_2, u_3, \hbar, x_{11}, x_{21}, x_{31}+x_{32}, x_{31}x_{32}, x_{41}+x_{42}, x_{41}x_{42}, x_{51}+x_{52}, x_{51}x_{52}$$

and in it the five subvarieties H_i defined by

$$x_{11}=\mathrm{Loc}_i(x_{11}),\dots,x_{51}+x_{52}=\mathrm{Loc}_i(x_{51}+x_{52}), x_{51}x_{52}=\mathrm{Loc}_i(x_{51}x_{52})$$

for $i=1,\dots,5$. The polynomials p_i can be considered to be polynomials on the H_i's, and the existence of F is rephrased as the existence of a polynomial on $\mathbb{C}^{12}$ that *restricts* to the given five-tuple. A necessary condition is, of course, that the p_i's agree on their pairwise intersections. These conditions are exactly (4.5). It can be shown that our varieties H_i intersect in such a general way that guarantees that the named necessary conditions are also sufficient. (For more sophisticated intersections of varieties such a statement does not hold, for example consider the polynomials $c_j x$ on the lines $y=jx$ for $j=1,2,3$, in the x,y-plane. They agree on their intersection, but they only extend to a polynomial in x,y if $c_1+c_3=2c_2$.) In fact the point of view of this remark is used in the *definition* of equivariant elliptic cohomology. Namely the elliptic counterpart of $\cup H_i$ is called the "elliptic cohomology scheme" (cf. [AO, Section 2.25-2.3], [FRV, Section 4], [RTV3, Section 7], [RSVZ1, Section 2]).

Now that (i) is verified for the table (*) above, it is worth verifying property (ii), that is the axioms of stable envelopes.

The *normalization axiom* is about the diagonal entries: for each vertex on the graph the directions of N^- are those that are *not* covered by the pink shading in the figure. Hence the diagonal entries need to be the products of their weights.

The *boundary axiom* holds because all below-diagonal entries are divisible by $\hbar$.

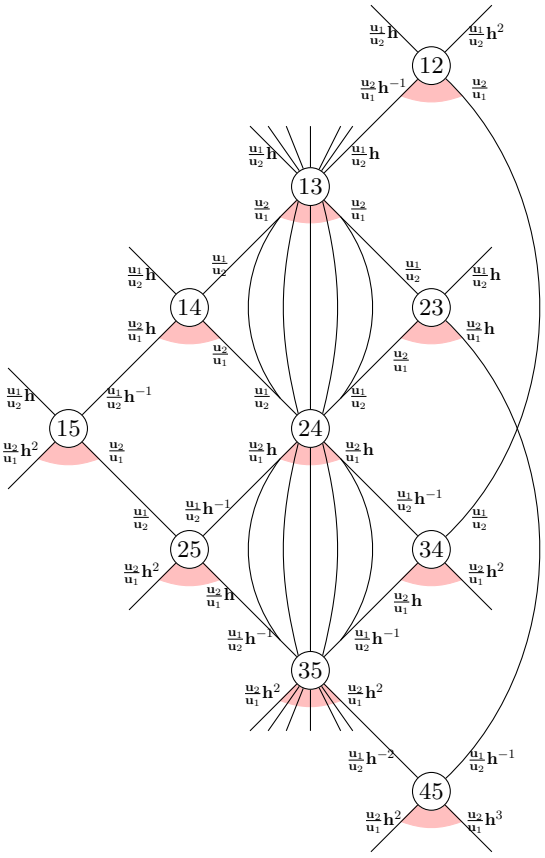

Figure 4.5: Illustration of $\mathbb{T}$-fixed points, invariant curves, poset structure, Leafs, Slopes, and N_f^+ spaces on $\mathcal{C}(/1/2/3/4/5\backslash 2\backslash)$, which is the 3d mirror dual of $T^*\mathrm{Gr}(2,5)$. See Section 4.3.4.

The *support-1 axiom* holds because the above-diagonal entries are all 0.

The *support-2 axiom* is a divisibility requirement for below-diagonal entries. Continuing Example 4.3.6 we see that the axiom requires that the (5,4), (5,3), (5,2), (5,1) entries of the table (*) are divisible by $u_1 - u_2 + 2\hbar$, 1, $u_2 - u_3 + \hbar$, 1, respectively.

4.3.4 Stable Envelope for $\mathcal{C}(/1/2/3/4/5\backslash 2\backslash)$

Consider $\mathcal{D} = /1/2/3/4/5\backslash 2\backslash$. The corresponding bow variety is (Hanany-Witten equivalent to) the 3d mirror dual of $T^*\mathrm{Gr}(2,5)$. Its $\mathbb{T}$ fixed points are in bijection with the 2-element subsets of $\{1,\dots,5\}$. The tie diagram corresponding to $\{k,l\}$ consists of 5 ties: U_2 is connected with V_k and V_l, and U_1 is connected with V_i for $i \neq k,l$. We denote this fixed point by kl. Figure 4.5 illustrates relevant information on the fixed point data.

In the table below we name the stable envelopes in the same manner as in Section 4.3.3. We used the following conventions: both horizontally and vertically we used the 45, 35, 34, 25, 24, 23,

15, 14, 13, 12 order of the vertices, and for brevity we write $u_{ij}^{(k)}$ for $(u_i - u_j + k\hbar)$.

45	35	34	25	24	23	15	14	13	12
$u_{12}^{(-1)}u_{12}^{(-2)}$	0	0	0	0	0	0	0	0	0
$u_{12}^{(-1)}\hbar$	$u_{12}^{(-1)}u_{12}^{(-1)}$	0	0	0	0	0	0	0	0
$u_{12}^{(-1)}\hbar$	$u_{12}^{(-1)}\hbar$	$u_{12}^{(0)}u_{12}^{(-1)}$	0	0	0	0	0	0	0
$u_{12}^{(-1)}\hbar$	$u_{12}^{(-1)}\hbar$	0	$u_{12}^{(0)}u_{12}^{(-1)}$	0	0	0	0	0	0
$u_{12}^{(-1)}\hbar$	$\hbar^2$	$u_{12}^{(0)}\hbar$	$u_{12}^{(0)}\hbar$	$u_{12}^{(0)}u_{12}^{(0)}$	0	0	0	0	0
$2\hbar^2$	$u_{12}^{(0)}\hbar$	$u_{12}^{(0)}\hbar$	$u_{12}^{(0)}\hbar$	$u_{12}^{(0)}\hbar$	$u_{12}^{(0)}u_{12}^{(1)}$	0	0	0	0
$u_{12}^{(-1)}\hbar$	$u_{12}^{(-1)}\hbar$	0	$u_{12}^{(-1)}\hbar$	0	0	$u_{12}^{(-1)}u_{12}^{(1)}$	0	0	0
$u_{12}^{(-1)}\hbar$	$\hbar^2$	$u_{12}^{(0)}\hbar$	$\hbar^2$	$u_{12}^{(0)}\hbar$	0	$u_{12}^{(1)}\hbar$	$u_{12}^{(0)}u_{12}^{(1)}$	0	0
$2\hbar^2$	$u_{12}^{(0)}\hbar$	$u_{12}^{(0)}\hbar$	$\hbar^2$	$\hbar^2$	$u_{12}^{(1)}\hbar$	$u_{12}^{(1)}\hbar$	$u_{12}^{(1)}\hbar$	$u_{12}^{(1)}u_{12}^{(1)}$	0
$2\hbar^2$	$2\hbar^2$	$2\hbar^2$	$u_{12}^{(1)}\hbar$	$u_{12}^{(1)}\hbar$	$u_{12}^{(1)}\hbar$	$u_{12}^{(1)}\hbar$	$u_{12}^{(1)}\hbar$	$u_{12}^{(1)}\hbar$	$u_{12}^{(1)}u_{12}^{(2)}$

To prove that the values of this table are correct we need to prove the properties (i) and (ii) as in Section 4.3.3. Property (ii) is done by observation. Property (i) is more sophisticated: either we use a computer to find representatives of the rows as polynomials in the $x_{ij}, u_i, \hbar$ variables, or one can use a formula presented in [RSVZ1, Section 5] specifically for stable envelopes on 3d mirror duals of T^*Gr spaces.

Remark 4.3.10. Note that property (i) can *not* be concluded by checking that neighboring components agree up to a substitution. This bow variety has infinitely many invariant curves, so it is not a GKM space. The subvarieties analogous to those called H_i in Section 4.3.3 do not intersect transversally. Hence, the GKM conditions on the components of an element in the image of Loc must be generalized to some coincidences of higher derivatives.

4.3.5 Stable Envelope for $\mathcal{C}(\backslash 1/2/2\backslash 2\backslash 1/)$.

Since the examples of Sections 4.3.3, 4.3.4 were both quiver varieties, we present one more example, for which neither $\mathcal{C}(\mathcal{D})$ nor its 3d mirror dual are Hanany-Witten equivalent to a quiver variety: $\mathcal{D} = \backslash 1/2/2\backslash 2\backslash 1/$. Calculation shows that its fixed point data relevant for stable envelopes

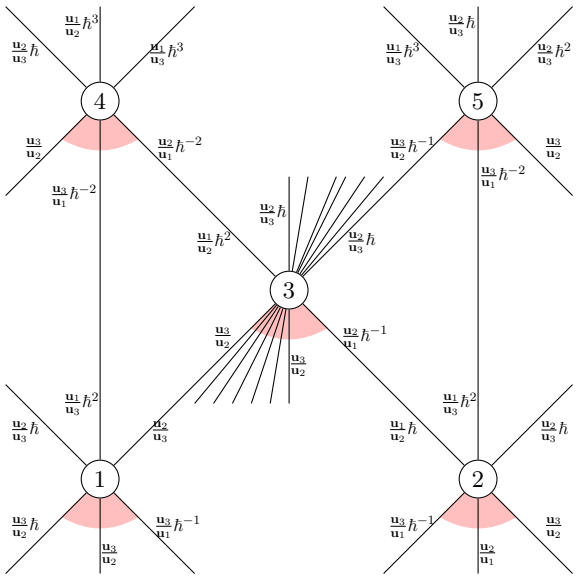

Figure 4.6: Illustration of $\mathbb{T}$-fixed points, invariant curves, poset structure, Leafs, Slopes, and N_f^+ spaces on $\mathcal{C}(\backslash 1/2/2\backslash 2\backslash 1/)$. See Section 4.3.5.

is in Figure 4.6, where the five fixed points denoted by 1, 2, 3, 4, 5 are

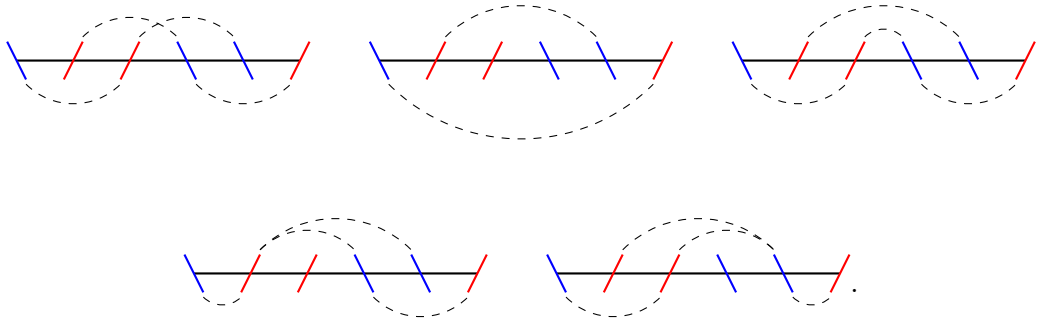

By methods similar to those in Section 4.3.4, it can be verified that the stable envelopes are

	1	2	3	4	5
1	$u_{23}^{(0)}u_{13}^{(2)}u_{23}^{(1)}$	0	0	0	0
2	0	$u_{13}^{(2)}u_{12}^{(1)}u_{23}^{(1)}$	0	0	0
3	$u_{13}^{(2)}u_{23}^{(1)}\hbar$	$u_{13}^{(2)}u_{23}^{(1)}\hbar$	$u_{12}^{(2)}u_{23}^{(1)}u_{23}^{(1)}$	0	0
4	$u_{32}^{(1)}u_{23}^{(1)}\hbar$	$u_{13}^{(2)}u_{23}^{(1)}\hbar$	$u_{23}^{(1)}u_{23}^{(1)}\hbar$	$u_{13}^{(3)}u_{12}^{(3)}u_{23}^{(1)}$	0
5	$u_{13}^{(2)}u_{23}^{(1)}\hbar$	$u_{21}^{(0)}u_{23}^{(1)}\hbar$	$u_{12}^{(2)}u_{23}^{(1)}\hbar$	0	$u_{13}^{(3)}u_{23}^{(1)}u_{23}^{(2)}$

.

It is instructive to verify the axioms from Definition 4.3.7 just by checking the entries against the structure of Figure 4.6. The fact that each line is in fact an element of $\mathbb{H}_{\mathbb{T}}(\mathcal{C}(\mathcal{D}))$ is verified by computer calculation.

4.3.6 Conjectural Formula for Cohomological Stable Envelopes

In the last three sections we presented formulas for stable envelopes that can be verified. The question remains how we came up with these formulas. We used the conjecture we present now.

Let us fix a brane diagram $\mathcal{D}$, and a fixed point $f \in \mathcal{C}(\mathcal{D})^{\mathbb{T}}$. Recall that

$$\mathrm{Loc}_f^K : K_{\mathbb{T}}(\mathcal{C}(\mathcal{D})) \to K_{\mathbb{T}}(f) = \mathbb{C}[\mathbf{u}_1^{\pm 1}, \mathbf{u}_2^{\pm 1}, \ldots, \mathbf{u}_n^{\pm 1}, \mathbf{h}^{\pm 1}]$$

is the restriction map in K-theory that we calculated explicitly in Section 3.2.3. The formula for $T\mathcal{C}(\mathcal{D})$ from Section 3.1.3 has the form

$$T\mathcal{C}(\mathcal{D}) = \sum_{x,y,k} \alpha_{x,y,k} \frac{x}{y} \mathbf{h}^k$$

where x and y are one of the Grothendieck roots of one of the tautological bundles or one of the u_i's, and $\alpha_{x,y,k} \in \mathbb{Z}$.

Definition 4.3.11. A term $\alpha_{x,y,k} \frac{x}{y} \mathbf{h}^k$ is *f-small*, if $\mathrm{Loc}_f^K(\frac{x}{y}) = \frac{u_i}{u_j}$ with $i < j$.

Let $\tilde{W}$ be the Euler class of the f-small part of $T\mathcal{C}(\mathcal{D})$:

$$\tilde{W}_f = e_{\mathbb{T}} \left(\sum_{f\text{-small}} \alpha_{x,y,k} \frac{x}{y} \mathbf{h}^k \right). \tag{4.6}$$

In other words, $\tilde{W}$ is the part of $T\mathcal{C}(\mathcal{D})$ that restricts to N_f^- at fixed point f. Now, $\tilde{W}_f$ is a rational expression in the Chern roots x_{ij} of the tautological bundles as well as u_i and $\hbar$. Let s be the number of segments in $\mathcal{D}$. We define

$$W_f = \frac{1}{n_f} \mathrm{Sym}\left(\tilde{W}_f\right)$$

where Sym is the symmetrizing operator $\mathrm{Sym}_1\mathrm{Sym}_2\cdots\mathrm{Sym}_s$ and

$$\mathrm{Sym}_i(\rho(x_{i1},\ldots,x_{i,d_{X_i}})) = \sum_{\sigma\in S_{d_{X_i}}} \rho(x_{i,\sigma(1)},x_{i,\sigma(2)},\ldots,x_{i,\sigma(d_{X_i})}).$$

The normalizing factor d_f is defined by

$$n_f = \prod_{U \text{ D5}} \prod_{i=1}^{s} d_i^U!.$$

Conjecture 4.3.12. *Cohomological stable envelopes exist for bow varieties. The stable envelope for the fixed point f is represented by W_f.*

We need to explain what "represented" means. The formula W_f is a rational function in the Chern roots of the tautological bundles as well as $u_i, \hbar$. The cohomological restriction map

$$\mathrm{Loc}_{f'} : H^*_{\mathbb{T}}(\mathcal{C}(\mathcal{D})) \to H^*_{\mathbb{T}}(f') = \mathbb{C}[u_1,u_2,\ldots,u_n,\hbar],$$

is a "substitution" map: we substitute certain $u, \hbar$ polynomials into the Chern roots. Hence, it can be applied to W_f. However, the result might have $0/0$ terms. The first part of the conjecture is that the *limit* of this substitution map exists and is a *polynomial*, i.e. that W_f *defines* an element in $\bigoplus_{f'} H^*_{\mathbb{T}}(f')$. The second part is that this element is in $\mathbb{H}_{\mathbb{T}}(\mathcal{C}(\mathcal{D}))$, and the third part is that it satisfies the axioms of Definition 4.3.7.

Remark 4.3.13. The phenomenon of naming a rational function whose fixed point restrictions are polynomials is not new in the theory of stable envelopes: the so-called "weight functions" of [RTV1, Ri] are also examples for that. The phenomenon that we need to take limits to restrict to fixed points is new.

Remark 4.3.14. Although the definition of W_f may sound technical, in plain language, it is just the natural formula we obtain if we want an expression symmetric in the Grothendieck roots that satisfies the normalization axiom of Definition 4.3.7. Remarkably, all our computations support the conjecture that the rest of the axioms also hold.

Remark 4.3.15. Hanany-Witten equivalent brane diagrams have tautological bundles of different ranks. Hence, the symmetrization part of the definition of W_f may be computationally much easier

for certain representatives in the HW equivalence class than for others. Our choice in Section 4.3.4, for instance, was made for this reason.

Example 4.3.16. Consider the brane diagram $\mathcal{D} = \backslash 1/2/2\backslash 2\backslash 1/$ of Section 4.3.5 (see Figure 4.6). In this section we show how Conjecture 4.3.12 produces some of the entries in the second line of the stable envelope table of Section 4.3.5.

According to Section 3.1.3, the first few terms of the tangent bundle $T\mathcal{C}(\mathcal{D})$ expressed in Grothendieck roots are

$$\frac{\mathbf{u}_1}{\xi_1}\mathbf{h} + \frac{\xi_1}{\xi_2^{(1)}}\mathbf{h} + \frac{\xi_1}{\xi_2^{(2)}}\mathbf{h} + \frac{\xi_2^{(1)}}{\xi_1} + \frac{\xi_2^{(2)}}{\xi_1} - 1 - (1+\mathbf{h})\left(\frac{\xi_2^{(1)}}{\xi_2^{(2)}} + \frac{\xi_2^{(2)}}{\xi_2^{(1)}} + 2\right) + \dots, \tag{4.7}$$

where ξ_1 is the first tautological bundle, and $\xi_2^{(1)}, \xi_2^{(2)}$ are the Grothendieck roots of the second tautological bundle, etc. According to Section 3.2.3, the localization map to the second fixed point maps $\xi_1 \mapsto \mathbf{u}_1\mathbf{h}, \xi_2^{(1)} \mapsto \mathbf{u}_1\mathbf{h}, \xi_2^{(2)} \mapsto \mathbf{u}_3\mathbf{h}^{-1}$. Under this substitution only a few terms from (4.7) will be f-small: from the displayed ones, only $\xi_1/\xi_2^{(2)}\mathbf{h}$ and $-(1+\mathbf{h})\xi_2^{(1)}/\xi_2^{(2)}$. For the sum $\sum_{f\text{-small}} \alpha_{x,y,k}\mathbf{h}^k x/y$ in equation (4.6), we obtain

$$\frac{\xi_1}{\xi_2^{(2)}}\mathbf{h} - \frac{\xi_2^{(1)}}{\xi_2^{(2)}} - \frac{\xi_2^{(1)}}{\xi_2^{(2)}}\mathbf{h} - \frac{\xi_3^{(1)}}{\xi_3^{(2)}} + \frac{\xi_3^{(1)}}{\mathbf{u}_2} + \frac{\xi_4^{(1)}}{u_3} + \frac{\xi_2^{(1)}}{\xi_3^{(2)}}\mathbf{h} - \frac{\xi_4^{(1)}}{\xi_4^{(2)}} + \frac{\xi_3^{(1)}}{\xi_4^{(2)}} - \frac{\xi_3^{(1)}}{\xi_4^{(2)}}\mathbf{h} + \frac{\mathbf{u}_2}{\xi_4^{(2)}}\mathbf{h} + \frac{\xi_3^{(1)}}{\xi_2^{(2)}} + \frac{\xi_4^{(1)}}{\xi_4^{(2)}}\mathbf{h}.$$

Hence, we have

$$\tilde{W}_2 = \frac{(x_{11}-x_{22}+\hbar)(x_{31}-u_2)(x_{41}-u_3)(x_{21}-x_{32}+\hbar)(x_{31}-x_{42})(u_2-x_{42}+\hbar)(x_{31}-x_{22})(x_{41}-x_{42}+\hbar)}{(x_{21}-x_{22})(x_{21}-x_{22}+\hbar)(x_{31}-x_{32})(x_{41}-x_{42})(x_{31}-x_{42}+\hbar)},$$

and W_2 is its $S_2 \times S_2 \times S_2$ symmetrization with respect to $(x_{2,1}, x_{2,2})$, $(x_{3,1}, x_{3,2})$, $(x_{4,1}, x_{4,2})$. For example, the (2,3) entry of the stable envelope table of Section 4.3.5 is the

$$x_{11} \mapsto u_1 + \hbar \quad x_{21} \mapsto u_1 + \hbar \quad x_{31} \mapsto u_2 \quad x_{41} \mapsto u_2 \quad x_{51} \mapsto u_2$$
$$x_{22} \mapsto u_3 - \hbar \quad x_{32} \mapsto u_3 \quad x_{42} \mapsto u_3$$

substitution into this symmetrized 8-term rational function (the substitutions are determined in Section 3.2.3). We get termwise 0, so the (2,3) entry is 0.

The (2,2) entry in the table is the

$$x_{11} \mapsto u_1 + \hbar \quad x_{21} \mapsto u_1 + \hbar \quad x_{31} \mapsto u_1 + \hbar \quad x_{41} \mapsto u_1 + \hbar \quad x_{51} \mapsto u_1 + \hbar$$
$$x_{22} \mapsto u_3 - \hbar \quad x_{32} \mapsto u_3 \quad x_{42} \mapsto u_3$$

substitution into the 8-term rational expression. The first term maps to $(u_1 - u_3 + 2\hbar)(u_1 - u_2 + \hbar)(u_2 - u_3 + \hbar)$ (a polynomial!) and all the other terms map to 0.

The (2,5) entry in the table is the

$$x_{11} \mapsto u_1 + \hbar \quad x_{21} \mapsto u_1 + \hbar \quad x_{31} \mapsto u_3 \qquad x_{41} \mapsto u_3 \qquad x_{51} \mapsto u_3 - \hbar$$
$$x_{22} \mapsto u_3 - \hbar \quad x_{32} \mapsto u_3 - \hbar \quad x_{42} \mapsto u_3 - \hbar$$

substitution into the 8-term rational expression. Six of those terms map to 0. However, the substitution does not make sense for the remaining two terms, because of the presence of the $(x_{32} - x_{41} + \hbar)$ factor in the denominator of these two terms. Yet, the sum of the terms *has* a limit, and it is 0. Thus we obtain that the (2,5) entry of the table is 0. The other entries follow similarly.

This example illustrates that Conjecture 4.3.12 typically does not provide the simplest representatives for the stable envelope classes. The F_j functions of (4.4) are, for example, much simpler representatives (they are polynomials to start with, not rational functions) than the formula of Conjecture 4.3.12.

4.4 Characteristic Classes of Separated Bow Varieties

The combinatorics of W_f and Conjecture 4.3.12 are subtle, especially due to the symmetrizations in the definition of W_f. Some of the difficulties are alleviated in the case of separated bow varieties. In this section, we analyze W_f for separated bow varieties, and discuss a possible approach for proving Conjecture 4.3.12 in this setting. Throughout this section, $\mathcal{D}$ will be a separated brane diagram with m NS5 branes, n D5 branes, and $s = m + n - 1$ segments. As usual, we denote the margin vectors by r, c and the Grothendieck roots of a bundle η by $\eta^{(1)}, ..., \eta^{(\text{rank}(\xi))}$.

4.4.1 Bundles on Separated Bow Varieties

We begin by analyzing the tautological bundles $\xi_1, ..., \xi_{m+n-1}$ on $\mathcal{C}(\mathcal{D})$. Let $f \in \mathcal{C}(\mathcal{D})^{\mathbb{T}}$. From Section 2.6, it follows that the fixed point restriction $\xi_i|_f$ for $m \leq i \leq m + n - 1$ does not depend on f. This fixed point restriction is a Laurent polynomial in $\mathbf{u}, \mathbf{h}$ variables, which we may interpret as global bundles to obtain bundles $\hat{\xi}_1, ..., \hat{\xi}_n$ over $\mathcal{C}(\mathcal{D})$. For $1 \leq j \leq n$, define the bundle $\hat{\xi}_{i,j} \to \mathcal{C}(\mathcal{D})$ by

$$\hat{\xi}_{i,j} = \begin{cases} \sum_{k=1}^{c_{n-j+1}} \mathbf{h}^{1-k}\mathbf{u}_j & \text{if } i \leq j, \\ 0 & \text{if } i > j. \end{cases}$$

From Section 3.2.3, we then have

$$\hat{\xi}_i = \sum_j \hat{\xi}_{i,j}.$$

Given any virtual bundle η expressed in terms of tautological bundles, let $\hat{\eta}$ denote the bundle resulting from the substitution $\xi_{m+i-1} \mapsto \hat{\xi}_i$. Note that if Loc^K is injective (see Section 4.3.1), then $\hat{\eta} = \eta$ in $K^0_{\mathbb{T}}(\mathcal{C}(\mathcal{D}))$. By Lemma 3.1.8, the A maps induce injections $\xi_{m+i} \to \xi_{m+i-1}$ for $1 \le i \le n-1$, and hence injections $\hat{\xi}_{i+1} \to \hat{\xi}_i$.

Next, we analyze $\widehat{T\mathcal{C}(\mathcal{D})}$. The formula of Theorem 3.1.15 gives the diagram

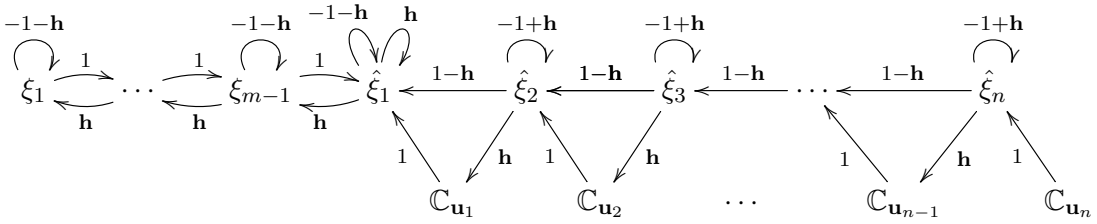

The multiplicity -1 of $\mathrm{End}(\hat{\xi}_1)$ is written as $(-1-\mathbf{h})+\mathbf{h}$ for reasons that will become clear in the Section 4.4.2. For now, just observe that we can split the diagram into two parts,

TW :

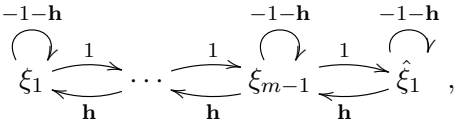

,

TR :

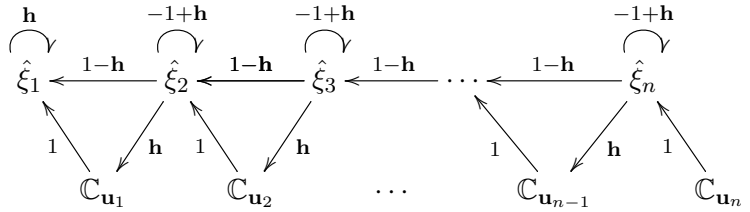

.

We will refer to these parts as TW and TR for "two-way" and "triangle", respectively.

4.4.2 Polarization

Though we do not incorporate the polarization in our definition of cohomological stable envelope (Definition 4.3.7), we will define a canonical choice of polarization for future reference. By *polarization*, we mean a virtual bundle $T^{1/2}\mathcal{C}(\mathcal{D})$ satisfying

$$\widehat{T\mathcal{C}(\mathcal{D})} = T^{1/2}\mathcal{C}(\mathcal{D}) \oplus \mathbf{h}(T^{1/2}\mathcal{C}(\mathcal{D}))^\vee.$$

Theorem 4.4.1. *Let* $P = \widehat{T\mathcal{C}(\mathcal{D})}|_{\mathbf{h}=0}$*, and* $P' = \sum_{i=1}^{n} \rho_{c_i}$*, where* $\rho_j = \sum_{i=1}^{j}(i-1)\mathbf{h}^{i-j}$*. Then,* $T^{1/2}\mathcal{C}(\mathcal{D}) = P + P'$ *is a polarization for* $\mathcal{C}(\mathcal{D})$*.*

Proof. In order to construct a polarization, we will construct virtual bundles $TW^{1/2}$ and $TR^{1/2}$ such that

$$TW = TW^{1/2} + \mathbf{h}(TW^{1/2})^{\vee}, \text{ and } TR = TR^{1/2} + \mathbf{h}(TR^{1/2})^{\vee}.$$

Then, $TW^{1/2}X + TR^{1/2}X$ is a polarization. A natural choice for $TW^{1/2}X$ is to take $TW|_{\mathbf{h}=0}$. Diagramatically, this is represented by

$$TW^{1/2}: \quad \overset{-1}{\circlearrowright}\ \hat{\xi}_1 \xrightarrow{1} \cdots \xrightarrow{1} \overset{-1}{\circlearrowright}\ \hat{\xi}_{m-1} \xrightarrow{1} \overset{-1}{\circlearrowright}\ \hat{\xi}_1 \ .$$

We would like to make the same choice for $TR^{1/2}$. Unfortunately, this is does not possess the necessary property.

Let $TR_1 = TR|_{\mathbf{h}=0}$ and TR_2 be the complement in TR. In other words, TR_1 is the part of TR with multiplicity ± 1, while TR_2 is the part with multiplicity $\pm\mathbf{h}$. Diagramatically, we have

$$TR_1: \quad \overset{\mathbf{h}}{\circlearrowright}\ \hat{\xi}_1 \xleftarrow{1} \overset{-1}{\circlearrowright}\ \hat{\xi}_2 \xleftarrow{1} \overset{-1}{\circlearrowright}\ \hat{\xi}_3 \xleftarrow{1} \cdots \xleftarrow{1} \overset{-1}{\circlearrowright}\ \hat{\xi}_n$$
$$\mathbb{C}_{\mathbf{u}_1} \xrightarrow{1} \hat{\xi}_1 \qquad \mathbb{C}_{\mathbf{u}_2} \xrightarrow{1} \hat{\xi}_2 \qquad \cdots \qquad \mathbb{C}_{\mathbf{u}_n} \xrightarrow{1} \hat{\xi}_n$$

$$TR_2: \quad \overset{\mathbf{h}}{\circlearrowright}\ \hat{\xi}_1 \xleftarrow{-\mathbf{h}} \overset{\mathbf{h}}{\circlearrowright}\ \hat{\xi}_2 \xleftarrow{-\mathbf{h}} \overset{\mathbf{h}}{\circlearrowright}\ \hat{\xi}_3 \xleftarrow{-\mathbf{h}} \cdots \xleftarrow{-\mathbf{h}} \overset{\mathbf{h}}{\circlearrowright}\ \hat{\xi}_n \ .$$
$$\mathbb{C}_{\mathbf{u}_1} \xrightarrow{\mathbf{h}} \hat{\xi}_1 \qquad \mathbb{C}_{\mathbf{u}_2} \xrightarrow{\mathbf{h}} \hat{\xi}_2 \qquad \cdots \qquad \mathbb{C}_{\mathbf{u}_{n-1}} \xrightarrow{\mathbf{h}} \hat{\xi}_{n-1}$$

Of course, $TR = TR_1 + TR_2$. Embedding all $\hat{\xi}_i$ into $\hat{\xi}_1$, we have

$$\begin{aligned}
TR_1 &= \mathrm{Hom}(\hat{\xi}_{1,2} + \cdots + \hat{\xi}_{1,n}, \hat{\xi}_{1,1} + \cdots + \hat{\xi}_{1,n}) + \mathrm{Hom}(\hat{\xi}_{1,3} + \cdots + \hat{\xi}_{1,n}, \hat{\xi}_{1,2} + \cdots + \hat{\xi}_{1,n}) + \cdots \\
&\quad + \mathrm{Hom}(\hat{\xi}_{1,n}, \hat{\xi}_{1,n-1} + \hat{\xi}_{1,n}) \\
&\quad - \mathrm{End}(\hat{\xi}_{1,2} + \cdots + \hat{\xi}_{1,n}) - \mathrm{End}(\hat{\xi}_{1,3} + \cdots + \hat{\xi}_{1,n}) - \cdots - \mathrm{End}(\hat{\xi}_{1,n}) \\
&\quad + \mathrm{Hom}(\hat{\xi}_{1,1}, \hat{\xi}_{1,1} + \cdots + \hat{\xi}_{1,n}) + \mathrm{Hom}(\hat{\xi}_{1,2}, \hat{\xi}_{1,2} + \cdots + \hat{\xi}_{1,n}) + \cdots + \mathrm{Hom}(\hat{\xi}_{1,n}, \hat{\xi}_{1,n}) \\
&= \mathrm{Hom}(\hat{\xi}_{1,2} + \cdots + \hat{\xi}_{1,n}, \hat{\xi}_{1,1}) + \mathrm{Hom}(\hat{\xi}_{1,3} + \cdots + \hat{\xi}_{1,n}, \hat{\xi}_{1,2}) + \cdots + \mathrm{Hom}(\hat{\xi}_{1,n}, \hat{\xi}_{1,n-1}) \\
&\quad + \mathrm{Hom}(\hat{\xi}_{1,1}, \hat{\xi}_{1,1} + \cdots + \hat{\xi}_{1,n}) + \mathrm{Hom}(\hat{\xi}_{1,2}, \hat{\xi}_{1,2} + \cdots + \hat{\xi}_{1,n}) + \cdots + \mathrm{Hom}(\hat{\xi}_{1,n}, \hat{\xi}_{1,n}),
\end{aligned}$$

and also

$$\begin{aligned}
\mathbf{h}^{-1}TR_2 &= \mathrm{End}(\hat{\xi}_{1,1} + \cdots + \hat{\xi}_{1,n}) + \mathrm{End}(\hat{\xi}_{1,2} + \cdots + \hat{\xi}_{1,n}) + \cdots + \mathrm{End}(\hat{\xi}_{1,n}) \\
&\quad - \mathrm{Hom}(\hat{\xi}_{1,2} + \cdots + \hat{\xi}_{1,n}, \hat{\xi}_{1,1} + \cdots + \hat{\xi}_{1,n}) - \mathrm{Hom}(\hat{\xi}_{1,3} + \cdots + \hat{\xi}_{1,n}, \hat{\xi}_{1,2} + \cdots + \hat{\xi}_{1,n}) - \cdots \\
&\quad - \mathrm{Hom}(\hat{\xi}_{1,n}, \hat{\xi}_{1,n-1} + \hat{\xi}_{1,n}) \\
&\quad + \mathrm{Hom}(\hat{\xi}_{1,2} + \cdots + \hat{\xi}_{1,n}, \hat{\xi}_{1,1}) + \mathrm{Hom}(\hat{\xi}_{1,3} + \cdots + \hat{\xi}_{1,n}, \hat{\xi}_{1,2}) + \cdots + \mathrm{Hom}(\hat{\xi}_{1,n}, \hat{\xi}_{1,n-1}) \\
&= \mathrm{Hom}(\hat{\xi}_{1,1}, \hat{\xi}_{1,1} + \cdots + \hat{\xi}_{1,n}) + \mathrm{Hom}(\hat{\xi}_{1,2}, \hat{\xi}_{1,2} + \cdots + \hat{\xi}_{1,n}) + \cdots + \mathrm{Hom}(\hat{\xi}_{1,n}, \hat{\xi}_{1,n}) \\
&\quad + \mathrm{Hom}(\hat{\xi}_{1,2} + \cdots + \hat{\xi}_{1,n}, \hat{\xi}_{1,1}) + \mathrm{Hom}(\hat{\xi}_{1,3} + \cdots + \hat{\xi}_{1,n}, \hat{\xi}_{1,2}) + \cdots + \mathrm{Hom}(\hat{\xi}_{1,n}, \hat{\xi}_{1,n-1}).
\end{aligned}$$

It follows that

$$\begin{aligned}
&\mathbf{h}^{-1}(TR - (TR_1 + \mathbf{h}TR_1^\vee)) \\
&\quad = \mathbf{h}^{-1}TR_2 - TR_1^\vee \\
&\quad = \mathrm{Hom}(\hat{\xi}_{1,1}, \hat{\xi}_{1,1} + \cdots + \hat{\xi}_{1,n}) + \mathrm{Hom}(\hat{\xi}_{1,2}, \hat{\xi}_{1,2} + \cdots + \hat{\xi}_{1,n}) + \cdots + \mathrm{Hom}(\hat{\xi}_{1,n}, \hat{\xi}_{1,n}) \\
&\qquad + \mathrm{Hom}(\hat{\xi}_{1,2} + \cdots + \hat{\xi}_{1,n}, \hat{\xi}_{1,1}) + \mathrm{Hom}(\hat{\xi}_{1,3} + \cdots + \hat{\xi}_{1,n}, \hat{\xi}_{1,2}) + \cdots + \mathrm{Hom}(\hat{\xi}_{1,n}, \hat{\xi}_{1,n-1}) \\
&\qquad - \mathrm{Hom}(\hat{\xi}_{1,1}, \hat{\xi}_{1,2} + \cdots + \hat{\xi}_{1,n}) - \mathrm{Hom}(\hat{\xi}_{1,2}, \hat{\xi}_{1,3} + \cdots + \hat{\xi}_{1,n}) - \cdots - \mathrm{Hom}(\hat{\xi}_{1,n-1}, \hat{\xi}_{1,n}) \\
&\qquad - \mathrm{Hom}(\hat{\xi}_{1,1} + \cdots + \hat{\xi}_{1,n}, \hat{\xi}_{1,1}) - \mathrm{Hom}(\hat{\xi}_{1,2} + \cdots + \hat{\xi}_{1,n}, \hat{\xi}_{1,2}) - \cdots - \mathrm{Hom}(\hat{\xi}_{1,n}, \hat{\xi}_{1,n}) \\
&\quad = \mathrm{End}(\hat{\xi}_{1,1}) + \cdots + \mathrm{End}(\hat{\xi}_{1,n}) - \mathrm{Hom}(\hat{\xi}_{1,1}, \mathbf{u}_1) - \cdots - \mathrm{Hom}(\hat{\xi}_{1,n}, \mathbf{u}_n).
\end{aligned}$$

Hence, we see that TR_1 is almost a polarization, but it is off by a Laurent polynomial in $\mathbf{h}$:

$$TR - (TR_1 + \mathbf{h}TR_1^\vee) = \rho \in \mathbb{Z}[\mathbf{h}^{\pm 1}],$$

where

$$\rho(\mathbf{h}) = \mathbf{h}(\mathrm{End}(\hat{\xi}_{1,1}) + \cdots + \mathrm{End}(\hat{\xi}_{1,n}) - \mathrm{Hom}(\hat{\xi}_{1,1}, \mathbf{u}_1) - \cdots - \mathrm{Hom}(\hat{\xi}_{1,n}, \mathbf{u}_n)).$$

If the $\hat{\xi}_{1,i}$'s are rank 1 bundles, then $\rho(\mathbf{h}) = 0$, and we can take $TR^{1/2} = TR_1$. This is the case for partial flag varieties. In general, we must polarize ρ. The terms of ρ of degree at most 0 form a polarization P'. □

4.4.3 Cohomological Stable Envelope for Separated Bow Varieties

We will consider a special version of Conjecture 4.3.12, adapted to separated bow varieties. To obtain this special version, define

$$\hat{W}_f = \frac{1}{\hat{n}_f}\mathrm{Sym}_1, ..., \mathrm{Sym}_{m-1}\tilde{W}_f,$$

where

$$\hat{n}_f = \prod_{U \text{ D5}} \prod_{i=1}^{m-1} d_i^U!.$$

Conjecture 4.4.2. *For $\mathcal{D}$ separated and $f \in \mathcal{C}(\mathcal{D})^{\mathbb{T}}$, the stable envelope class of f is represented by $\hat{W}_f$.*

Refer to Section 4.3.6 for the meaning of "represented". Alternatively, one may obtain Conjecture 4.4.2 by repeating the constructions of Section 4.3.6 with $\widehat{T\mathcal{C}(\mathcal{D})}$ instead of $T\mathcal{C}(\mathcal{D})$.

Remark 4.4.3. In the general case, there may be tautological bundles ξ_X whose fixed point restrictions are all equal. One may modify the formula for W_f by not symmetrizing over the Chern roots of ξ_X to obtain a simpler formula $\hat{W}_f$. In all examples we calculated, the fixed point restrictions of W_f and $\hat{W}_f$ agree up to modifying the normalization factor n_f appropriately. Conceptually, assuming injectivity of Loc, these bundles split into honest line bundles. Hence, there is no need to symmetrize over their Chern roots. The combinatorics of which tautological bundles have this property is subtle in general, but simple in the separated case.

To illustrate the advantages of $\hat{W}_f$, we will prove the normalization axiom for stable envelopes (Definition 4.3.7). Here, we assume that the limit of the fixed point restrictions of $\hat{W}_f$ exist.

Lemma 4.4.4. *The fixed point restrictions of $\hat{W}_f$ satsify the normalization axiom for stable envelopes.*

Proof. Let $\vec{\sigma} \in S_{d_{X_1}} \times \cdots \times S_{d_{X_{m-1}}}$. Given an expression $\rho(x_{i,1}, ..., x_{i,d_{X_i}})_{i=1}^{m-1}$, define

$$\vec{\sigma}(\rho) = \rho(x_{i,\sigma_i(1)}, ..., x_{i,\sigma_i(d_{X_i})})_{i=1}^{m-1}.$$

Note that $\mathrm{Sym}(\hat{\rho}) = \sum_{\vec{\sigma}} \vec{\sigma}(\rho)$. We may extend this definition to K-theory by replacing Chern roots with Grothendieck roots. Clearly, we have $\vec{\sigma}(e_{\mathbb{T}}(\eta)) = e_{\mathbb{T}}(\vec{\sigma}(\eta))$.

Consider the f-small (Definition 4.3.11) terms of $\mathrm{Hom}(\xi_{i-1}, \xi_i) \oplus \mathbf{h}\mathrm{Hom}(\xi_i, \xi_{i-1}) \oplus (-1-\mathbf{h})\mathrm{End}(\xi_i)$, the part of $\widehat{T\mathcal{C}(\mathcal{D})}$ pictured by

$$S_i: \qquad \xi_{i-1} \underset{\hbar}{\overset{1}{\rightleftarrows}} \xi_i \ \circlearrowright^{-1-\hbar}.$$

Denote the sum of these terms by S_i. Note that S_i and $S_{i'}$ share no Chern roots if $i \neq i'$. For $1 \leq i \leq m$ and $1 \leq k \leq n$, define $\xi_{i,k}^{(1)}, ..., \xi_{i,k}^{(d_i^{U_k})}$ to be the Grothendieck roots of ξ_i that restrict to $\mathbf{h}^l \mathbf{u}_k$ at f for some $l \in \mathbb{Z}$. Section 3.2.3 gives the explicit formula

$$\xi_{i,k}^{(j)}|_f = \frac{\mathbf{u}_k}{\mathbf{h}^{m+j-i-1}}.$$

Let $\xi_{i,k} = \sum_j \xi_{i,k}^{(j)}$. Finally, define S to be the f-small part of $\widehat{T\mathcal{C}(\mathcal{D})}$. We have $\hat{W}_f = \frac{1}{\hat{n}_f}\mathrm{Sym}(S)$.

The only source of -1 terms in $\vec{\sigma}(S)|_f$ is $\vec{\sigma}((-1-\mathbf{h})\mathrm{End}(\xi_i))$, where $1 \leq i \leq m-1$. Namely, each -1 term comes from a pair $\xi_{i,k}^{(j)}, \xi_{i,k}^{(j+1)}$ such that $\vec{\sigma}^{-1}(\xi_{i,k}^{(j)})$ is a Grothendieck root of $\xi_{i,a}$ and $\vec{\sigma}^{-1}(\xi_{i,k}^{(j+1)})$ is a root of $\xi_{i,b}$, where $b > a$. In this case, $-\mathbf{h}\xi_{i,k}^{(j+1)}/\xi_{i,k}^{(j)}$ is a root of $-\mathbf{h}\mathrm{End}(\xi_i)$ that appears in $\vec{\sigma}(S_i)$, and

$$-\frac{\mathbf{h}\xi_{i,k}^{(j+1)}}{\xi_{i,k}^{(j)}}\bigg|_f = -\mathbf{h}\frac{\mathbf{u}_k/\mathbf{h}^{(m+j-i)}}{\mathbf{u}_k/\mathbf{h}^{(m+j-i-1)}} = -1.$$

We have $0 \leq d_{X_i}^{U_k} - d_{X_{i-1}}^{U_k} \leq 1$. Hence, $j \leq d_{X_{i-1}}^{U_k}$, and $\xi_{i-1,k}^{(j)}|_f = \xi_{i,k}^{(j)}|_f/\mathbf{h}$. Assume $\vec{\sigma}^{-1}(\xi_{i-1,j}^{(k)})$ is a root of $\xi_{i-1,c}$. There are two cases. First, if $c \leq a$, then $\xi_{i,k}^{(j+1)}/\xi_{i-1,k}^{(j)}$ is a root of $\mathrm{Hom}(\xi_{i-1}, \xi_i)$ that

appears in $\vec{\sigma}(S_i)$. We have

$$\left.\frac{\xi_{i,k}^{(j+1)}}{\xi_{i-1,k}^{(j)}}\right|_f = \frac{\xi_{i,k}^{(j+1)}|_f}{\xi_{i,k}^{(j)}|_f/\mathbf{h}} = 1.$$

Second, if $c > a$, then $\mathbf{h}\xi_{i-1,k}^{(j)}/\xi_{i,k}^{(j)}$ is a root of $\hbar\mathrm{Hom}(\xi_i, \xi_{i-1})$ that appears in $\vec{\sigma}(S_i)$. We have

$$\left.\mathbf{h}\frac{\xi_{i-1,k}^{(j)}}{\xi_{i,k}^{(j)}}\right|_f = \mathbf{h}\frac{\xi_{i,k}^{(j)}|_f/\mathbf{h}}{\xi_{i,k}^{(j)}|_f} = 1.$$

In either case, the -1 is cancelled out. Repeating this argument for all such pairs shows that all -1 roots of $\vec{\sigma}(S_i)|_f$ are cancelled out. Since we do not permute the Chern roots of ξ_i for $i \geq m$, and $d_{X_1}^{U_k} \leq 1$ for all $1 \leq k \leq m$, varying i from 2 to $m-1$ accounts for all possible sources of -1 terms in $\vec{\sigma}(S)|_f$. We can therefore conclude that all -1 roots of $\vec{\sigma}(S)|_f$ are cancelled out. Thus, the virtual Euler class $e_{\mathbb{T}}(\vec{\sigma}(S)|_f)$ is defined. As a consequence of an elementary analytic argument, if the limit $\hat{W}_f|_f$ converges, then it must converge to $\sum_{\vec{\sigma}} e_{\mathbb{T}}(\vec{\sigma}(S)|_f)$.

We want to show that $e_{\mathbb{T}}(\vec{\sigma}(S)|_f) = 0$ if $\vec{\sigma}$ does not fix $\xi_{i,k}$ for all $i \leq m-1$ and k. Suppose $\vec{\sigma}$ does not fix $\xi_{m-1,k}$ for all k. Then, there must exist a root $\xi_{m-1,k}^{(j)}$ such that $\vec{\sigma}^{-1}(\xi_{m-1,k}^{(j)})$ is a root of $\xi_{m-1,k'}$, where $k' > k$. It follows that $\mathbf{h}\xi_{m-1,k}^{(j)}/\xi_{m,k}^{(j)}$ is a root of $\mathbf{h}\mathrm{Hom}(\xi_m, \xi_{m-1})$ that appears in $\vec{\sigma}(S)$. Note that this root is not present in the S_i bundles we considered before. We have $d_{X_m}^{U_k} \geq d_{X_{m-1}}^{U_k}$, and $\xi_{m-1,k}^{(j)}|_f = \xi_{m,k}^{(j)}/\mathbf{h}|_f$. Therefore, $\mathbf{h}\xi_{m-1,k}^{(j)}/\xi_{m,k}^{(j)}|_f = 1$. This results in a factor of 0 in $\vec{\sigma}(e(S))|_f$. We conclude that the only $\vec{\sigma}$ giving nonzero $\vec{\sigma}(e(S))|_f$ are those which fix $\xi_{m-1,k}$ for all k. We can now take $\vec{\sigma}$ fixing $\xi_{m-1,k}$ for all k and apply the same argument to conclude that $\vec{\sigma}$ must fix $\xi_{m-2,k}$ for all k in order to get a nonzero value of $e_{\mathbb{T}}(\vec{\sigma}(S)|_f)$. Our claim follows from induction.

Due the natural symmetry present in S, $\vec{\sigma}(S) = S$ if $\vec{\sigma}$ fixes $\xi_{i,k}$ for all $i \leq m-1$ and k. The number of such $\vec{\sigma}$ is precisely $\hat{n}_f$, and $e_{\mathbb{T}}(S)|_f = N_f^-$ by construction. The normalization axiom follows. □

In the proof of Lemma 4.4.4, we see that passing from W_f to $\hat{W}_f$ causes terms of the symmetrization to vanish upon restriction. In the diagonal restrictions, all nonvanishing terms are equal to the restriction of the unsymmetrized expression $\tilde{W}_f$. In the off-diagonal restrictions, more kinds of terms will appear. In Section 4.3.6, we identify three precise statements ("parts") that need to

be proven in order to prove Conjecture 4.3.12. The first part is that the limits in the fixed point restrictions exist and are polynomials, the second is that the restrictions lie in $\mathbb{H}_{\mathbb{T}}(\mathcal{C}(\mathcal{D}))$, and the third is that they satisfy the stable envelope axioms. For Conjecture 4.4.2, we expect the third part to follow from similar arguments to that of Lemma 4.4.4. Some of the ideas of this argument also pertain to the first part. The second part is a difficult interpolation problem, which likely requires more sophisticated techniques.

Remark 4.4.5. In our example computations, the fixed point restrictions of each term of the symmetrization in the formula for $\hat{W}_f$ converge. They do not, in general, converge to polynomials, however. Polynomials are only realized after cancellations with other terms of the symmetrization. We have also found that $\hat{W}_f|_{f'} = \sum_{\vec{\sigma}} e_{\mathbb{T}}(\vec{\sigma}(S)|_{f'})$. The latter is much faster to compute than the limits in the former.

4.5 Switching Consecutive 5-Branes of the Same Type

Consider the combinatorial transition of brane diagrams from Remark 2.4.1, that is, for $d_1 + d_3 = d_2 + \tilde{d}_2$ the local changes

Under these transitions the charges of the branes do not change, but the branes themselves switch places. Hence, the table-with-margins code for the diagram changes by switching two consecutive components either in c (for (TU) transition) or in r (for (TV) transition). Hence, permitting (TU) transition we may achieve that c is weakly decreasing, and permitting (TV) transition we may achieve that r is weakly increasing. Comparing with Theorem 2.5.1 and Corollary 2.5.2 we obtain

Proposition 4.5.1. *Any brane diagram is equivalent to a balanced one using Hanany-Witten and (TV) transitions. Any brane diagram is equivalent to a co-balanced one (ie. whose associated variety is a quiver variety) using Hanany-Witten and (TU) transitions.*

By permitting (TV) transitions (as well as HW transitions) cotangent bundles of different partial flag varieties become equivalent—which are C^∞ but not algebraically isomorphic. Namely, let $\lambda_1, \lambda_2, \ldots, \lambda_N$ and $\mu_1, \mu_2, \ldots, \mu_N$ be sequences of non-negative integers that are permutations of each other. Then as bow varieties $T^*\mathcal{F}_{\lambda_1, \lambda_1+\lambda_2, \ldots, \lambda_1+\lambda_2+\ldots+\lambda_N}$ and $T^*\mathcal{F}_{\mu_1, \mu_1+\mu_2, \ldots, \mu_1+\mu_2+\ldots+\mu_N}$ are

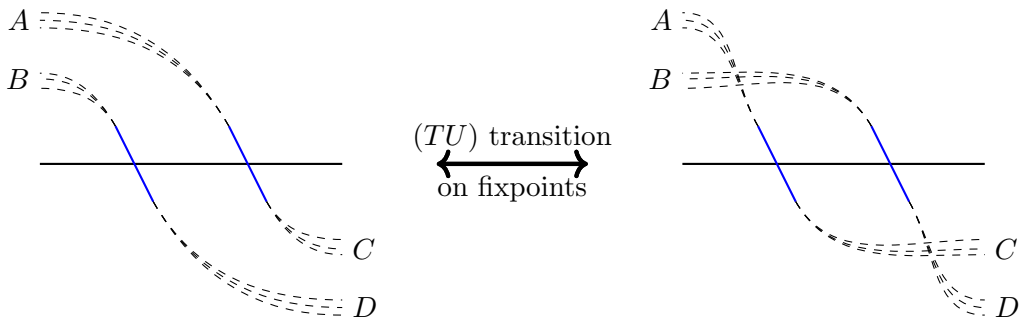

Figure 4.7: Bijection between fixed point codes for brane diagrams related by a (TU) transition.

equivalent using HW and (TV) transitions (their tables-with-margins only differ by permuting r).

Figure 4.7 illustrates a natural bijection between torus fixed points of $\mathcal{C}(\mathcal{D})$ and torus fixed points of $\mathcal{C}(\tilde{\mathcal{D}})$ for a (TU) transition. It is worth verifying the $d_1 + d_3 = d_2 + \tilde{d}_2$ relation in the figure. An analogous picture (in fact, this one upside down) provides the bijection for a (TV) transition.

Theorem 4.5.2. *Let $\mathcal{D}$ and $\tilde{\mathcal{D}}$ be related by (TU) transition. We have*

$$\mathbb{K}_{\mathbb{T}}(\mathcal{C}(\mathcal{D})) \cong \mathbb{K}_{\mathbb{T}}(\mathcal{C}(\tilde{\mathcal{D}})), \qquad \mathbb{H}_{\mathbb{T}}(\mathcal{C}(\mathcal{D})) \cong \mathbb{H}_{\mathbb{T}}(\mathcal{C}(\tilde{\mathcal{D}})).$$

Proof. The proof depends on the combinatorics of fixed point restrictions, namely the structure of the butterfly diagrams of Section 3.2.3. Let U_k and U_{k+1} be the two consecutive D5 branes switched at the (TU) transition, and let X_1, X_2, X_3 be the D3 branes adjacent to these 5-branes, in this order. We define a map

$$s : \bigoplus_{f \in \mathcal{C}(\mathcal{D})^{\mathbb{T}}} \mathbb{C}[\mathbf{u}_1^{\pm 1}, \ldots, \mathbf{u}_n^{\pm 1}, \mathbf{h}^{\pm 1}] \to \bigoplus_{\tilde{f} \in \mathcal{C}(\tilde{\mathcal{D}})^{\mathbb{T}}} \mathbb{C}[\tilde{\mathbf{u}}_1^{\pm 1}, \ldots, \tilde{\mathbf{u}}_n^{\pm 1}, \mathbf{h}^{\pm 1}]$$

as follows. The f-component maps to the $\tilde{f}$-component where f and $\tilde{f}$ are related as in Figure 4.7. The map between these components is $\mathbf{u}_i \mapsto \tilde{\mathbf{u}}_i$ for $i \neq k, k+1$, and $\mathbf{u}_k \mapsto \tilde{\mathbf{u}}_{k+1}$, $\mathbf{u}_{k+1} \mapsto \tilde{\mathbf{u}}_k$. This map restricts to a map $s' : \mathbb{K}_{\mathbb{T}}(\mathcal{C}(\mathcal{D})) \to \mathbb{K}_{\mathbb{T}}(\mathcal{C}(\tilde{\mathcal{D}}))$ because we claim that

$$s\left(\mathrm{Loc}_f(\xi_{X_2})\right) = \mathrm{Loc}_{\tilde{f}}(\xi_{X_1} \oplus \xi_{X_3} \ominus \xi_{X_2}). \tag{4.8}$$

holds for corresponding fixed points f and $\tilde{f}$. Indeed, according to Section 3.2.3, Loc_f^K maps the

relevant Grothendieck roots of ξ_1, ξ_2, ξ_3 to

$$\begin{aligned}
&\{\mathbf{u}_k, \mathbf{u}_k\mathbf{h}^{-1}, \dots, \mathbf{u}_k\mathbf{h}^{1-b}, \qquad \mathbf{u}_{k+1}, \mathbf{u}_{k+1}\mathbf{h}^{-1}, \dots, \mathbf{u}_{k+1}\mathbf{h}^{1-a}\} \\
&\{\mathbf{u}_k\mathbf{h}^{d-b}, \dots, \mathbf{u}_k\mathbf{h}^{1-b}, \qquad \mathbf{u}_{k+1}, \mathbf{u}_{k+1}\mathbf{h}^{-1}, \dots, \mathbf{u}_{k+1}\mathbf{h}^{1-a}\} \\
&\{\mathbf{u}_k\mathbf{h}^{d-b}, \dots, \mathbf{u}_k\mathbf{h}^{1-b}, \qquad \mathbf{u}_{k+1}\mathbf{h}^{c-a}, \dots, \mathbf{u}_{k+1}\mathbf{h}^{1-a}\}
\end{aligned}$$

respectively, where a, b, c, d are the number of ties in A, B, C, D in the figure. Similarly $\mathrm{Loc}_{\tilde{f}}^K$ maps the relevant Grothendieck roots of $\xi_1, \tilde{\xi}_2, \xi_3$ to

$$\begin{aligned}
&\{\tilde{\mathbf{u}}_k, \tilde{\mathbf{u}}_k\mathbf{h}^{-1}, \dots, \tilde{\mathbf{u}}_k\mathbf{h}^{1-a}, \qquad \tilde{\mathbf{u}}_{k+1}, \tilde{\mathbf{u}}_{k+1}\mathbf{h}^{-1}, \dots, \tilde{\mathbf{u}}_{k+1}\mathbf{h}^{1-b}\} \\
&\{\tilde{\mathbf{u}}_k\mathbf{h}^{c-a}, \dots, \tilde{\mathbf{u}}_k\mathbf{h}^{1-a}, \qquad \tilde{\mathbf{u}}_{k+1}, \tilde{\mathbf{u}}_{k+1}\mathbf{h}^{-1}, \dots, \tilde{\mathbf{u}}_{k+1}\mathbf{h}^{1-b}\} \\
&\{\tilde{\mathbf{u}}_k\mathbf{h}^{c-a}, \dots, \tilde{\mathbf{u}}_k\mathbf{h}^{1-a}, \qquad \tilde{\mathbf{u}}_{k+1}\mathbf{h}^{d-b}, \dots, \tilde{\mathbf{u}}_{k+1}\mathbf{h}^{1-b}\},
\end{aligned}$$

and (4.8) indeed holds. The map s' is clearly invertible hence the isomorphism in K theory is proved. The isomorphism in cohomology is proved similarly. □

For (TV) transition the counterpart of Theorem 4.5.2 does not hold; it holds only after substituting $\mathbf{h} = 1$ ($\hbar = 0$), that is, turning off the $\mathbb{C}_\hbar^\times$ action.

APPENDIX A

COMPARISON WITH THE BOW VARIETIES OF [NT]

In this appendix, we show how to obtain our special bow varieties from the more general construction of [NT]. First, we take stability conditions $\nu^{\mathbb{R}} = -1$ and $\nu_{\mathbb{C}} = 0$. In this case, the semi-stable and stable locus agree, giving a smooth variety. The (ν_1) condition of [NT, Section 2.4.2] is automatically satisfied, and our (ν) condition (Lemma 3.1.4) is (ν_2) from [NT, Section 2.4.2]. We also consider only finite type A bow varieties, while [NT] defines affine type A bow varieties. To pass from affine to finite, simply set one of the vector spaces $V_\zeta = 0$. This is consistent with the 0 multiplicity of the infinite left and right segments in Section 2.1. One can think of the more general affine construction as taking both of these multiplicities to be nonzero, but equal and taking the one-point compactification. With the exception of brane charge and BCTs, we believe our constructions generalize easily to affine type A. Finally, we explain how our torus action relates to that of [NT, Section 6.9.3].

Assume that the generator of $K^0_{\mathbb{C}^\times_\hbar}(\mathrm{pt})$, denoted by $\mathbf{h}$, has a formal square root and denote it by $\mathbf{h}^{1/2}$. Let k_X be the number of NS5 branes left of the D3 brane X. If we reparameterized

- W_X by $\mathbf{h}^{k_X/2}$ (X is a D3 brane), and
- $\mathbb{C}_U$ by $\mathbf{h}^{(-1+d_{U^-}-d_{U^+}+k_{U^+})/2}$ (U is a D5 brane),

then the $\mathbb{C}^\times_\hbar$-degrees would change from

$$\deg_{\mathbf{h}}(A) = 0, \qquad \deg_{\mathbf{h}}(B) = 1, \qquad \deg_{\mathbf{h}}(B') = 1, \qquad \deg_{\mathbf{h}}(C) = 1, \qquad \deg_{\mathbf{h}}(D) = 0,$$

$$\deg_{\mathbf{h}}(a) = 0, \qquad \deg_{\mathbf{h}}(b) = 1 \qquad \text{(the values of this paper)}$$

to the values

$$\deg_{\mathbf{h}^{1/2}}(A) = 0, \qquad \deg_{\mathbf{h}^{1/2}}(B) = 2, \qquad \deg_{\mathbf{h}^{1/2}}(B') = 2, \qquad \deg_{\mathbf{h}^{1/2}}(C) = 1, \qquad \deg_{\mathbf{h}^{1/2}}(D) = 1,$$

$$\deg_{\mathbf{h}^{1/2}}(a_U) = 1 + d_{U^+} - d_{U^-}, \qquad \deg_{\mathbf{h}^{1/2}}(b_U) = 1 + d_{U^-} - d_{U^+},$$

that agree with the degrees in [NT, Section 6.9.3]. Although the [NT] convention has conceptual

advantages, in this paper we will stick with our convention.

APPENDIX B

MAYA DIAGRAMS

In this appendix we describe the relation between our combinatorial codes and the ones called Maya diagrams in [N3, Appendix A].

Let us consider an affine type A brane diagram, that is, let the 5-branes be arranged around a cycle. Instead of drawing the diagram on the cycle, we draw it on the universal cover, that is, a periodic brane diagram on an infinite line, see Figure B.1. By applying some Hanany-Witten transitions we may assume that the NS5 branes and the D5 branes are separated on the cycle—we call this brane diagram *separated*. In our figure then the D5 branes come in groups, say, around integer positions, and the NS5 branes come in groups positioned at half-integer positions.

Tie diagrams of fixed point codes for such a brane diagram continue to make sense. However, the notion of brane charge is not defined; hence the table-with-margin code does not make sense. Instead, the analogous code is described in [N3], that we sketch now, together with the corresponding tie diagram.

Consider a representative of a tie diagram of a fixed point where all the ties are attached to the D5 branes in the group *at position 0*. Then the ties come in blocks corresponding to half integers, according to the position of the other end of the tie—see the figure. Consider the "BCTs" of the ties in block $\frac{k}{2}$ as follows:

- for $k > 0$, the (U, V) entry is 0 if there is a U-V tie, otherwise 1;
- for $k < 0$, the (U, V) entry is 1 if there is a U-V tie, otherwise 0.

Then glue these "BCTs" together to form an $n \times \infty$ table, called *Maya diagram*, see the bottom table in Figure B.1. By abuse of language, the 'BCT' corresponding to block $\frac{k}{2}$ will also be called "block $\frac{k}{2}$".

The following properties of the obtained Maya diagram can be read from the corresponding tie diagram.

1. For large enough k all entries of block $\frac{k}{2}$ are 1, and all entries of block $\frac{-k}{2}$ are 0.

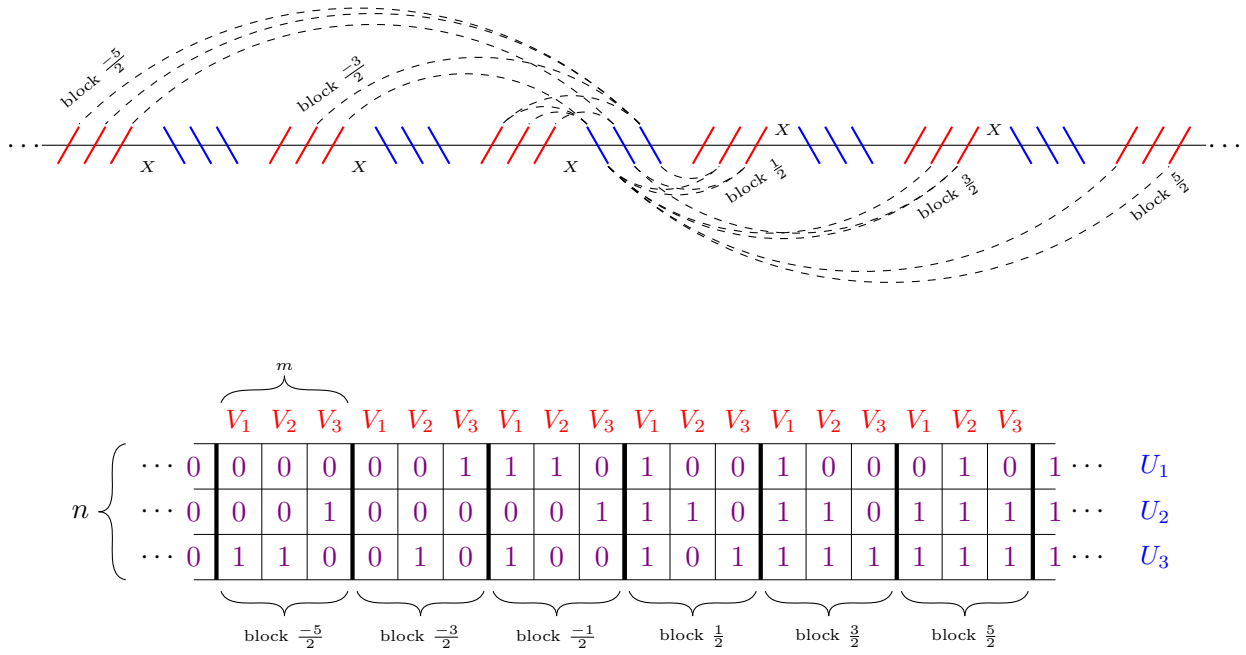

Figure B.1: Top: a tie diagram of a fixed point in $\mathcal{C}(\mathcal{D})$ where $\mathcal{D}$ is a separated brane diagram of affine type A. Bottom: the corresponding Maya diagram of [N3, Appendix A].

2. For $1 \leq i \leq n$ we have that $d_{U_i^+} - d_{U_i^-} =$

$$\#\{\text{0s in row } i \text{ of positive blocks}\} - \#\{\text{1s in row } i \text{ of negative blocks}\}.$$

3. For $1 \leq j \leq m$ we have that $d_{V_j^+} - d_{V_j^-} =$

$$\#\{\text{1s in a } V_j \text{ column of negative blocks}\} - \#\{\text{0s in a } V_j \text{ column of negative blocks}\}.$$

4. Let X be the D3 brane for which X^+ is a D5 brane and X^- is an NS5 brane. Then

$$\begin{aligned} d_X =& \#\{1s \text{ in block } \frac{-1}{2}\} + 2\#\{1s \text{ in block } \frac{-3}{2}\} + 3\#\{1s \text{ in block } \frac{-5}{2}\} + \dots \\ &+ \#\{0s \text{ in block } \frac{3}{2}\} + 2\#\{0s \text{ in block } \frac{5}{2}\} + 3\#\{0s \text{ in block } \frac{7}{2}\} + \dots . \end{aligned}$$

It is proved in [N3] that Maya diagrams (ie. $n \times \infty$ tables that come as a union of ∞ many $n \times m$ tables called blocks, that have properties (1)–(4)) are in bijection with the torus fixed points of a

bow variety associated with a separated affine type A brane diagram.

Since Figure 2.12 still holds as a proof of bijection between torus fixed points of HW equivalent brane diagrams, this statement describes the fixed points of all affine type A bow varieties.

REFERENCES

[AD] S. Abeasis, A. Del Fra. Degenerations for the representations of an equioriented quiverof type A_m. Boll. Un. Mat. Ital. Suppl. 1980, 157–171.

[AO] M. Aganagic, A. Okounkov. Elliptic stable envelopes. Preprint arXiv:1604.00423

[AM1] P. Aluffi, L. C. Mihalcea. Chern classes of Schubert cells and varieties. J.Algebraic Geom., 18(1):63–100, 2009

[AM2] P. Aluffi, L. C. Mihalcea. Chern-Schwartz-MacPherson classes for Schubert cells in flag manifolds, Comp. Math., Vol. 152, Issue 12, 2016, pp. 2603–26

[AMSS1] P. Aluffi, L. C. Mihalcea, J. Schürmann, C. Su. Shadows of characteristic cycles, Verma modules, and positivity of Chern-Schwartz-MacPherson classes of Schubert cells. ArXiv:1709.08697.

[AMSS2] P. Aluffi, L. Mihalcea, J. Schürmann, C. Su. Motivic Cherm classes of Schubert cells, Hecke algebras,and applications to Casselman's problem. Preprint 2019, arXiv 1902.10101.

[B] A. Barvinok. On the number of matrices and a random matrix with prescribed row and column sums and 0-1 entries. Adv. Math., Vol. 224, Issue 1, 2010, 316–339.

[BFN] A. Braverman, M. Finkelberg, H. Nakajima. Coulomb branches of $3d$ $N = 4$ quiver gauge theories and slices in the affine Grassmannian. With two appendices by Braverman, Finkelberg, Kamnitzer, Kodera, Nakajima, Webster and Weekes. Adv. Theor. Math. Phys., 23(1), 75–166, 2019.

[BL] L. Borisov, A. Libgober. Elliptic genera of singular varieties. Duke Math. J. 116 (2003), no. 2,319–351

[Br] R. A. Brualdi. Algorithms for constructing $(0, 1)$-matrices with prescribed row and column sum vectors. Discrete Math., Vol 306, Issue 23, 2006, 3054–3062.

[BFR] A. S. Buch, L. Fehér, R. Rimányi. Positivity of quiver coefficients through Thom polynomials. Adv. Math. 197 (2005) 306–320.

[BDG] M. Bullimore, T. Dimofte, and D. Gaiotto. The Coulomb Branch of $3d$ $N = 4$ Theories. Commun. Math. Phys., 354(2):671–751, 2017.

[BDGH] M. Bullimore, T. Dimofte, D. Gaiotto, and J. Hilburn. Boundaries, Mirror Symmetry, and Symplectic Duality in $3d$ $N = 4$ Gauge Theory. JHEP, 10:108, 2016.

[BSY] J.-P. Brasselet, J. Schürmann, and S. Yokura. Hirzebruch classes and motivicChern classes for singular spaces. J. Topol. Anal., 2(1):1–55, 2010

[Ch09] S. A. Cherkis. Moduli spaces of instantons on the Taub-NUT space, Comm. Math. Phys. 290 (2009), no. 2, 719–736.

[Ch10] S. A. Cherkis. Instantons on the Taub-NUT space, Adv. Theor. Math. Phys. 14 (2010), no. 2, 609–641.

[Ch11] S. A. Cherkis. Instantons on gravitons, Comm. Math. Phys. 306 (2011), no. 2, 449–483.

[FR] L. Fehér, R. Rimányi. Chern-Schwartz-MacPherson classes of degeneracy loci, Geom. & Top. 22 (2018) 3575-3622

[FRV] G. Felder, R. Rimányi, A. Varchenko. Elliptic dynamical quantum groups and equivariant elliptic cohomology. SIGMA 14 (2018), 132, 41 pages, DOI 10.3842/SIGMA.2018.132.

[FRW1] L. M. Fehér, R. Rimányi, A. Weber. Motivic Chern classes and K-theoretic stable envelopes. arXiv 1802.01503, 201

[FRW2] Fehér L.M., Rimányi R., Weber A. (2020) Characteristic Classes of Orbit Stratifications, the Axiomatic Approach. In: Hu J., Li C., Mihalcea L.C. (eds) Schubert Calculus and Its Applications in Combinatorics and Representation Theory. ICTSC 2017. Springer Proceedings in Mathematics & Statistics, vol 332. Springer, Singapore. DOI 10.1007/978-981-15-7451-1_9

[G] Gale, D. (1957). A theorem on flows in networks. Pacific Journal of Mathematics, 7, 1073-1082.

[GR] N. Ganter, A. Ram. Generalized Schubert Calculus. Journal of the Ramanujan Mathematical Society 28A (Special Issue 2013) pp. 1–42.

[GKM] M. Goresky, R. Kottwitz, R. MacPherson. Equivariant cohomology, Koszul duality, and the localization theorem. Inv. Math. 131 (1998), 25–83.

[GW] D. Gaiotto and E. Witten. S-Duality of Boundary Conditions In $N = 4$ Super Yang-Mills Theory. Adv. Theor. Math. Phys., 13(3):721–896, 2009.

[GMMS] D. V. Galakhov, A. D. Mironov, A. Y. Morozov, and A. V. Smirnov. Three-dimensional extensions of the Alday-Gaiotto-Tachikawa relation. Theoret. and Math. Phys., 172(1):939–962, 2012.

[HW] A. Hanany, E. Witten. Type IIB superstrings, BPS monopoles, and threedimensional gauge dynamics. Nucl. Phys., B492:152–190, 1997.

[HHH] M. Harada, A. Henriques, T. S. Holm. Computation of generalized equivariant cohomologies of Kac–Moody flag varieties. Adv. Math., 197:1, 2005, 198–221.

[IS] K. Intriligator, N. Seiberg. Mirror symmetry in three-dimensional gauge theories. Phys. Lett. B,387(3):513–519, 1996.

[JKK] L. Jeffrey, Y.-H. Kiem, F. Kirwan. On the cohomology of hyperkähler quotients. Transformation Groups 14(4):801-823, 2008

[KRW] S. Kumar, R. Rimányi, A. Weber. Elliptic classes of Schubert varieties. Math. Ann., 378(1), 703-728, DOI 10.1007
colorred/s00208-020-02043-z

[KS] Y. Kononov, A. Smirnov. Pursuing quantum difference equations II: 3D-mirror symmetry. arXiv:2008.06309, Aug. 2020.

[LZ] C. Lenart, K. Zainoulline. A Schubert basis in equivariant elliptic cohomology. New York Journal ofMathematics 23, 711–737, 2017.

[MG1] K. McGerty, T. Nevins. Kirwan surjectivity for quiver varieties. Inv. Math., Vol. 212, 161–187 (2018).

[MG2] K. McGerty, T. Nevins. Counterexamples to hyperkahler Kirwan surjectivity. Preprint, arXiv:1904.12003.

[M] R. MacPherson. Chern classes for singular algebraic varieties. Ann. of Math. 100 (1974), 421–432.

[MO] D. Maulik, A. Okounkov. Quantum Groups and Quantum Cohomology. Astérisque 408, Société Mathématique de France, 2019.

[N1] Hiraku Nakajima. Instantons on ALE spaces, quiver varieties, and Kac-Moody algebras. Duke Mathematical Journal, Duke Math. J. 76(2), (1994), 365-416

[N2] H. Nakajima. Lectures on Hilbert Schemes of Points on Surfaces University Lecture Series 18; AMS 1999.

[N3] H. Nakajima. Towards geometric Satake correspondence for Kac-Moody algebras—Cherkis bow varieties and affine Lie algebras of type A. arXiv:1810.04293.

[NT] H. Nakajima, Y. Takayama. Cherkis bow varieties and Coulomb branches of quiver gauge theories of affine type A, Selecta Mathematica 23 (2017), no. 4, 2553–2633.

[O] A. Okounkov. Lectures on K-theoretic computations in enumerative geometry. In: Geometry of Moduli Spaces and Representation Theory, IAS/Park City Math. Ser., 24, AMS, Providence, RI, (2017), pp. 251–380.

[Oh1] T. Ohmoto. Equivariant Chern classes of singular algebraic varieties withgroup actions, Math. Proc. Cambridge Phil. Soc. 140 (2006), 115–134

[Oh2] T. Ohmoto. Singularities of maps and characteristic classes, Adv. Stud. PureMath., School on Real and Complex Singularities in São Carlos 2012, R. N.Araújo dos Santos, V. H. Jorge Pérez, T. Nishimura and O. Saeki, eds. (Math.Soc. of Japan, 2016), 191–265

[Ro] L. Rozansky. In preparation. 2020.

[Ri] R. Rimanyi. $\hbar$-deformed Schubert calculus in equivariant cohomology, K theory, and elliptic cohomology. To appear in the proceedings of the Geometry and Topology of Singularities, Némethi-60 conference, Birkhäuser, Springer 2020.

[RS] R. Rimányi, Y. Shou. Bow varieties—geometry, combinatorics, characteristic classes. Preprint arXiv:2012.07814

[RSVZ1] R. Rimányi, A. Smirnov, A. Varchenko, Z. Zhou. 3d mirror symmetry and elliptic stable envelopes. Preprint arXiv:1902.03677.

[RSVZ2] R. Rimányi, A. Smirnov, A. Varchenko, Z. Zhou. Three dimensional mirror self-symmetry of the cotangent bundle of the full flag variety. SIGMA 15 (2019), 093, 22 pages, DOI 10.3842/SIGMA.2019.093.

[RTV1] R. Rimányi, V. Tarasov, A. Varchenko. Partial flag varieties, stable envelopes and weight functions. Quantum Topol. 6 (2015), no. 2, 333–364.

[RTV2] R. Rimányi, V. Tarasov, A. Varchenko. Trigonometric weight functions as K-theoretic stable envelope maps for the cotangent bundle of a flag variety. J. Geom. Phys. 94 (2015), 81–119, DOI 10.1016/j.geomphys.2015.04.002.

[RTV3] R. Rimányi, V. Tarasov, A. Varchenko. Elliptic and K-theoretic stable envelopes and Newton polytopes. Selecta Math. (2019) 25:16, DOI 10.1007/s00029-019-0451-5.

[RV] R. Rimányi, A. Varchenko. Equivariant Chern-Schwartz-MacPherson classes in partial flag varieties: interpolation and formulae. In *Schubert Varieties, Equivariant Cohomology and Characteristic Classes*, IMPANGA2015 (eds. J. Buczynski, M. Michalek, E. Postingel), EMS 2018, pp. 225–235.

[RW1] R. Rimányi, A. Weber. Elliptic classes of Schubert varieties via Bott-Samelson resolution. J. of Topology, Vol. 13, Issue 3, September 2020, 1139-1182, DOI 10.1112 colorred/topo.12152.

[RW2] R. Rimányi, A. Weber. Elliptic classes on Langlands dual flag varieties. Preprint arXiv:2007.08976.

[Sch] M.-H. Schwartz. Classes caractéristiques définies par une stratification d'une variété analytique complexe. I. C. R. Acad. Sci. Paris, 260:3262–3264, 196

[Sm] A. Smirnov. Elliptic stable envelope for Hilbert scheme of points in the plane. Preprint, arXiv:1804.08779.

[St] R. P. Stanley. Enumerative Combinatorics. Cambridge, Vol. 2, 1999

[SZ] A. Smirnov, Z. Zhou. 3d Mirror Symmetry and Quantum K-theory of Hypertoric Varieties. arXiv:2006.00118, May 2020.

[T] Y. Takayama. Nahm's equations, quiver varieties and parabolic sheaves. Publ. Res. Inst. Math. Sci. 52(1), 1–41 (2016)

[W1] A. Weber. Equivariant Chern classes and localization theorem. J. of Singular-ities, Vol. 5 (2012), 153–176

[W2] A. Weber. Equivariant Hirzebruch class for singular varieties. Selecta Math.(N.S.) 22 (2016), no. 3, 1413–1454